Aus der

Abteilung für Neuropsychologie und Verhaltensneurobiologie

Zentrum für Kognitionswissenschaften (ZKW)

Electrophysiological and functional magnetic resonance imaging investigations on the influence of spatial and feature-based attention on the flanker effect

vorgelegt dem Fachbereich 2 (Biologie/Chemie)

der Universität Bremen als

DISSERTATION

zur Erlangung des akademischen Grades

Doktor der Naturwissenschaften (Dr. rer. nat.)

von

M.Sc. Julia Siemann

Tag des öffentlichen Kolloquiums:
Erstgutachter der Dissertation: Prof. Dr. med. Dr. phil. Manfred Herrmann
Zweitgutachter der Dissertation: Prof. Dr. med. Manfred Fahle

Table of contents

"*All truths are easy to understand once they are discovered; the point is to discover them*."

(Galileo Galilei)

Preface

Attention represents an almost ubiquitous field in neuroscientific research. It can be manipulated in many ways including direction, intensity or selectivity of attention. An unanswered question remains concerning the possibility to suppress distracting information through top-down attentional control. The present doctoral thesis addresses this topic and furthermore contrasts two main attention types (spatial and feature-based allocation). For this purpose, both anatomical and temporal data were collected and brought together in a common source analysis.

The reported experiments were conducted at the University of Bremen (Department of Neuropsychology and Behavioral Neurobiology) and financially supported by a grant from the German Research Foundation (DFG; GA1806/2-1, "Zeitlich-räumliche Charakterisierung neuronaler Konflikt-Verarbeitungsprozesse unter dem Einfluss räumlicher und eigenschaftsbasierter Aufmerksamkeitsausrichtung"). The project was supervised by Dr. Daniela Galashan (project leader) and Prof. Dr. Dr. Manfred Herrmann (head of department).

Abstracts

Experiment I: Spatial cueing in the flanker task

In daily life, the brain frequently needs to select certain items out of an incoming stream of information in order to react adequately based on its current goals. A central question in the literature concerns the temporal locus of this selection process. This either may be early after low-level perceptual analysis of late after processing of all information units.

Experiment I addresses the question whether enhanced perception of items at attended location can inhibit the involuntary processing of information that is irrelevant for the current task but shares similarities with the relevant information. For this purpose, a non-centrally presented interference task was combined with spatial cues, which could be valid or invalid with respect to the actual target location. In addition, neutral cues were included that directed attention to both possible target locations. Functional imaging and electroencephalographic data were collected from 20 healthy volunteers and combined in a common source analysis.

The results suggest that valid cueing reduced conflict detection during the N200 component, whereas invalidly cued trials apparently led to enhanced conflict processing. According to source waveform differences, the putative neural generators of these effects were located in visual brain regions (parietooccipital negativity) and the anterior cingulate cortex (frontocentral positivity). Correct spatial attention probably involved early attentional window adjustments in order to suppress flankers. Overall, experiment I corroborates the assumption that focused spatial attention can reduce the impact of distracting information.

Experiment II: Feature-based cueing in the flanker task

While early modulations of spatial attention have been reported in numerous studies, top-down feature-based effects are less well established. Findings in the literature hint at later differences

between attended and unattended conditions when cueing features compared with spatial cueing.

Experiment II aimed at identifying differences between both attention types with regard to influences on early stimulus processing and the capacity to suppress irrelevant information. For this purpose, the experimental design used in experiment I was replicated using color cues. Functional imaging and electroencephalographic data were collected from 21 healthy volunteers and combined in a common source analysis. Comparing both experiments, there was overlapping activity during interference processing with valid cueing in dorsal frontoparietal brain regions. This suggests that there is a common network for top-down control during conflict processing. Globally directed feature-based attention possibly involved initial attentional captures to the stimulus location followed by similar focusing processes as in experiment I.

In experiment II, validly cued conflict trials additionally activated cingulate and motor regions. Source waveform data originating in these regions hint at a late response-based stage of conflict. Response selection was probably more difficult compared to experiment I because of enhanced activation of competing response channels due to an initial global search mode.

Integration: Spatial and feature-based attention in the present experiments

Different attentional mechanisms were postulated for both experiments that might explain the observed results patterns. In order to substantiate these assumptions, spatial and feature-based attention were directly compared with each other. For this end, anatomical and temporal data of both experiments were analyzed with regard to potential influences of the factor ‘attention mode’.

Conjunction analyses of the reorientation contrast (invalid > neutral) and of the facilitation contrast (valid > neutral) over both attention modes revealed a broad frontoparietal network. This overlap shows that non-spatial attention recruits similar structures in order to shift attention after invalid cueing. Moreover, both experiments possibly involved saliency detection signals during processing of the task-relevant attribute (location/color). Thus, there were activation clusters in ventral frontoparietal regions that trigger salience signals and are putative generators of the P300 component. In accordance with this suggestion, there were validity effects for both attention modes during the analyzed P300 time window. The observed overlap between experiments may be explained by early attentional capture mechanisms, which interrupted the global focus commonly associated with feature-based attention. Therefore, spatial attentional adjustments may have played a central role during both experiments.

German abstracts

Experiment I: Räumliche Hinweisreize in der Flanker-Aufgabe

Im täglichen Leben muss das Gehirn fortlaufend bestimmte Objekte aus einem hereinströmenden Informationsfluss auswählen, um basierend auf den aktuellen Zielen adäquat reagieren zu können. Eine zentrale Fragestellung befasst sich mit der zeitlichen Lokalisation dieses Auswahlprozesses.

Experiment I befasst sich mit der Frage, ob die erhöhte Wahrnehmung von Objekten an attendierten Orten die unwillkürliche Verarbeitung von Informationen unterdrücken kann, die für die momentane Aufgabe irrelevant sind, jedoch Ähnlichkeiten mit den relevanten Informationen aufweisen. Zu diesem Zweck wurde eine nicht-zentrale Interferenzaufgabe mit räumlichen Hinweisreizen kombiniert, die valide oder invalide sein konnten in Bezug auf den tatsächlichen Zielreizort. Zusätzlich wurden neutrale Hinweisreize mit einbezogen, die die Aufmerksamkeit auf beide mögliche Zielreizorte lenkten. Funktionell bildgebende und elektroenzephalographische Daten von 20 gesunden Freiwilligen wurden erhoben und in einer gemeinsamen Quellenanalyse kombiniert.

Die Ergebnisse deuten darauf hin, dass valide Hinweisreize die Konfliktwahrnehmung während der N200-Komponente reduzierten, während invalide Durchgänge offensichtlich zu erhöhter Konfliktverarbeitung führten. Entsprechend den Unterschieden zwischen den Quellen-wellenformen liegen die mutmaßlichen neuronalen Generatoren dieser Effekte in visuellen Hirnarealen (parietookzipitale Negativierung) und im anterioren zingulären Kortex (frontozentrale Positivierung). Korrekt ausgerichtete räumliche Aufmerksamkeit beinhaltete wahrscheinlich eine frühe Anpassung des Aufmerksamkeitsfensters, um die Flankierreize zu unterdrücken. Insgesamt bekräftigt Experiment I die Annahme, dass fokussierte räumliche Aufmerksamkeit den Einfluss störender Information reduzieren kann.

Experiment II: Eigenschaftsbasierte Hinweisreize in der Flanker-Aufgabe

Während frühe Modulationen durch räumliche Aufmerksamkeit in zahlreichen Studien berichtet wurden, sind willentlich gesteuerte eigenschaftsbasierte Effekte weniger gesichert. Befunde in der Literatur deuten auf spätere Unterschiede zwischen attendierten und nicht attendierten Bedingungen hin, wenn Eigenschaften vorhergesagt werden im Vergleich zu räumlichen Hinweisreizen.

Experiment II zielte darauf ab, Unterschiede zwischen den Aufmerksamkeitsarten zu identifizieren in Bezug auf Einflüsse auf die frühe Stimulusverarbeitung und die Fähigkeit, irrelevante Informationen zu unterdrücken. Zu diesem Zweck wurde das experimentelle Design aus Experiment I repliziert unter Einbeziehung von Farb-Hinweisreizen. Funktionell bildgebende und elektroenzephalographische Daten wurden von 21 gesunden Freiwilligen erhoben und in einer gemeinsamen Quellenanalyse kombiniert. Im Vergleich beider Experimente zeigten sich überlappende Aktivierungsmuster während der Interferenzverarbeitung mit validen Hinweisreizen in dorsalen frontoparietalen Hirnregionen. Dies deutete darauf hin, dass es ein gemeinsames Netzwerk willentlich gesteuerter Kontrolle während der Konfliktverarbeitung gibt. Global ausgerichtete eigenschaftsbasierte Aufmerksamkeit beinhaltete möglicherweise eine frühe Aufmerksamkeitslenkung auf die Stimulusposition, worauf ähnliche Fokussierungsmechanismen wie in Experiment I folgten.

In Experiment II aktivierten valide vorhergesagte Konfliktdurchgänge zusätzlich zinguläre und motorische Regionen. Quellenwellenform-Daten aus diesen Regionen deuten auf eine späte Antwort-basierte Konfliktverarbeitungsstufe hin. Die Auswahl der Antwort war wahrscheinlich schwieriger in Vergleich zu Experiment I aufgrund einer erhöhten Aktivierung konkurrierender Antwortkanäle bedingt durch die anfänglich globale Suchstrategie.

Integration: Räumliche und eigenschaftsbasierte Aufmerksamkeit in den vorliegenden Experimenten

Verschiedene Aufmerksamkeitsmechanismen wurden für die beiden Experimente vorgeschlagen, die die beobachteten Ergebnisse erklären könnten. Um diese Annahmen zu begründen, wurden räumliche und eigenschaftsbasierte Aufmerksamkeit direkt miteinander verglichen. Hierfür wurden die anatomischen und zeitlichen Datensätze beider Experimente in Hinblick auf potentielle Einflüsse des Faktors „Aufmerksamkeitsmodus“ analysiert.

Gemeinsame Analysen des Reorientierungskontrastes (invalid > neutral) und des Faszilitationskontrastes (valid > neutral) über beide Aufmerksamkeitsmodi ergaben ein umfassendes frontoparietales Netzwerk. Diese Überlappung zeigt, dass nicht-räumliche Aufmerksamkeit ähnliche Strukturen rekrutiert, um die Aufmerksamkeit nach invaliden Hinweisreizen zu verschieben. Darüber hinaus beinhalteten beide Experimente womöglich Signale zur Salienz-Detektion während der Verarbeitung der aufgabenrelevanten Attribute (Lokation/Farbe). So gab es Aktivierungsbereiche in ventralen frontoparietalen Regionen, die Salienzsignale weiterleiten und vermeintliche Generatoren der P300-Komponente sind. In Übereinstimmung mit dieser Vermutung gab es Validitätseffekte beider Aufmerksamkeitsmodi im analysierten P300-Zeitfenster. Die beobachtete Überlappung zwischen den Experimenten kann durch frühe Mechanismen der Aufmerksamkeitslenkung erklärt werden, die den globalen Fokus unterbrachen, welcher allgemein mit eigenschaftsbasierter Aufmerksamkeit assoziiert wird. Darum könnte eine räumliche Aufmerksamkeitsanpassung eine zentrale Rolle in beiden Experimenten gespielt haben.

Abbreviations

ACC	anterior cingulate cortex
ANOVA	analysis of variance
BA	Brodmann area
BOLD	blood oxygenation level dependent
CON	congruent
dFPN	dorsal frontoparietal network
EEG	electroencephalography
EPI	echo-planar imaging
ERP	event-related potential
FEF	frontal eye field
fMRI	functional magnetic resonance imaging
FWHM	full width at half maximum
IFG	inferior frontal gyrus
INC	incongruent
IOG	inferior occipital gyrus
IPL	inferior parietal lobule
IPS	intraparietal sulcus
ISI	interstimulus interval
ITI	intertrial interval
MFG	middle frontal gyrus
MOG	middle occipital gyrus
MTG	middle temporal gyrus
PCA	principle component analysis
PHG	parahippocampal gyrus
RMS	root mean square
RS	regional source
RT	reaction time
SD	standard deviation
SEM	standard error of the mean
SFG	superior frontal gyrus
SMA	supplementary motor area
SN	selection negativity
SOG	superior occipital gyrus
SPL	superior parietal lobule
SR	stimulus-response
SS	stimulus-stimulus
STG	superior temporal gyrus
TPJ	temporoparietal junction
vFPN	ventral frontoparietal network

2. GENERAL INTRODUCTION: VISUAL SELECTIVE ATTENTION

Visual selective attention is one of the main areas of cognitive research, leading to a vast amount of studies in many branches of fundamental as well as applied research. In the online search engine ‘pubmed’ (http://www.ncbi.nlm.nih.gov/pubmed/), the entry ‘visual selective attention’ delivers 3530 hits, of which 1961 stem from the past 10 years alone (date of search: 13.10.2015, 11am). The term attention subsumes several distinct but related cognitive processes. The present study addresses two main attention modes (spatial and feature-based attention) and their influence on the processing of irrelevant distracting information (interference). The first chapter serves as a background providing general information about the cognitive processes investigated in the two experiments and the methods applied for this end. In Chapter 2, the objectives and applied methods are described in more detail. Chapters 3 and 4 describe the experiments, including a detailed outline of the experimental questions, a methods section, a results part, and a critical discussion respectively. In Chapter 5, both experiments are directly compared with regard to commonalities and differences of the applied attention modes. Chapter 6 serves to integrate the results into the theoretical background of the thesis.

1.1 Dimensions of attention

The term ‘attention’ generally refers to the conscious focusing of cognitive resources on certain information units (James, 1950) and comprises several components. First, attention can vary as a function of **selectivity**, being either directed to a single element (selective attention), shift between elements (shifts of attention) or be divided between several elements simultaneously (divided attention). In addition, there are different levels of attentional **intensity**, including alertness (short-term activation), sustained attention (long-term activation towards frequently presented stimuli) and vigilance (long-term activation towards occasional target stimuli) (Sturm, 2004, according to van Zomeren & Brouwer, 1994).

There are also different modes of visual selective attention. In **spatial** attention, so-called cues can direct attention to a certain location in the visual field that receive processing priorities over the rest of the scene (Posner, 1980). When **features** are the target of attention, there is a global enhancement of all stimuli containing the attended feature (Allport, 1971), whereas attending to a feature conjunction (**object)** leads to enhancement of that object's representation with all of its features (Duncan, 1984).

Attending to a location in space leads to better performance in response to goal-relevant information. Given that visual search in naturalistic scenes typically involves eye movements, past research concentrated on the question whether spatial attention is directly linked to and thus possibly even explained by gaze direction (Carrasco, 2011). Posner (1980) investigated the possibility that focused attention could be effective without eye movements and found 'covert' orienting to be possible, i.e., looking at a fixation point while attending to another location in the visual display. In the literature, there is general agreement that focused spatial attention leads to increased spatial resolution at the attended location independent of gaze direction (e.g. Carrasco et al., 2006; Cutrone et al., 2014).

1.2 Models of visual selective attention

Several models have evolved in the literature regarding the neurophysiological basis of attentional mechanisms and the underlying computational processes that these brain regions may perform. Thus, Posner and Petersen (1990) made a distinction between anterior and posterior brain structures involved in different attention-related processes. First, an **anterior network** is presumably engaged in target detection and selective attention, i.e. executive control functions, and recruits frontal and cingulate parts of the brain. Second, a **posterior network** comprises posterior parts of the parietal cortex and subcortical regions for orienting, e.g. in visual search, which guides covert shifts of attention.

The temporal characteristics of the anterior network suggest that there are further subcomponents: One component is defined for transient within-trial adjustments (e.g. during task switching) and one for sustained top-down control over several trials (Dosenbach et al., 2006; Dosenbach et al., 2008). The transient network is associated with dorsolateral prefrontal cortex, inferior parietal lobule (IPL), dorsal frontal cortex, intraparietal sulcus (IPS), precuneus, and cingulate cortex. Cingulo-opercular regions including anterior prefrontal cortex, anterior insula, frontal operculum, anterior cingulate cortex (ACC), medial superior frontal cortex, and thalamus are involved in the sustained top-down control network (Dosenbach et al., 2006; Dosenbach et al., 2008).

Another anatomical distinction has emerged in the literature between dorsal and ventral attentional structures. Dorsal frontoparietal cortices including the frontal eye fields (FEF), superior parietal lobules (SPL), and IPS are most likely involved in correctly (validly) directed attention and top-down strategic control, whereas attentional reorienting during incorrectly (invalidly) cued trials seem to activate temporoparietal junction (TPJ) and ventral frontal cortex predominantly of the right hemisphere, i.e. right ventral brain regions (Corbetta & Shulman, 2002; Petersen & Posner, 2012). The *dorsal frontoparietal network* (dFPN) appears to have a higher spatial resolution in order to precisely localize target items, while the *right ventral frontoparietal network* (vFPN) sends interruption signals upon detection of behaviorally relevant stimuli outside the current attentional focus (Corbetta & Shulman, 2002, see Figure 1).

In contrast to the aforementioned anatomical networks, attention models have also been formulated on a micro-level. Thus, Desimone and Duncan (1995) defined a *biased competition model* according to which neuronal signals evoked by external stimuli are compared with a top-down attentional template that represents the current task demands. When the template and the stimulus match, the visual system is biased towards that stimulus. Moreover, bottom-up factors such as stimulus saliency also create biases (Desimone & Duncan, 1995).

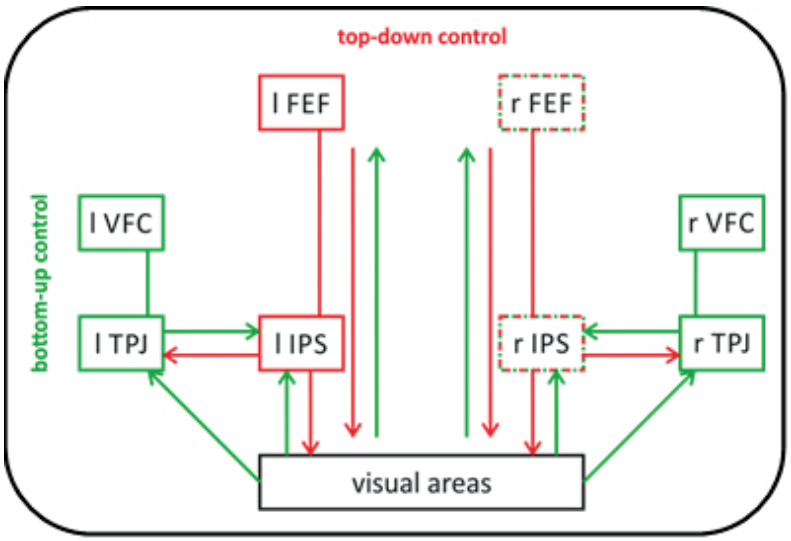

Figure 1: Schematic illustration of the interplay of dorsal and ventral frontoparietal structures during voluntary top-down control (red stream) and involuntary bottom-up captures (according to Corbetta & Shulman, 2002).

Labels:
FEF = frontal eye field
IPS = intraparietal sulcus
l = left
r = right
TPJ = temporoparietal junction
VFC = ventral frontal cortex

Top-down biasing apparently involves three distinct mechanisms: neuronal response enhancement for attended stimuli or locations and simultaneous suppression of unattended information, elevation of a neuron's baseline activity in response to attentional cues in the absence of stimulation, and raised neuronal response sensitivity (Kastner & Ungerleider, 2000). Without focused attention, competition of two stimuli located in the receptive field of a neuron leads to reduced activity of surrounding neurons and consequently to reduced overall activity of that neuronal population compared to the presentation of each stimulus in isolation (Desimone, 1998). The central role ascribed to attention is to increases the signal difference between signals evoked by attended and unattended stimuli (Kastner et al., 1998).

1.3 Vulnerabilities of visual selective attention: Interference effects

The core function of visual selective attention is to minimize influences from irrelevant information in order to improve target processing (Carrasco, 2011). However, numerous study designs show that unattended information also influences behavior. For example, when a target stimulus appears together with stimuli (flankers) which activate a deviating response (incongruent), there is a performance decline compared to congruent trials (Eriksen & Eriksen, 1974). Such interference effects may arise from different kinds of overlaps (Kornblum et al., 1990). In the flanker task, targets and flankers belong to the same dimension (letters). Therefore,

there is a conflict at the perceptual and the conceptual level (Zhang et al., 1999). Moreover, different conflict constellations exist. The classical letter flanker task is an example of a stimulus-stimulus conflict (SS conflict), because the flanker stimuli overlap with the target stimulus but not with the response (Zhang et al., 1999). An irrelevant attribute of the target stimulus may also interfere with the response (SR conflict), e.g. when the presentation side of the target is opposite to the response side (Simon, 1969). Various other conflict types exist which overlap in different dimensions. The present thesis focuses on SS conflicts in a variant of the letter flanker task.

The biased competition model can account for performance declines in interference tasks, because distractors resembling the target lead to smaller signal differences (i.e. biases) than distractors which are dissimilar to the target (Desimone & Duncan, 1995). Due to the known influence of top-down control on neuronal responses, the question arises whether attention can alter interference processing in order to reduce performance cost effects.

1.4 Top-down control during interference processing

Information processing involves several distinct stages, including sensory analysis, stimulus evaluation, response selection, and response execution (Birbaumer & Schmidt, 2010). According to Broadbent's (1958) filter model, attention modulates information processing early after sensory analysis by preventing the transmission of unattended information units. In the filter model, simple perceptual properties are processed in parallel, while higher-order properties require serial processing with limited capacities, which makes filtering necessary. Similarly, Treisman and Gelade (1980) suggested a 'feature integration model' in which feature processing occurs without capacity limits (parallel processing of all features), whereas integration of features from different spatial locations requires spatial attention (serial processing of locations). However, various types of interference effects show that unattended information is processed beyond the perceptual stage, e.g. in the flanker task. Deutsch and

Deutsch (1963) developed an alternative account assuming unlimited capacities. Here, attention serves to select those stimuli that enter working memory for active manipulation and conscious perception.

Lavie (1995) reconciled these opposing viewpoints by proposing that information processing is a function of perceptual load. This assumption postulates an inverse correlation between amount of perceptual load and amount of irrelevant information processed. Apparently, past studies found evidence for early selection when the perceptual load was high, whereas low load studies more frequently supported late selection (Lavie & Tsal, 1994). Alternatively, processing of irrelevant information may also be ascribable to visual interference diluting attention (Benoni & Tsal, 2010). Moreover, the capacity of irrelevant stimuli to capture attention could also depend on the degree to which they are target-related. Thus, interference may arise when attention involuntarily spreads to locations containing behaviorally relevant distractors ('slippage theory'; (Gaspelin et al., 2014). Accordingly, several studies found reduced interference effect when participants closely focused on the target location following valid spatial cues (Fournier & Shorter, 2001; McCarley & Mounts, 2008; Munneke et al., 2008). However, spatially cueing the target location does not necessarily reduce the size of interference effects (e.g. Fox, 1995; Ro et al., 2002; Theeuwes, 1994). Lupiáñez and Jesús Funes (2005) propose that successful inhibition of distracting information depends on the locus of the interference effect. SS conflicts may be sensitive to early attentional effects while SR conflicts are potentially unaffected.

Few studies addressed this matter on a neurophysiological level. Electrophysiological studies on macaque monkeys suggest that spatial attention affects stimulus processing as early as 50ms after stimulus onset (Luck et al., 1997), whereas non-spatial attention effects occur around 170ms (Chelazzi et al., 1998). Neurons in visual cortex demonstrate a response pattern with an initial phase of parallel processing of all stimuli followed by early attentional biases. The

neurons are mutually inhibitory, which is in line with limited amounts of capacity (Desimone & Duncan, 1995). This inhibitory process is susceptible to top-down and bottom-up influences, as predicted by the biased competition model (Desimone & Duncan, 1995). Similarly, O'Connor and colleagues (2002) found attention effects already in lateral geniculate nucleus of the thalamus. As was predicted by the biased competition model, they reported both response enhancement for attended stimuli and suppressions for unattended material as well as attention-related raised baseline activity.

These findings imply that attention can suppress interfering information before response selection stages. Research in this area is therefore an important contribution to the knowledge about selective attentional processes and the locus of selection in face of interference.

2. SCOPE OF THE PRESENT THESIS AND METHODICAL IMPLEMENTATION

2.1 Objectives of the present thesis

The present thesis deals with the interaction of different attentional mechanisms and stimulus-driven conflict effects. It centers on the basic question whether top-down control can alter early stages of interference processing and in this context compares different attention modes with each other. In two experiments, the same flanker task was manipulated using spatial and feature-based attentional cueing respectively. The flanker stimuli varied with regard to spatial position (above or below central fixation) and color (red or green). In the first experiment, cues informed about stimulus position to investigate whether an improved spatial focus can increase selectivity of information processing. Experiment II used color cues to test how globally directed feature-based attention differs with regard to effects on early perceptual selectivity from spatially directed attention.

The methods of functional magnetic resonance imaging (fMRI) and electroencephalography (EEG) were applied to inform about the spatial and temporal dynamics in the brain respectively. Moreover, these data sets were linked using an fMRI-constrained source analysis to provide insights into the chronometry of brain activity during attentional processing and interference resolution. Finally, both attention modes were directly contrasted with each other.

2.2 Magnetic Resonance Imaging – functional and structural imaging of the brain

Magnetic Resonance Imaging (MRI) is a technique that provides noninvasive insights into the human body. In the present study, it was applied to the brain to provide a high-resolution image of participants' brains (structural MRI) and their activity patterns during task completion

(functional MRI; fMRI). Both structural and functional MRI make use of the abundance of hydrogen molecules in the human brain. In a natural environment, these hydrogen nuclei demonstrate a spin around their axis. Due to the strong magnetic field inside the MRI scanner, these spins become aligned (longitudinal magnetization; Huettel et al., 2004). By adding a short high-frequency magnetic pulse, the nuclei's spin can be deflected into a transversal magnetization (orthogonal to the longitudinal field). Afterwards, the spins slowly recover into the original longitudinal direction (relaxation). MRI makes use of the fact that different tissue types in the body demonstrate different relaxation times depending on their respective density properties. With the help of a read-out gradient, the resonance of these tissue types can be coded into different signal intensities, leading to a high-resolution image of the observed body part (in Huettel et al., 2004).

Functional images of the brain using fMRI are based on different local blood oxygenation levels that vary with neuronal activity (blood oxygenation level dependent; BOLD; (Huettel et al., 2004). Local blood flow increases during neuronal activity lead to a higher concentration of oxygenated blood due to an oversupply of oxygen. Oxygenated blood leads to a slower decay of the transversal magnetization (induced by the high-frequency pulse) compared with deoxygenated blood. This is measurable as signal intensity differences depending on the relative local concentration of oxygen (BOLD signal). The fMRI signal is therefore an indirect measure of neuronal activity derived from putative distortions of the signal that are weaker with high concentrations of oxygen during neuronal activity ((in Huettel et al., 2004).

2.3 Electroencephalography and event-related brain potentials

Electroencephalography (EEG) describes the measurement of electrical activity on the scalp originating in the brain. By averaging the same repetitively occurring event within this data stream, a signal can be extracted which is time-locked to that event. This is called event-related potential (ERP). EEG records a dipole that arises as the sum of co-occurring differences in

charges within a circumscribed patch of brain. These charge differences originate from cellular activity which occurs in the form of postsynaptic potentials and action potentials (Luck, 2005a). During excitatory action potentials, positively charged ions flow into the cell and are propagated along the axon until this change in charge reaches the synapse. These depolarizations occur at a very short time scale. Postsynaptic potentials occur as an action potential reaches another cell's dendrite, where current intrudes the dendrite, leaving a net negativity in the extracellular space around the dendrite. Furthermore, there is a concurrent efflux of current at the cell body so that a net positivity emerges at this location. These two processes (negativity at dendrites; positivity at cell body) create a dipole.

EEG cannot measure action potentials directly due to the short timing (≤1ms), as the action potentials of nearby cells are usually non-synchronous and cancel each other out (Luck, 2005a). Postsynaptic potentials are local dipoles gathering for ≥10ms. When a large number of cells is depolarized simultaneously and the cells are spatially aligned and perpendicular to the surface (i.e., their dipoles do not cancel each other out), the resulting joint dipole can be recorded from the scalp. Therefore, postsynaptic potentials are the values that are measurable using EEG recordings (Luck, 2005a).

Whilst EEG measures brain activity nearly in real-time, it is not suited to inform about the generators of this activity. Voltage always spreads to all directions and is sensitive to resistances. Therefore, any tissue exhibiting high resistance such as the skull will cause the voltage to divert laterally. Therefore, the signal measured at one point of the scalp can originate from almost any source within the brain (Luck, 2005a).

2.4 fMRI-constrained source analysis

In order to investigate the spatio-temporal dynamics involved in the present experiments an fMRI-constrained source analysis was computed in each experiment following the basic approaches of previous studies (Bledowski et al., 2007; Galashan et al., 2015; Miedl et al.,

2014). For this end, clustered fMRI peak coordinates of the respective experiments were used as constraints during source analysis of the ERP data. Both data sets (ERP and fMRI) were transferred into Talairach space ('mni2tal.m'; http://imaging.mrc-cbu.cam. ac.uk/imaging/Mni Talairach) in order to ensure identical spatial reference frames of the data sets (Hopfinger et al., 2005). Details of the applied steps are reported for each experiment separately in the respective 'Material and methods' sections.

2.5 Methods applied in experiment I and II

2.5.1 Study design and experimental procedure

The target stimulus set consisted of the letters 'H' and 'S', leading to two congruent (CON) stimulus combinations (target letter flanked by four identical letters) and two incongruent (INC) combinations (flanker letters of the opposite stimulus category). The combination of three cue validity levels (valid/neutral/invalid) and two congruency levels (CON/INC) resulted in six conditions appearing with equal frequencies (congruency = 50%; overall validity = 33.33%) in five runs. To control for congruency sequence effects (Gratton et al., 1992) the experimental runs consisted of 144 (EEG) or 72 (fMRI) pseudo-randomly distributed trials (EEG = 24 trials/condition; fMRI = 12 trials/condition) with each of the six conditions following any of the others equally often in each run.

All participants completed a training session on a separate day before the experimental sessions. A standardized written task instruction file was used to familiarize with the experimental design and the response procedure and to inform about the equiprobable cue validity (see Appendix A). The parameters of the training session matched those of the experiment except for the first training run, which provided written feedback ('correct', 'incorrect' or 'too slow' for responses > 1000ms after stimulus onset). Figure 2 illustrates sample trials for both experiments without feedback presentation.

Each trial started with the presentation of a cue word in white (800ms; Arial; lower case). Cues either predicted a stimulus appearance above (’oben’; 3.38° x 1.25°) or below fixation (‘unten’; 3.75° x 1.2°) or did not display relevant information (‘xxxx’; 3.2° x 0.9°). Next, a smoothed fixation point (1.23° x 1.23°) appeared for a jittered interstimulus interval (ISI, EEG: 950 ±150ms; fMRI: 1400 ±200ms), followed by the presentation of the target letter string (1000ms). The stimulus array appeared in red or green above or below fixation (Arial; upper case; 2.4° from fixation point to center of stimulus) and was either a string of ‘HHHHH’ (8.45° x 1.88°), ‘SSSSS’ (7.8° x 1.93°), ‘SSHSS’ (8.01° x 1.93°) or ‘HHSHH’ (8.28° x 1.93°). Each trial ended with the reappearance of the fixation point for a jittered intertrial interval (ITI, EEG: 950 ±150ms; fMRI: 1500 ±200ms).

Participants were instructed to make use of the cue information and to direct their attention covertly (without eye movements) to the corresponding location (experiment I) or color (experiment II). They responded manually to the central letter with their right index and middle fingers with stimulus-finger mapping counterbalanced across participants.

Experimental measurements with fMRI and EEG took place on two separate days. Half of the male and half of the female participants first took part in the EEG session followed by the fMRI session and vice versa. The order of experimental runs was counterbalanced across participants.

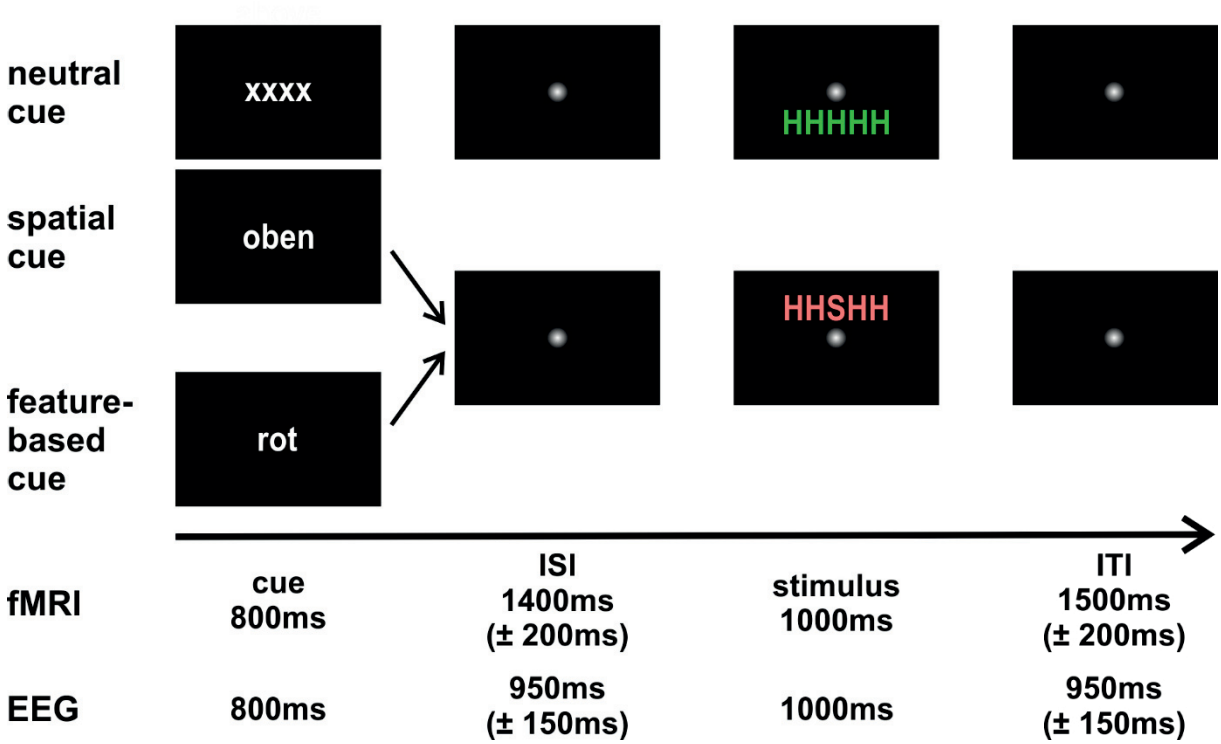

Figure 2: Sample trials showing neutrally (top) and validly cued trials (middle: experiment I; bottom: experiment II). A trial started with cue presentation (experiment I = location; experiment II = color). After a jittered ISI (interstimulus interval) displaying a smoothed fixation point, the stimulus was presented above or below fixation in red or green. Participants responded to the central letter (H or S) with a right-hand click on the respective button. At the end, the fixation point was presented for a jittered ITI (intertrial interval).

2.5.2 Data acquisition

Training and EEG data acquisition

Training and experimental sessions took place in a dimly lit room where participants sat on a height adjustable chair in front of the computer screen. They positioned their heads on a chin and forehead rest to ensure a fixed distance (55cm) from a 19-inch computer monitor (Belṅea 1970 S1). Stimuli were presented using Presentation®-Software (Neurobehavioral Systems; https://nbs.neuro-bs.com). During all sessions, an in-house developed (MRI compatible) eye-tracking device allowed monitoring of eye movements to ensure that participants continued to fixate the center throughout the experiment.

EEG data were recorded from 64 channels (Neurofax μ EEG 9110; Nihon Kohden Systems; Tokyo, Japan) with the recording program eemagine EEG 3.3 (Medical Imaging Solutions GmbH; Berlin, Germany). The REFA® multichannel system (TMS International; Oldenzaal, Netherlands; www.tmsi.com) served as a direct-coupled (DC) amplifier (sampling rate: 512 Hz; average-reference; impedances≤10kΩ). An array of 64 Ag/AgCl head electrodes was arranged according to the extended international 10-20 system using a standard elastic cap (Fp1, Fp2, AF7, AF3, AFz, AF4, AF8, F7, F5, F3, F1, Fz, F2, F4, F6, F8, FT7, FC5, FC3, FC1, FCz, FC2, FC4, FC6, FT8, T7, C5, C3, C1, Cz, C2, C4, C6, T8, TP9, TP7, CP5, CP3, CP1, CPz, CP2, CP4, CP6, TP8, TP10, P7, P5, P3, P1, Pz, P2, P4, P6, P8, O1, Oz, O2, PO9, PO7, PO3, POz, PO4, PO8, PO10; EASYCAP, www.easycap.de, Herrsching–Breitbrunn, Germany;). The ground electrode was placed at the left mouth angle and four additional electrodes (infra- and supraorbitally and at the outer canthi) were used for recording of an electrooculogram (EOG).

(f)MRI data acquisition

MRI measurements were conducted on a 3 Tesla Siemens Skyra® whole body scanner using a 20 channel head coil. Participants lay on a scanner couch inside the tube of the MRI scanner. The room was dimly lit and participants wore foam earplugs. Stimuli were presented with Presentation® Software (Neurobehavioral Systems; https://nbs.neuro-bs.com) on a computer connected to a JVC video projector (distance to projection area: 140cm). Participants watched the stimulation via a mirror attached to the head coil and gave manual responses on an MRI-compatible computer mouse.

Functional scans were obtained via T2* echo-planar imaging (EPI) sequences to derive BOLD signals (TR= 2210ms; TE= 30ms; flip angle= 81°; matrix= 64*64; FOV=192*192; voxel size= $3mm^3$; 41 slices; no gap; ascending acquisition order). There were five functional runs, each covering 163 volumes (approx. six minutes). To investigate activity during color processing, two color localizers were additionally acquired after the main experiments. In both localizers,

four chromatic blocks were interleaved with four achromatic blocks, each lasting approximately 20s (see Appendix B). These were separated by baseline epochs of 10s in which the fixation point was shown. During the first localizer, the letter array from the experimental runs was presented in various colors (chromatic blocks) or shades of grey that were isoluminant with the single colors of the chromatic blocks (achromatic blocks). The letters rapidly (8Hz) switched between the positions used in the experiment (above/below fixation). During the second localizer, a checkerboard was shown that covered the entire screen. It also switched between colors (chromatic) or shades of grey (achromatic) at 8Hz. Each measurement included 143 volumes (TR= 1800ms; 33 slices; approx. four minutes), and a short (5 volumes) functional whole-brain scan was recorded for coregistration purposes of the functional localizer scans. To acquire an anatomical scan, a T1-weighted MPRAGE sequence was applied (TR=1900ms; TE=2.07ms; TI=900ms; flip angle= 9°; FOV= 256*256; voxel size= $1mm^3$; 176 slices; approx. 4 minutes acquisition time).

3. EXPERIMENT I: SPATIAL CUEING IN THE FLANKER TASK

3.1 Introduction

The present study investigated the influence of spatially focused attention on processing of CON and INC flanker stimuli. To operationalize this purpose, the letter flanker task was modified by presenting the stimulus array above or below fixation and instructing participants to attend to one of the two possible locations. Spatial cues directed attention on a trial-by-trial basis and were valid or invalid (equiprobable). In addition, neutral cues could occur containing no spatial information. Parameters of interest were the spatial and temporal information of the fMRI and ERP signals respectively. The experiment focused on the question whether areas known to be involved in processing mechanisms during interference processing would show validity-specific modulations and whether the conflict-related N200 ERP component would be sensitive to differences between validity-levels. In addition, a source analysis of the ERP waveforms based on coordinates from fMRI was computed.

3.1.1 Neuronal mechanisms of flanker processing

Numerous fMRI studies on flanker processing show overlapping activation clusters in ACC and prefrontal regions (see e.g. Fan et al., 2007; van Veen et al., 2001; Wei et al., 2013). Of these, ACC has become a major region of interest regarding conflict processing in the flanker and several other conflict tasks. Botvinick and colleagues (2001) proposed a *conflict monitoring theory* centered on the ACC, which deals with the recruitment of control in response to conflict. The theory assumes that control processes must be initialized in response to conflict, optimized when control demands change, and withdrawn when no longer needed (Botvinick et al., 2001). The theory assumes that ACC detects conflict between simultaneously active streams of information and subsequently initializes control. Accordingly, many cognitive operations

appear to elicit ACC activation, including response inhibition, error commission, and divided attention (Botvinick et al., 2001). Several computational models (Botvinick et al., 2001; Yeung et al., 2004) account for ACC activation in face of conflict and established its role in conflict monitoring. Interestingly, conflict monitoring theory also correctly predicts that correct conflict trials and error trials recruit ACC (Botvinick et al., 2004). As a complementary finding, the corresponding ERP components (N200 and error-related negativity) have presumed neuronal generators in ACC (Bocquillon et al., 2014; Van Veen & Carter, 2002).

Despite the ubiquity of ACC activation in conflict tasks, a meta-analysis demonstrates low consistencies between flanker tasks (Nee et al., 2007). Only two structures were reliably active across six flanker studies. These were right dorsolateral prefrontal cortex and right insula. Another meta-analysis investigating executive functions in general found a large network of regions overlapping between diverse conflict tasks, encompassing frontal and parietal regions and ACC (Niendam et al., 2012). However, this was primarily due to Stroop and Go/nogo studies, which mainly involve SR-conflict (Stroop task) and response inhibition (Go/nogo task) whereas the flanker task constitutes a SS conflict task.

Several other regions may also contribute to flanker task processing, including parts of the frontal and parietal cortices (Fan et al., 2003; Fan et al., 2008; Ullsperger & von Cramon, 2001). These findings are in line with suggestions of an executive control network comprising frontal, parietal and cingulate cortex (Corbetta & Shulman, 2002; Dosenbach et al., 2008; Petersen & Posner, 2012). Accordingly, regions in this network yielded overlapping activation clusters in various executive function tasks (Niendam et al., 2012). While frontal parts seem to contribute to top-down control processes, possibly through connections with motor cortices, parietal cortex may respond to bottom-up factors such as stimulus saliency (Niendam et al., 2012).

3.1.2 Temporal characteristics of flanker processing

Investigations of flanker conflict processing using EEG have consistently shown a modulation by target-flanker congruency peaking between 250ms and 350ms at frontocentral sites (Larson et al., 2014). In the literature, a negative-going deflection at this latency is termed N200 or N2, apparently incorporating several independent subcomponents (Folstein & Van Petten, 2008; Larson et al., 2014). The N200 is sensitive to various experimental manipulations including novelty induced by low-probability targets, mismatches between expected and actually presented stimuli, and the need to inhibit a response (Folstein & Van Petten, 2008). In addition, its scalp topography is context-specific, leading to overlapping N200 effects within some experiment. Thus, in an oddball task where participants must respond to rare target stimuli, a posterior N200 responds to targets only, whereas a frontocentral N200 is generally larger for non-targets but also responds to stimulus novelty irrespective of targetness (Folstein & Van Petten, 2008).

Several suggestions have emerged regarding the underlying mechanisms of the N200-family. Suwazono and colleagues (2000) found a larger anterior N200 in response to rare cues which predicted subsequent targets. The authors suggest a link between anterior N200 and alerting mechanisms rather than a low-level perceptual mismatch response. The posterior N200 meanwhile appears to be target-specific and stronger contralateral to the hemifield of target presentation. The posterior N200 therefore seems to reflect attentional processes (Suwazono et al., 2000) that serve to decrease distractor processing (Luck & Hillyard, 1994).

Another class of N200 components is elicited by response inhibition, e.g. in go/nogo and flanker tasks. Even though all of these tasks require response inhibition, there is disagreement about the underlying mechanism of this N200 subcomponent. In go/nogo tasks, higher N200 amplitudes on nogo trials go along with better performance, suggesting a role in inhibition (Folstein & Van Petten, 2008). However, in the flanker task a frontally distributed N200 is

sensitive to stimulus probability (Bartholow et al., 2005) and larger for INC than congruent stimuli. The anterior N200 may therefore be a sign of control signaling rather than of response inhibition (Folstein & Van Petten, 2008).

A frontocentrally distributed N200 was also found to be larger for response-incongruent than stimulus-incongruent stimuli, despite equal levels of perceptual mismatch (Van Veen & Carter, 2002). Therefore, it appears to be distinct from the previously mentioned perceptual mismatch or novelty N200 (Van Veen & Carter, 2002). Nieuwenhuis and Yeung (2003) found both the flanker N200 latency and amplitude to correlate positively with RTs, suggesting that the flanker N200 reflects conflict processing. In keeping with this finding, the neuronal generator of the flanker N200 is located in the medial frontal gyrus, which is associated with conflict detection mechanisms (Van Veen & Carter, 2002).

Additional evidence for control-related mechanisms of anterior N200 comes from studies showing increased amplitudes when INC flankers occur in close proximity to the target (Danielmeier et al., 2009). Moreover, Yeung et al. (2007) found no relation between perceptual flanker properties and N200 amplitude when varying flanker brightness. These data might show that the N200 amplitude is related to the strength of attention directed on the flankers (Larson et al., 2014).

3.1.3 Objectives of experiment I

In experiment I, spatial visual selective attention was combined with an interference task. Spatial cues predicted the location of flanker stimuli either correctly (valid cueing) or incorrectly (invalid cueing) or contained no predictive value (neutral cueing). To inform about the spatio-temporal dynamics, fMRI and EEG data were collected and analyzed in an fMRI-constrained source analysis.

Previous studies could show that top-down control and bottom-up reactions recruit partly overlapping brain regions of the dorsal and ventral frontoparietal networks (Macaluso &

Doricchi, 2013). Based on these observations, activation patterns in the present study should differ between validly and invalidly cued flanker interference, because the first facilitates stimulus processing at the attended location, whereas the latter leads to shifts of attention from the attended location to the position containing the target stimulus (Posner, 1980; Posner & Petersen, 1990). On a behavioral level, an interaction of the factors *cue validity* and *flanker congruency* was expected following previous reports of reduced interference effects with focused spatial attention (McCarley & Mounts, 2008; Yantis & Johnston, 1990). Such interactions are ascribable to the simultaneous processing of two operations (here: selective attention and interference control) at one processing stage (see Sternberg, 1966). On a temporal level, the N200 component was therefore assumed to show differential influences of flanker congruency (INC > CON) depending on cue validity levels.

3.2 Material and methods

3.2.1 Study participants

EEG and MRI data were collected from 20 healthy and right-handed (median = 100%; range = 84.6% - 100% according to the Edinburgh Inventory; Oldfield, 1971) volunteers (10 male; mean age = 25.6 years; standard deviation (SD) = 4.7) with normal or corrected-to-normal vision. No participant showed signs of color-blindness according to a modified version of the Ishihara Test (Ishihara, 1917) including the colors used in the present experiment (see Appendix C). Every participant took part in a training session, an EEG experiment, and an MRI experiment on separate days (time between EEG and fMRI sessions: median = 2 days; range = 1 – 14). Artifacts and low behavioral performance led to the exclusion of one data set from both fMRI and ERP analyses. Another data set was excluded from ERP and source analysis due to an insufficient amount of trials remaining after trial rejection.

3.2.2 Data protection, data security, and legal framework

The study protocol of both experiments reported here (I and II) was in line with the Helsinki Declaration of the World Medical Association (Rickham, 1964) and approved by the local ethics committee of the University of Bremen (see Appendix D). Participants were informed about data collection, data protection, and data security of all experimental and personal data, including the pseudonymization procedure. The potential risk factors of the MRI scanner were highlighted and no participant was measured who showed one or more of the exclusion criteria (see Appendix E). Based on this procedure, all participants gave written and informed consent before participating in the study (see Appendices F and G) and they were allowed to quit the experiment at any time without giving reasons. All participants received 30€ or were given course credits.

3.2.3 Data analysis

3.2.3.1 Behavioral data analysis

Behavioral data were analyzed with the software SPSS (Version 11.5, SPSS Incorporation, Chicago, USA). Only correct trials were included in the analysis of reaction times (RTs) and participants with an average accuracy below 75% were excluded to correct for extreme values (one data set). RTs were investigated using a repeated-measures analysis of variance (ANOVA) with factors *method (EEG/fMRI) x cue validity (valid/neutral/invalid) x flanker congruency (CON/INC)*. Error rates (percentage of incorrect trials and misses per condition) were analyzed using Friedman tests. The significance level was set α=0.05 for all behavioral and electrophysiological analyses. Greenhouse Geisser corrected epsilon values are reported if the assumption of sphericity was violated (Mauchly´s Test). Significant effects were further investigated using post hoc paired t-tests (with Bonferroni-Holm correction when required) and Wilcoxon tests for RTs and error rates respectively.

3.2.3.2 (f)MRI data analysis

Preprocessing of the (f)MRI data with the software 'Statistical Parametric Mapping' (version SPM8, SPM®; Wellcome Trust Centre for Neuroimaging, London, UK, http://www.fil.ion.ucl.ac.uk/spm/software/) included the following pipeline: Functional data were spatially realigned to the 10^{th} volume of the first run with 4^{th} degree B-Spline interpolation and six parameter rigid-body transformation (reslice option: mean image). Thereafter, the data were temporally resliced to the middle slice acquired after half the TR (slice 21). Structural data analysis involved reorientation and segmentation into grey matter, white matter, and cerebrospinal fluid. Functional data were co-registered to the anatomical data with the T1 as reference image and the resliced mean functional image as source image. Normalization to the standard MNI space of both functional and structural images was performed with 4^{th} degree B-Spline interpolation and standard resampling to 2 mm^3 isotropic voxels. Smoothing of the functional images involved an 8mm full width at half maximum (FWHM) Gaussian kernel. To

account for serial correlations, an autoregressive AR(1) model was used. Low frequency drifts were removed using the standard high-pass filter of 128s.

A fixed-effects analysis was performed on the individual data with the correct trials of all six conditions and the cue period, the ISI and the ITI as separate regressors, which were modeled as events using the canonical hemodynamic response function (Della-Maggiore et al., 2002). To account for motion artifacts, the six motion parameters (rotation and translation along x- y- and z direction, (Johnstone et al., 2006)) were used as regressors of no interest. Group-specific activation based on the single-subject contrasts of 19 participants was analyzed with a random-effects analysis using a full factorial design with the factors *cue validity (valid/neutral/invalid)* and *congruency (CON/INC)*. Post hoc paired t-tests were performed on the INC > CON contrast pooled over cue validity levels and separately for each cue validity level. For all contrasts, the significance threshold was set to $p<.001$ (uncorrected) with an extent threshold of $k\geq10$ voxels.

The MNI coordinates of all peaks and sub-peaks were transformed into Talairach space (‘mni2tal.m’; http://imaging.mrc-cbu.cam.ac.uk/imaging/MniTalairach) and their anatomical locations were derived from the ‘Talairach Daemon Client’ software (http:// http://www.talairach.org/daemon.html) and the automated anatomical labeling toolbox (‘AAL‘; http://www.gin.cnrs.fr/AAL-217?lang=en).

3.2.3.3 ERP data analysis

EEG data were filtered (high-pass filter 0.05; Notch filter 50Hz) and analyzed with BESA® 6.0 (Brain Electrical Source Analysis; MEGIS Software GmbH, Munich, Germany). After visual inspection of every channel electrodes were interpolated (spherical spline interpolation; mean = 2 channels ±2, maximum = 5 channels) or defined as bad (mean = 1 channel ±1, maximum = 3 channels) when necessary. EEG epochs of correct trials were averaged stimulus-locked from -200ms to 900ms. This procedure resulted in a mean of 76 trials (60-90 trials) per condition and participant which were distributed over the whole length of the experiment, resulting in equal

numbers of trials between conditions throughout the sample. Trials with eye blinks, excessive eye movements or muscle activity were manually excluded from further analyses during averaging. From the whole data set (N=20), data of two participants had to be excluded (low behavioral performance; high level of noise and eye blinks).

To analyze the N200 component, mean amplitude values were extracted in five consecutive time windows of 20ms between 200ms and 300ms post-stimulus from electrodes F3, Fz, F4, C3, Cz, C4, P3, Pz, P4, PO7, POz and PO8. Within these windows, separate repeated-measures ANOVAs with the factors *cue validity (valid/neutral/invalid)* x *flanker congruency (CON/INC)* x *frontality (F/C/P/PO)* x *laterality (left/midline/right)* were conducted using SPSS (Version 21.0. Armonk, NY: IBM Corp). Post hoc paired t-tests were computed for significant main and interaction effects using Bonferroni-Holm corrected threshold values.

3.2.3.4 fMRI-constrained source analysis

In the fMRI constrained source analysis, the seed points were derived from activation clusters of the MRI data obtained from the same individuals in the same task as in the EEG experiment. For this end, two fMRI contrasts were computed based on a second level fMRI analysis including the six conditions (single subject level) contrasted against the fixation point (ITI). The contrasts used were the conjunction analyses (see Nichols et al., 2005) of the CON and INC conditions pooled over validity levels. A liberal threshold of $p<.005$ uncorrected and an extent threshold of $k\geq10$ voxels was applied in order to obtain all relevant sources. Application of these criteria resulted in 31 distinct peak coordinates. The MNI coordinates of all peaks and subpeaks of the two conjunctions were transformed into Talairach space (‘mni2tal.m’;http:// imaging.mrc-cbu.cam.ac.uk/downloads/MNI2tal/) and subsequently clustered using a nearest-neighbor approach: First, the distance (root mean square of the x-, y- and z-coordinates) between each pair of coordinates was computed to identify the nearest neighbors (minimal distance compared to the distance to all other coordinates). For distances below the minimal

distance criterion of 30mm (e.g. Miedl et al., 2014), the coordinates were averaged (arithmetic mean). This was done for all coordinates and further for all derived coordinates meeting these criteria until all peaks and derived peaks were at least 30mm apart from each other. The maximally allowed distance between the derived coordinates and their original peaks was 25mm. This procedure resulted in a set of ten distinct Regional Sources (RSs). One of these was situated in the left cerebellum. According to Luck (2005a), EEG rarely takes up cerebellar activity due to the dense folding of the cerebellar cortex, which leads to cancelling of the signal. Therefore, the cerebellar RS was excluded from the source model.

The grand average of the ERP data over all conditions and 18 participants was computed and interpolated (spherical spline interpolation) from the recorded 64 electrodes to a standard configuration of 81 electrodes using BESA® 6.0 (MEGIS Software GmbH, Munich, Germany). This montage was transformed into Talairach space using the Brain Voyager QX software package (Brain Innovation, Maastricht, The Netherlands) in order to guarantee that both data sets (ERP and fMRI) were in the same coordinate system. This required fitting of the 81 electrode positions and three fiducial points (nasion; left and right preauricular points) to the head surface of the Talairach template. Afterwards, the clustered fMRI sources were assigned as RSs to this grand average using the source analysis function embedded in BESA® 6.0 (MEGIS Software GmbH, Munich, Germany). Each RS is composed of three equivalent current dipoles, which are orthogonal to each other (Scherg & Von Cramon, 1986; Scherg, 1990). The source sensitivity of each RS was reviewed using BESA® 6.0 (Brain Electrical Source Analysis; MEGIS Software GmbH, Munich, Germany) in order to ensure that the single RSs primarily reflected activity arising from the respective location and not from neighboring RSs (see Appendix H for the single source sensitivity plots). The resulting source model was applied to the individual ERP data. To analyze the differences between source waveforms of INC and CON trials within each cue validity level, BCa bootstrap 95%-confidence intervals (Efron &

Tibshirani, 1993) were computed on the root mean square (RMS) of all three dipoles per RS. Only epochs of ≥20ms were considered to reflect meaningful differences between conditions.

3.3 Results

3.3.1 Behavioral data

Table 1 summarizes RTs and error rates across all conditions for both the EEG and the fMRI session. One data set exceeded the maximum criterion of erroneous trials (>25%) and was therefore excluded from further analyses. The remaining 19 data sets were analyzed using a repeated-measures ANOVA with the within-subject factors *method (EEG/fMRI)* x *cue validity (valid/neutral/invalid)* x *flanker congruency (CON/INC).* There were significant main effects of *cue validity* ($F_{[1.2;20.7]} = 17.8$, $p < .001$), *flanker congruency* ($F_{[1;18]} = 93.2$, $p < .001$), and *method* ($F_{[1;18]} = 82.8$, $p < .001$). Post hoc testing on the *cue validity* factor yielded significantly faster RTs for valid trials than for neutral ($t_{[18]} = -3.8$, $p < .005$) and invalid trials ($t_{[18]} = -4.4$, $p < .001$). In addition, invalid cueing resulted in significantly increased RTs compared to neutral cueing ($t_{[18]} = 4.1$, $p < .005$). Furthermore there was a congruency effect with significantly higher RTs for INC compared to CON stimuli ($t_{[18]} = -9.7$, $p < .001$; see Figures 3 and 4). Additionally, RTs were found to be generally faster during EEG measurements compared to MRI sessions ($t_{[18]} = -9.1$, $p < .001$).

Table 1: Summary of the mean reaction times (RTs) and error rates (top and bottom respectively) with standard deviations (SD) of the six conditions during the EEG (left) and the fMRI session (right). N = 19.

		EEG			fMRI		
	condition	**congruent**	**incongruent**	**total EEG**	**congruent**	**incongruent**	**total fMRI**
RTs [ms] ± SD	**valid**	488.8 ± 76.3	527.5 ± 73.9		548.3 ± 70.8	589.8 ± 74.4	
	neutral	502.4 ± 85.9	544.9 ± 76	520.8	570.1 ± 75.8	605.6 ± 76.7	581.5
	invalid	523.5 ± 92.7	565.2 ± 83.6		583.3 ± 74.4	622.6 ± 67.9	
error rates [%] ± SD	**valid**	3.6 ± 2.7	6.3 ± 4.3		3.7 ± 4	5.5 ± 5.8	
	neutral	2.6 ± 2.4	6.1 ± 3.7	5.7	3.1 ± 3.8	4.2 ± 3.3	4.8
	invalid	4.7 ± 3.1	5.9 ± 3.4		2.7 ± 2.9	4.6 ± 4.7	

Analysis of error rates with the factors *method* x *cue validity* x *congruency* yielded significant differences (Friedman test: $\chi_{[11]} = 52.7$, $p < .001$). Post hoc Wilcoxon tests demonstrated a significant *congruency* effect ($Z = -3.7$; $p<.001$) with more errors on INC than CON trials. The

factor *method* also showed significant differences (Z= -2.4; p<.05) due to higher error rates during EEG measurements.

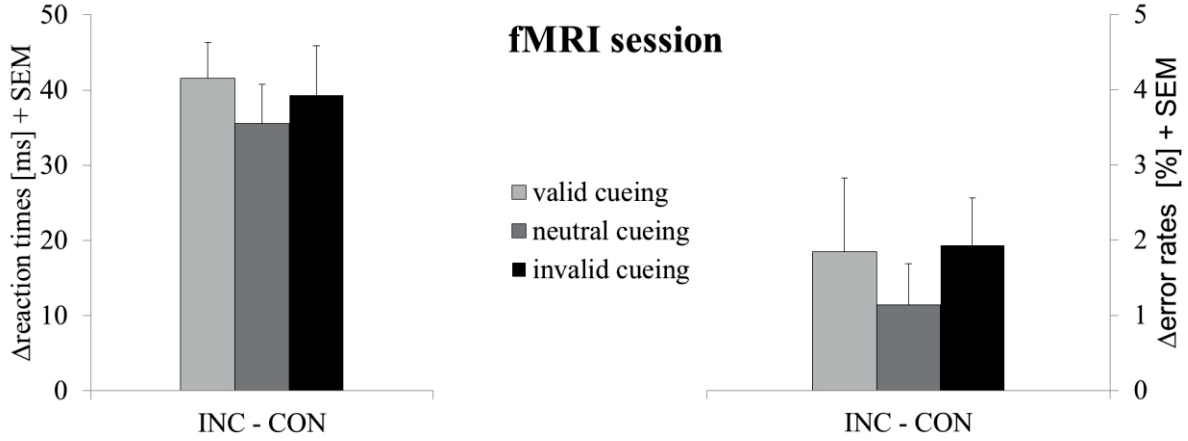

Figure 3: fMRI session: Differences (Δ) of the reaction times (left) and percent error rates (right) between incongruent (INC) and congruent (CON) flanker conditions during valid (light grey), neutral (medium grey), and invalid cueing (black). Error bars show standard error of the mean (SEM). N = 19.

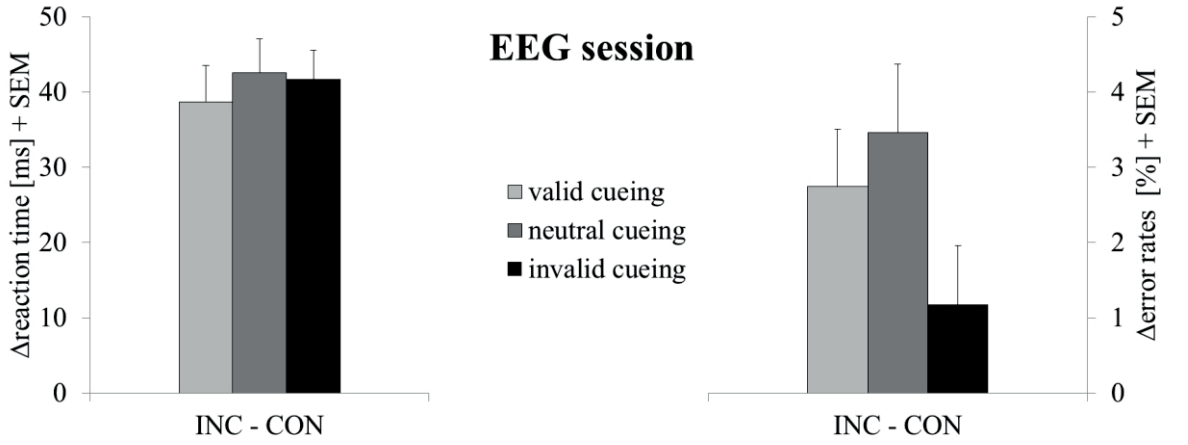

Figure 4: EEG session: Differences (Δ) of the reaction times (left) and percent error rates (right) between incongruent (INC) and congruent (CON) flanker conditions during valid (light grey), neutral (medium grey), and invalid cueing (black). Error bars show standard error of the mean (SEM). N = 19.

3.3.2 fMRI data

Analysis of the fMRI data showed significant activation clusters for the contrast INC > CON located in left middle frontal gyrus (MFG) and precuneus (see Table 2 and Figure 5). Post hoc analyses of the congruency effect separately for each cue validity level revealed several activation foci for the difference between INC and CON when attentional cueing was valid,

including bilateral SPL/precuneus, left superior frontal gyrus (SFG), superior temporal gyrus (STG), inferior occipital gyrus (IOG), and MFG, as well as right middle temporal gyrus (MTG). There were no supra-threshold clusters for the INC > CON contrast with invalid or neutral cueing.

Table 2: Talairach peak coordinates of significant activation clusters for the comparison of incongruent (INC) and congruent (CON) flanker conditions pooled over validity levels (top) and during valid cueing (bottom; p<.001, k≥10 voxels). BA = Brodmann area; L = left; r = range of nearest grey matter (mm); R = right. N = 19.

contrast	cluster size	t-value	r	peak coordinates (Talairach space)			side	anatomical region (BA)
INC > CON (all validities)	35	3.7	1	-24	-56	49	L	Precuneus (7)
	16	3.6	2	-26	-8	41	L	Middle Frontal Gyrus (6, 2)
INC> CON (valid cues)	85	4.4	1	-24	-58	53	L	Precuneus (7)
	127	4.2	1	22	-61	55	R	Superior Parietal Lobule (7)
	28	3.9	5	50	-37	-5	R	Middle Temporal Gyrus
	54	3.9	2	-44	-70	-7	L	Inferior Occipital Gyrus (19)
	40	3.7	3	-18	58	-5	L	Superior Frontal Gyrus (10)
	10	3.5	4	-40	-48	13	L	Superior Temporal Gyrus (39)
	14	3.5	0	-16	-69	51	L	Precuneus (7)
	11	3.4	0	-24	-4	43	L	Middle Frontal Gyrus (6)

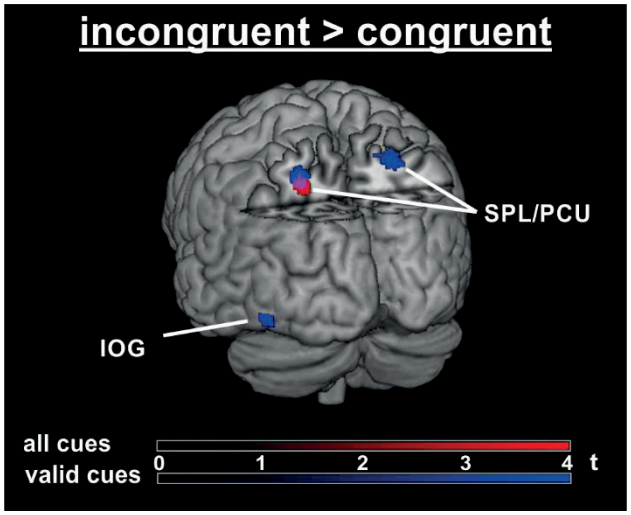

Figure 5: Overlay of activation clusters derived from the contrast incongruent > congruent pooled over all cue validity levels (red) and for valid cueing only (blue) thresholded at p<.001, k≥10. N = 19.

Labels:
IOG = inferior occipital gyrus
PCU = precuneus
SPL = superior parietal lobule

3.3.3 ERP data

To analyze the N200 component, the mean amplitude values of INC and CON trials of each cue validity level were examined between 200-300ms. For this purpose, separate repeated-measures ANOVAs with the factors *frontality (F/C/P/PO)* x *laterality (left/midline/right)* x *cue*

validity (valid/neutral/invalid) x *flanker congruency (CON/INC)* were computed in consecutive time bins of 20ms each. In general, the comparison between INC and CON was characterized by an early relative negativity of INC stimuli at bilateral parietooccipital electrode sites. In addition, there was a simultaneous frontocentral positivity.

These analyses revealed an interaction of the factors *congruency* and *cue validity* between 200-220ms ($F_{[2;\ 34]}$ = 3.4, p < .05). Post hoc paired t-tests showed that INC stimuli resulted in significantly more positive amplitude values than CON stimuli ($t_{[17]}$ = -3.3; p<.01), and that this effect was significant for validly cued trials only ($t_{[17]}$ = -3.1; p<.01). Moreover, there were four-way interactions of all factors (*frontality* x *laterality* x *cue validity* x *congruency*) in the time windows between 240ms-260ms ($F_{[12;\ 204]}$ = 2.7; p<.005) and 280ms-300ms ($F_{[5.1;\ 86.1]}$ = 2.4; p<.05; see Figure 6 and Appendix I1 – I3).

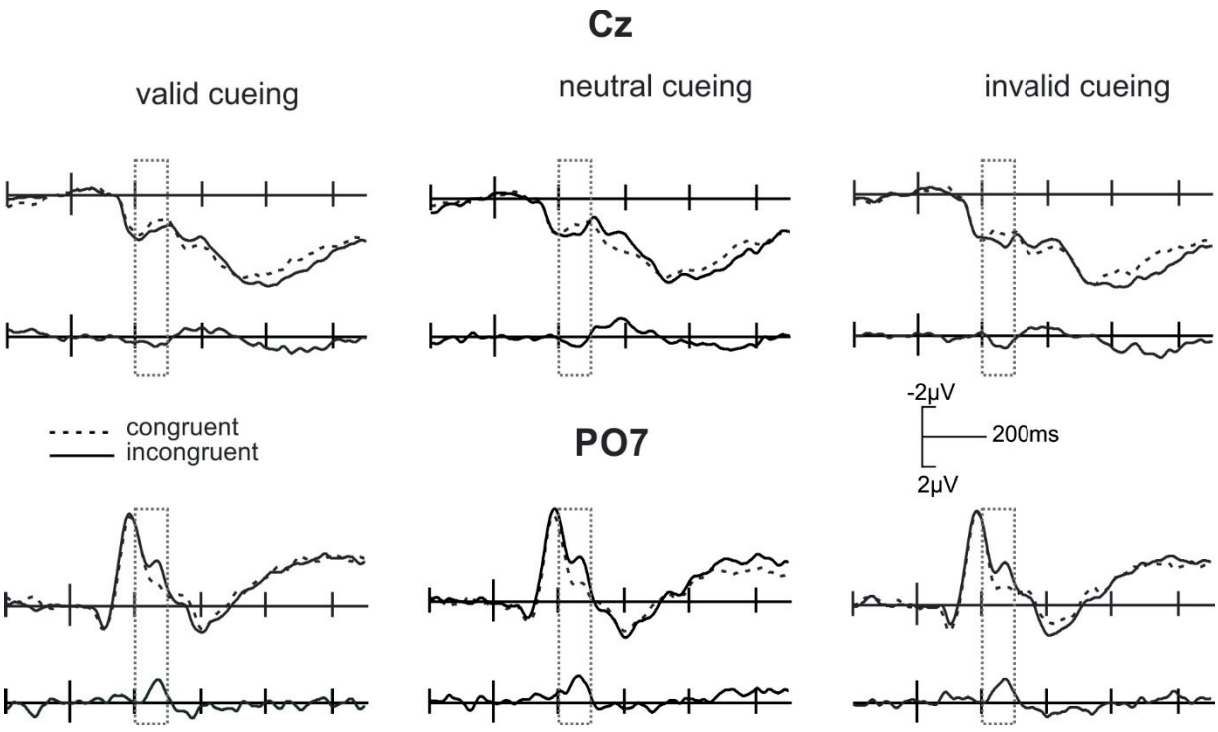

Figure 6: Group ERPs and difference waves during flanker processing at electrodes Cz and PO7: ERPs (stimulus-locked grand average: -200ms to 900ms) of congruent and incongruent conditions with valid (left), neutral (center) and invalid (right) cueing; difference waves (incongruent > congruent) are plotted below the grand averages. Boxes indicate the analyzed N200 time window. N = 18.

Post hoc analyses showed that between 240-260ms the *congruency* manipulation was significant with invalid cueing at electrodes C3 ($t_{[17]}$ = -5.6; p<.001) and PO7 ($t_{[17]}$ = 4.1; p<.005), and with neutral cueing at electrode PO7 ($t_{[17]}$ = 4.4; p<.001). From 280-300ms, the

difference between INC and CON stimuli with invalid cueing was significant at electrode C3 ($t_{[17]} = -4.1$; $p<.005$). No other post hoc tests at the single electrode positions yielded significant results.

3.3.4 fMRI-constrained source analysis

3.3.4.1 Clustering of fMRI peak coordinates

Talairach coordinates used for the source analysis were derived as described in section 2.4 and following Bledowski and colleagues (2006). The clustering method resulted in 10 RSs located in precuneus, ACC, insula, cerebellum, MTG, and precentral gyrus (two RSs) of the left hemisphere and in inferior frontal gyrus (IFG), IPL, and parahippocampal gyrus (PHG) of the right hemisphere (see Table 3). One of the sources located in the left precentral gyrus was derived from several averaged peaks located in IFG, pre- and postcentral gyri, and insula. Because the coordinates were similar to those of the RS in the right IFG (distance = 20.3mm from an IFG location with homologous coordinates in the left hemisphere), it was considered to reflect activity originating in the left IFG, comparable to the source in the right IFG.

Given that the cerebellar cortex consists of highly folded gyri, it is unlikely that activity generated in the cerebellum reaches the scalp as a recordable voltage difference (Luck, 2005a). Accordingly, the cerebellar RS explained <0.5% of the overall variance. Therefore, the cerebellar RS was excluded from the source model (see e.g. Galashan et al., 2015).

A Principle Component Analysis (PCA) of the residual signal (BESA®) that remained after seeding of the nine fMRI-constrained RSs yielded one principle component explaining 2.8% of the residual variance between 50ms and 150ms. This component presumably reflects perceptual processing of the visual stimulus properties. Therefore, two further RSs were added to account for early visual processing. Hence, between 50ms and 150ms the additional RSs were fitted symmetric to each other to account for the fact that visual information is processed in both hemispheres when presented to both visual hemifields (Engel et al., 1997). The procedure

resulted in RSs in the bilateral lingual gyri (BA18), which are related to processing of visual information and of letters in particular (Mechelli et al., 2000).

Table 3: Left: Talairach peak coordinates of significant activation clusters when contrasting all congruent trials against the ITI (CON) and all incongruent trials against the ITI (INC) pooled over validity levels respectively (p<.005, k≥10). Right: Labels of regional sources and their locations in Talairach space, resulting from averaging of the corresponding peak coordinates on the left side that were within a distance of 30mm to each other. RSs in italics were not included in the final source model. BA = Brodmann area; conj = conjunction; r = range of nearest grey matter (mm); RS = regional source; WM = white matter (no grey matter within 5mm distance. N = 18.

conj	anatomical region (BA)	r	peak coordinates (Talairach space)			RS region (BA)	RS coordinates (Talairach space)		
			X	Y	Z		X	Y	Z
CON	Inferior Frontal Gyrus (9)	1	-59	7	27				
INC	Precentral Gyrus (6)	0	-59	5	27				
CON	Postcentral Gyrus (4)	0	-57	-19	41				
INC	Postcentral Gyrus (2)	1	-57	-19	43	Precentral Gyrus (6)	-49	-11	24
CON	Insula (13)	0	-48	-22	20				
CON/INC	Insula (13)	1	-40	-3	11				
CON	Claustrum	1	-34	-19	8				
CON	Middle Occipital Gyrus (19)	2	-38	-64	9	WM (near middle temporal gyrus)	-34	-56	8
CON/INC	Parahippocampal (30)	5	-30	-48	6				
CON/INC	Culmen	0	-34	-40	-28	*Culmen*	*-34*	*-40*	*-28*
INC	Precentral Gyrus (6)	0	-34	-12	61	Precentral Gyrus (6)	-33	-12	62
CON	Precentral Gyrus (6)	0	-32	-12	63				
CON	Insula (13)	0	-32	14	10	Insula (13)	-31	14	10
INC	Insula (13)	1	-30	14	10				
INC	Inferior Parietal Lobule (7)	1	-32	-56	42	Precuneus (7)	-28	-51	48
INC	Sub-Gyral (7)	0	-24	-46	54				
INC	Anterior Cingulate (32)	1	-6	10	38	Anterior Cingulate (24)	-5	5	43
CON/INC	Medial Frontal Gyrus (6)	0	-4	-1	48				
CON/INC	Declive	0	22	-59	-14				
CON/INC	Parahippocampal (30)	2	22	-38	7				
CON/INC	Caudate (Tail)	4	22	-42	15	Parahippocampal Gyrus (37)	27	-46	-7
CON	Hippocampus	4	28	-45	2				
INC	Hippocampus	4	30	-45	2				
CON/INC	Culmen	0	34	-38	-27				
CON/INC	Insula (13)	3	40	2	2				
CON	Inferior Frontal Gyrus (9)	0	61	9	22	Inferior Frontal Gyrus (44)	54	7	16
INC	Inferior Frontal Gyrus (9)	0	61	9	25				
INC	Postcentral Gyrus (40)	0	46	-29	47				
CON	Postcentral Gyrus (40)	0	48	-31	48	Inferior Parietal Lobule (40)	53	-31	35
INC	Inferior Parietal Lobule (40)	0	59	-32	22				
CON	Inferior Parietal Lobule (40)	0	57	-32	24				
	RS fitted (no reference to original fMRI clusters)					Lingual Gyrus (18)	-27	-77	-7
	RS fitted (no reference to original fMRI clusters)					Lingual Gyrus (18)	26	-77	-7

With these RSs incorporated in the model, PCA demonstrated only components that explained less than 1% of variance. The model is therefore likely to be saturated, with a Goodness of Fit (=100% minus residual variance) of 99% ±0.6 for CON stimuli and 99% ±0.5 for INC stimuli.

As the residual variance explained by the second and third dipole of some RS contributed substantially to the overall variance in the model, the power (RMS) of all three dipoles was used for further analyses.

3.3.4.2 Source waveform data

BCa bootstrap 95%-confidence intervals (Efron & Tibshirani, 1993) were computed for the comparison of INC vs. CON stimuli separately for all three cue validity levels. These delivered various cue validity-specific differences for the comparison of INC and CON trials (see Figure 7 and Table 4 as well as Appendices J, K, and L).

The RS in left IFG was sensitive to stimulus congruency relatively late during stimulus processing irrespective of validity. Right IFG showed early congruency effects with neutral cueing and late effects on invalidly cued trials. The ACC RS demonstrated an early and a later phase of differences between INC and CON with invalid cueing. Late source waveform differences were also evident with valid cueing. The source in precentral gyrus contributed to source waveform differences depending on stimulus congruency both early (with invalid and neutral cueing) and later in the analyzed time window (valid and invalid cueing). The differences with neutral cueing were evident during the N200 time window. Early signal differences originating in right lingual gyrus were evident irrespective of the validity level. These intervals partially overlapped with the N200 time window, but the significant epoch did not meet the pre-defined minimal length (20ms) when cues were invalid. At later phases, both validly and invalidly cued trials demonstrated congruency effects in right lingual gyrus, and the left lingual gyrus source also yielded waveform differences on validly cued trials distributed over both early and late phases.

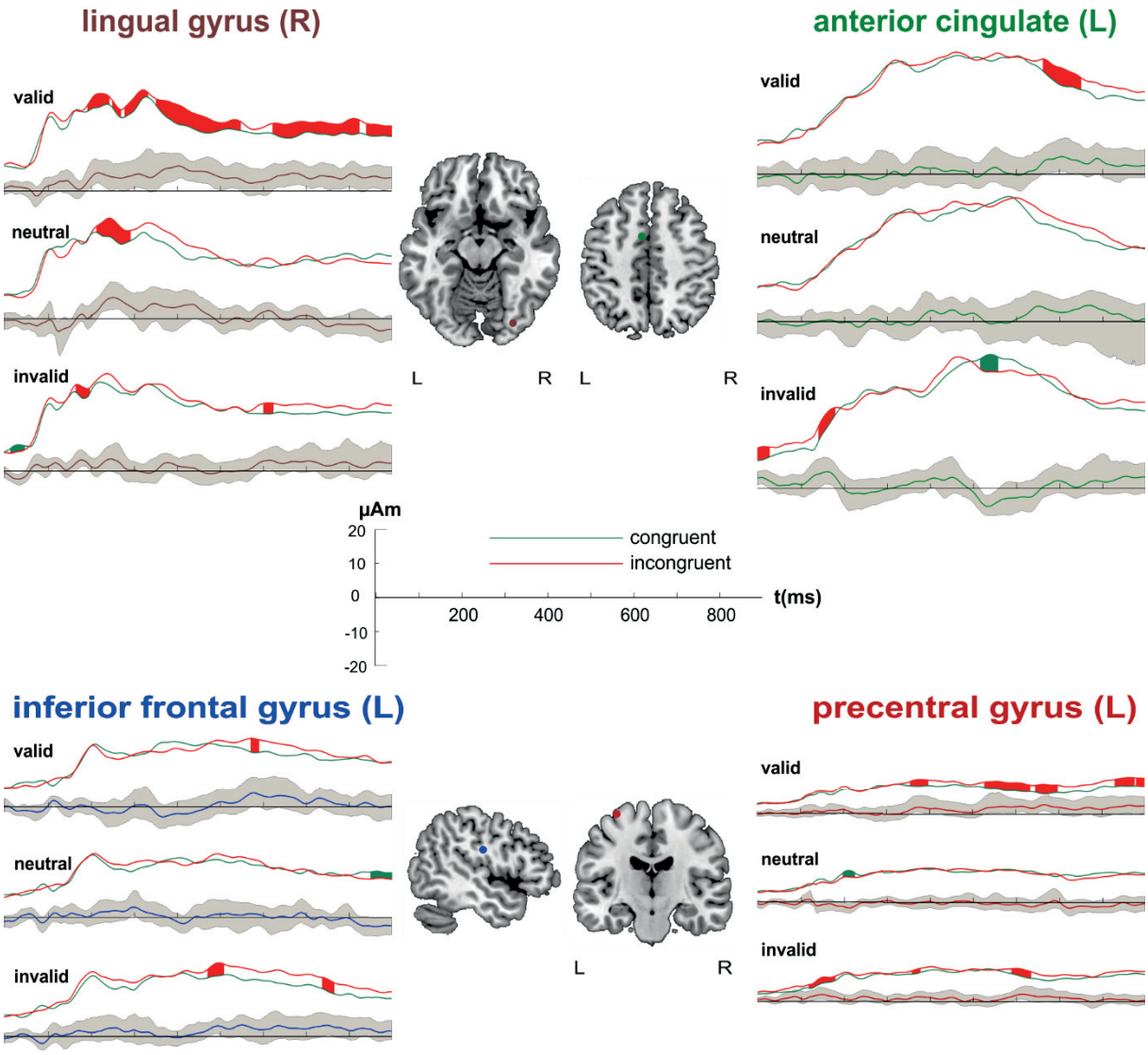

Figure 7: Group source waveforms and BCa bootstrap 95%-confidence intervals. Central column: positions of the regional sources in right lingual gyrus, left anterior cingulate gyrus, left inferior frontal gyrus, and left precentral gyrus projected onto the MNI brain. For each regional source, the corresponding root mean square source waveform time course is shown (0-900ms). Green source waveforms indicate congruent conditions, incongruent conditions are presented in red. Difference waves (incongruent > congruent) are depicted in the respective color of the regional source below the source waveforms. The grey area surrounding the difference waves represents the 95%-confidence interval. Epochs deviating from zero for a period of at least 20ms are presented in green (congruent > incongruent) and red (incongruent > congruent). L = left hemisphere; R = right hemisphere. N = 18.

Table 4: Significant time epochs (ms) in which the BCa bootstrap 95%-confidence interval for the difference between incongruent and congruent trials did not include zero for at least 20ms separately for each validity level (left = valid cueing; middle = neutral cueing; right = invalid cueing). N = 18.

Regional Source	valid cueing	neutral cueing	invalid cueing
left Inferior Frontal Gyrus	570-590	850 - 900	471-507 735-765
left Middle Frontal Gyrus	126-154 238-272 326-575 748-781		538-558 669-804
left Precentral Gyrus	355-402 527-633 645-698 828-876 879-900	193-224	116-179 357-385 588-634
left Insula		65-100 132-215	122-149 337-363 435-455
left Precuneus	105-135 229-301 503-690		324-372 404-484 752-827
left Anterior Cingulate Cortex	660-749		0-25 140-178 515-558
right Inferior Frontal Gyrus		64-150	604-670
right Inferior Parietal Lobule		78-110 414-475 685-713	114-136 505-531
right Parahippocampal Gyrus		439-479 505-705 715-791 816-900	109-131 157-181 364-404 424-631
left Lingual Gyrus	103-146 165-190 423-447 486-540		
right Lingual Gyrus	189-242 248-269 277-331 350-546 621-825 839-900	213-290	11-44 163-196 599-623

The RS in the precuneus showed congruency effects at early phases including the N200 component, but only with valid cueing. During later phases of stimulus processing, there were congruency effects irrespective of validity level. RSs in the insula and IPL yielded early differences with both invalid and neutral cueing, and later differences with invalid (insula and IPL) and neutral cueing (only IPL). Finally, there were early congruency effects with valid cueing in left MTG and with invalid cueing in right PHG. Additionally, amplitude differences were evident between INC and CON stimuli with valid and invalid cueing at later phases,

though with several consecutive intervals each <20ms on validly cued trials in right PHG. Neutral cueing also showed late congruency effects in right PHG.

3.4 Discussion

3.4.1 Behavioral data

The behavioral data analysis demonstrated significant RT effects with respect to *flanker congruency* (CON < INC), *cue validity* (valid < neutral < invalid) and *method* (EEG<fMRI). Longer RTs during fMRI sessions have been reported repeatedly and might be explained by slowed response execution in the MRI scanner (Fehr et al., 2014; Galashan et al., 2015; van Maanen et al., 2015). More errors were committed on INC compared to CON trials.

In contrast to expectations based on the literature, valid cueing of the target location did not reduce flanker interference. Comparing the present study design with past studies using cued interference tasks shows that there are several potential reasons for the present pattern of results. First, other studies usually used valid cues only and either contrasted them against neutrally cued trials (Correa et al., 2009; Klemen et al., 2011) or against trials without cues (McCarley & Mounts, 2008; Munneke et al., 2008). In the latter studies, cue validity was always 100% on cued trials. Fournier and Shorter (2001) directly manipulated cue validity levels and found decreased flanker interference effects with 100% valid cues, whereas uninformative cues with 50% validity had no such effect. This may be due to more focused spatial attention in trials in which the target location is certain compared to trials with uncertainty.

The present study design included neutral and invalid cues with equal frequencies to overcome several potential problems. For example, comparing cued trials to uncued trials would introduce different levels of alertness as a possible confounding factor between conditions. Without alertness, participants cannot prepare for upcoming stimulus presentation and are typically slower in responding, leading to larger interference effects compared to fast responses (e.g. Burle et al., 2014; Mattler, 2003). Any differences between cued and uncued interference effects are thus partly explicable by varying levels of alertness. Furthermore, using invalidly cued trials allows a comparison of correct as well as incorrect spatial attention independently.

As there were only two possible stimulus positions, valid cueing alone may not have sufficed to increase focused attention relative to neutral trials. A comparison of valid and invalid trials may be more appropriate. Finally, 50% cue validity of valid and invalid cues prevents oddball effects for cues with lower probabilities. Past studies using equal levels of valid and invalid cues either found no cueing benefit on flanker processing, i.e. equal levels of interference for both validity levels (Ro et al., 2002), or increased flanker effects when flankers appeared at exogenously cued locations (Facoetti, 2001).

Many of the past studies combining spatial cueing and flanker stimuli used crowded displays (Fournier & Shorter, 2001; Klemen et al., 2011; McCarley & Mounts, 2008), leading to high perceptual load. According to perceptual load theory, high load displays more strongly engage attentional capacities, thus resulting in fewer cognitive resources for distractor processing (Lavie, 1995). In addition, the applied target-flanker separation was often relatively large (Chao, 2011; Fox, 1995; Yantis & Johnston, 1990). Such designs may lead to generally improved focused attention because target stimuli are easily distinguishable from flanker stimuli. Paquet (2001) manipulated target-flanker proximity and found a cueing benefit with reduced interference effects for large distances, whereas flanker stimuli located close to the target evoked stronger interference. In the present study, perceptual load was rather low and target-flanker separation was small (around 0.36° angular size). Thus, the present design was more similar to the design introduced by Eriksen and Eriksen (1974) who found most robust flanker effects with high target-flanker proximity. With this design, it may be assumed that the modulations of interference processing found in the present study are more likely attributable to the cueing manipulation than to factors related to stimulus parameters. Moreover, due to equal cue frequencies, the distinct effects of each cue on flanker processing cannot be attributed to different levels of expectancies. Likewise, CON and INC flanker stimuli were equiprobable, excluding the possibility that processing of one condition would become more automatic than that of the other. The ERP and fMRI data show that despite comparable effects in the behavioral

measures cueing altered flanker processing in various brain regions and with distinct temporal patterns.

3.4.2 Neurophysiological data

Both the fMRI and the ERP data hint at an early modulation of flanker processing in visual brain regions. Data of the source analysis derived from separate measurements provide further evidence that this finding might reflect the same underlying neuronal process, i.e. an early adjustment of the attentional focus depending on the initially attended location.

The fMRI data show that contrasting INC > CON resulted in significant signal increase in left frontal (MFG) and parietal cortices (SPL/precuneus). The same contrast for the subset of validly cued trials additionally activated left SFG, IOG and MTG, as well as right SPL and STG. There were no significant clusters on invalidly or neutrally cued trials. The ERP data displayed significant differences between flanker conditions at frontocentral and parietooccipital sites. Detailed ERP analyses in consecutive time windows revealed modulations by flanker congruency and interactions with electrode site and cue validity. In a time bin from 200-220ms, only validly cued trials demonstrated a significant *congruency* effect with more positive amplitude values for INC compared to CON trials. No comparable effect was found when comparing the flanker conditions within the other cue validity levels. Visual inspection of the scalp topography of the difference wave shows that this positive difference is derived from amplitude differences at centroparietal electrodes. In the following 20ms time windows, there was a negative-going deflection on INC trials with a posterior scalp distribution and a concurrent relative positivity at frontocentral electrode sites in all three validity levels.

Concerning the difference between INC and CON stimuli on validly cued trials, the initial relative positivity at centroparietal sites in the ERP data, followed by a negativity with a bilateral posterior distribution, as well as the fMRI cluster in IOG both fit with the idea that the cueing manipulation led to flexible changes of the focus of spatial attention. Advance

knowledge of the correct stimulus location on validly cued trials possibly allowed participants to detect the mismatch between target and flankers on an early perceptual level. As the perceptual load was higher for INC than CON stimuli, it seems plausible that spatial attention became more focused early during stimulus processing to inhibit flanker processing. Thus, distractor suppression has been found to increase BOLD activity in visual cortex (Serences et al., 2004), possibly through biased competition mechanisms when targets and distractors activate overlapping receptive fields (Munneke et al., 2011). These effects are apparently restricted to higher visual areas, where it is more likely that both targets and distractors share the same receptive field (Munneke et al., 2011). This might explain the lack of significant differences between flanker conditions in early visual areas in the fMRI analysis. Similarly, de Haas el al. (2014) could show that high perceptual load leads to the suppression of distracting information that is presented at locations surrounding an attended region. Thus, the receptive fields of visual neurons which process the locations of irrelevant stimuli increase, leading to a blurry representation of these stimuli in visual cortex. In the present study, the early centroparietal difference between congruency conditions with valid cueing was characterized by less negative amplitude values for INC than CON stimuli. As the amplitude of the N200 is assumed to be indicative of the degree of processing of the flankers (Larson et al., 2014), less attention may have been directed to the flanker stimuli on INC trials in the present study.

Based on these findings, the early congruency effect on validly cued trials during the N200 time window might derive from activity in visual brain regions, in line with perceptual-load induced effects in visual cortex (de Haas et al., 2014). This finding is corroborated by the source analysis data which demonstrate that with valid cueing, early phases of stimulus processing including the N200 time window showed higher source activity for INC than CON stimuli in RSs representing brain areas involved in visual processing, including the bilateral lingual gyri. A similar pattern became evident when comparing INC and CON trials with invalid cueing, whereas neutral cueing did not show congruency effects in these RSs during the N200. While

validly cued trials potentially led to increased focusing on the target letter on INC but not CON trials (de Haas et al., 2014), invalidly cued trials might initially have involved disengagement of attention from the incorrect location and a subsequently redirection to the target location (Posner & Petersen, 1990). Here, INC stimuli might have consumed more attentional capacity before control mechanisms were initiated to adjust the spatial focus. By contrast, neutral cues were used to direct participants' attention to both possible location so that they initially evoked divided attention. In that case, the strength of attention directed to each location only needed to be adjusted during stimulus presentation. Therefore, neutral trials possibly involved re-weighting of the attentional foci instead of switching or enhanced focusing. This pattern may also explain the lack of differences of INC and CON trials between 200 and 300ms for neutral cueing in RSs located in visual areas during the N200 time window.

The fMRI activation data similarly point to adjustments of the attentional focus: Parietal clusters activated in the validly cued INC > CON contrast overlap with a frontoparietal orienting network (Corbetta & Shulman, 2002). Brain regions involved in that network respond to attentional switches and comprise right ventral portions of frontal and parietal cortices. In line with the present data, right IPS of that network is reported to show more activity both in response to covert shifts of attention (dFPN) and attentional orienting during target detection (vFPN, Corbetta & Shulman, 2002). In the present study, enhanced activation on validly cued INC trials was evident in bilateral SPL adjacent to IPS. SPL activity might have induced an adjustment of the attentional window in response to an early detection of the perceptual mismatch of INC stimuli. It might also have assisted in target detection later after completion of the proposed focusing process. In addition, Fan et al. (2007) reported SPL and MFG to be active both in response to alertness cues and during conflict processing. The authors interpreted this overlap as a sign of executive control adjustments. In the present study, there were frequent switches between correct and incorrect attentional allocations due to equal probabilities of valid and invalid cues. These may have led to activation of MFG and SPL in general. The need to

adjust the width of the attentional window on INC trials might additionally explain why these regions were more active on INC compared to CON trials with valid cueing. The fact that invalidly cued INC stimuli did not significantly increase activity in SPL appears to contradict the current interpretation of focus adjustments on INC trials. However, there was probably enhanced SPL activity on all invalid trials when attention switched to the correct location, regardless of flanker congruency (Corbetta & Shulman, 2002). In contrast to validly cued trials, this may have led to a ceiling effect shadowing additional SPL activity in response to flanker conflict.

Bunge et al. (2002) found activity in parietal regions for conflict processing in general and in addition on trials involving maintenance of several response alternatives compared to trials activating only one response. Thus, INC trials usually involve more SPL activity than CON trials due to later response selection in frontal brain areas, leading to prolonged phases of maintaining the response alternatives in parietal cortex (Bunge et al., 2002). Assuming that valid cueing led to fast attentional adjustments after the perceptual mismatch was detected on INC trials, it seems plausible that SPL was less active on CON than on INC trials because the response representations were quickly updated from two alternatives to one. By contrast, on invalidly cued trials the initial switch might have provided enough time to find the correct response regardless of the congruency level so that there was no difference between CON and INC stimuli in parietal regions.

The ERP data demonstrated cue validity-specific modulations of the congruency effect in the N200 time window that are compatible with source activity differences in ACC and precentral gyrus. These ERP deflections might reflect conflict detection (ACC) and response competition (precentral gyrus) during early stimulus processing. Thus, between 240-260ms, only invalidly cued trials yielded a significant positive difference between INC and CON at frontocentral sites and both neutrally and invalidly cued trials were associated with significant relative negativities

at parietooccipital sites. There was no significant congruency modulation on validly cued trials. In addition, there was a congruency effect between 280 and 300ms due to a relative positivity at central sites, and this effect was evident on invalidly cued trials only. Likewise, in the source analysis data, source activity in trials with invalid cueing differed between congruency levels in the RS in ACC during the first 300ms. Assuming that the anterior N200 reflects control signals arising in ACC (Carter & van Veen, 2007), this pattern of results may represent conflict detection in trials where the stimulus location was unknown in advance. Correspondingly, there was a simultaneous early difference of INC and CON trials with invalid cues in the RS in precentral gyrus, which might reflect activation of two competing response channels (Bunge et al., 2002; Ullsperger & von Cramon, 2001). Concurrent activation of both ACC and precentral gyrus might suggest that in contrast to validly cued trials, the conflicting information was processed beyond the low-level perceptual stage with invalid cueing and initiated preliminary response preparation. On invalidly cued trials, the spatial focus initially had to switch from the incorrect to the actual stimulus location so that attention was not focused on the target letter (Posner, 2014). By contrast, on validly cued trials conflict detection was possibly attenuated due to an early focusing on the target in the time window from 200-220ms.

The findings discussed above point to separate neuronal generators underlying different effects in the N200 time window. The frontocentral positive effect is likely to originate from activity differences between INC and CON trials in ACC (Van Veen & Carter, 2002), while the posterior negative differences may derive from bilateral activation of visual cortical regions in line with the posterior bilateral scalp topography. Similarly, a posterior N200 has been reported for visual search tasks (Hopf et al., 2006) with a neuronal generator in the occipital cortex (Luck et al., 1997). As outlined previously, these regions are involved in distinct processes with regard to attentional control mechanisms, namely task-related control signaling (ACC) and spatial selection via adjustments of the attentional focus (visual cortex).

In the source analysis data, early source activity differences between congruency levels in visual areas as well as ACC and precentral gyrus were complemented by signal differences during late phases of stimulus processing originating in the RS in left IFG, and these occurred earlier with invalid (~500ms) than valid (~580ms) or neutral cueing (~570ms). IFG appears to be involved in the selection among response alternatives (Bunge et al., 2002). Enhanced recruitment of IFG on INC compared to CON trials might thus reflect increased difficulties to distinguish between two simultaneously active response channels causing transient activation of control mechanisms triggered by IFG (Dosenbach et al., 2007). This effect possibly occurred earlier with invalid cueing than in the other cueing conditions because of an early activation of competing response channels, which is as also reflected in early effects in the RSs in ACC and precentral gyrus. In line with this argumentation, there was a late congruency effect in the RS in ACC and a subsequent activity difference in the RS in precentral gyrus on invalidly cued trials. This source waveform pattern corroborates the assumption of different origins of conflict processing for different types of cueing. With invalid cueing, early conflict detection on INC trials might later have activated ACC in order to initiate conflict monitoring, thus enabling the selection of the correct response (Botvinick et al., 2004; van Veen et al., 2001). On validly cued trials source waveform differences in the precentral gyrus RS preceded significant effects originating in the cingulate RS. This pattern might be a result of the detection of the perceptual mismatch during early stimulus processing, possibly leading to the maintenance of both response alternatives and early response selection. Therefore, enhanced activation in the precentral gyrus on validly cued INC trials may originate from the simultaneous maintenance of two response alternatives in general (Bunge et al., 2002; Ullsperger & von Cramon, 2001), whereas on invalidly cued trials, the underlying process might have been competition between response alternatives. With valid cueing, the congruency-related effects in the RS in ACC showed later differences than with invalid cueing. ACC seems to be involved in strategic behavioral adjustments in response to conflict (Botvinick et al., 2001). Therefore, the difference

observed in the present study might be due to the evaluation of the flanker stimuli after a broadened attentional focus initiated control signals, leading to reactivation of both response channels on INC trials.

3.4.3 Critical reflections

The results of the source analysis must be interpreted cautiously. Thus, in the precentral gyrus RS differences between flanker conditions were briefly significant at stimulus onset with invalid cues (0-16ms). This hints at baseline problems rather than effects related to the flanker manipulation. Likewise, there were baseline shifts of source waveforms in the IFG RS with valid cues (0-13ms) and in the cingulate RS with invalid cueing (0-25ms). These baseline problems either may be due to noise in the ERP data or alternatively to enhanced interindividual variabilities. The latter could result from differing performance evaluation styles or strategic adaptation to previous trial history (Gratton et al., 1992). Such dynamic changes have been found in the literature to be mediated by the cingulate cortex (Sheth et al., 2012). Strategic modulations initiated by the cingulate gyrus would also explain baseline shifts in the precentral gyrus and IFG RSs, as these structures demonstrate high functional connectivity patterns (Koski & Paus, 2000) and are coactivated during conflict processing (Corbetta & Shulman, 2002). Nevertheless, the early INC vs. CON differences between source waveforms originating in these RSs are probably not related to current-trial conflict processing.

In the fMRI analysis, the contrast INC > CON did not result in significant differences on neutrally or invalidly cued trials. Based on the data pattern derived from source analysis, it is reasonable to assume that this is due to the transient activation of several different brain regions. While occipital and frontal RSs demonstrated long phases of significant differences between CON and INC stimuli with valid cueing, regions such as ACC yielded transient differences in the other cueing conditions. The latter may not have been detected by fMRI due to the slow nature of the BOLD signal (Huettel et al., 2004).

In addition, neither of the INC > CON contrasts (pooled over validity levels and in the single cueing conditions) resulted in ACC activation. Executive control processes are expected to recruit a fronto-cingulo-parietal network (Dosenbach et al., 2007), where frontal and parietal cortices seem to regulate top-down control processes through short-scale adjustments. By contrast, cingulate structures operate on a more tonic time-scale to maintain the current task goal, enabling conflict detection between different response alternatives inherent in a stimulus array (Dosenbach et al., 2008). As comparisons in the present study were not based on blocks of different attentional states, activity of ACC related to task set maintenance is probably not reflected in the fMRI contrasts. Instead, the data more likely represent within-trial adjustments related to top-down control triggered by frontoparietal networks.

3.4.4 Conclusions

To summarize, the present results pattern hints at early modulations of flanker processing induced by spatial cueing with different informative properties. Correct attentional allocation presumably induced more focused attention on INC trials, whereas invalidly cued trials might have increased flanker conflict due to unfocused attention after switches to the stimulus location. Thus, a posterior bilateral negativity in the N200 time window together with an fMRI cluster in IOG points towards brain mechanisms to control the attentional focus. A concurrent relative ERP positivity at frontocentral sites was specific to invalidly cued trials and may reflect enhanced interference due to a broad spatial focus resulting from switching the attentional focus from the attended location to the target location. The fMRI-constrained source analysis further points to separate neuronal generators for these readjustment processes. Early stimulus processing within the N200 time window was associated with activity in visual RSs, corroborating the proposal that the posterior bilateral negativity might reflect mechanisms related to modifications of the attentional focus. In addition, a RS in ACC was differentially sensitive to flanker processing depending on cue validity, as it demonstrated an early congruency effect only with invalid cueing. There was a simultaneous source waveform

difference between INC and CON stimuli with invalid cueing in the RS in precentral gyrus, possibly reflecting initial activation of the incorrect response. The fact that the congruency effects in ACC differed between valid and invalid cueing may further suggest that the conflict sources differed. With valid cueing, conflict might have resulted from the perceptual mismatch between CON and INC stimuli, whereas invalidly cued INC trials were possibly triggered by the competition among response channels. The source analysis data thus extended the fMRI and ERP findings by demonstrating source waveform differences in regions possibly involved in early and later phases of conflict detection and attentional adjustment procedures.

4. EXPERIMENT II: FEATURE-BASED CUEING IN THE FLANKER TASK

4.1 Introduction

In experiment II, feature cues were used in an experimental design that was in all other respects identical to experiment I. Cues directed participants' attention to the upcoming color of the flanker stimulus or were neutral. Recording of EEG and fMRI data with identical parameters to experiment I provided optimal conditions for comparison between experiments. Experiment II was centered on the question whether feature-based cueing would have the same effect on the conflict-related N200 ERP component as spatial information, and whether the same or different brain regions demonstrating validity-specific modulations during interference processing in experiment I would also be differentially affected by cue validity of color cues. Finally, a source analysis of the ERP waveforms based on coordinates from fMRI was computed and with compared the results of experiment I.

4.1.1 Models of feature-based attention

In general, the term 'attention' describes the concentration of available resources on a subset of all incoming information units at a given time. This ability is not restricted to locations in space. Rather, non-spatial information such as features (Allport, 1971) or entire objects (Duncan, 1984) can serve as entities to guide attention. The question whether these attentional selection mechanisms are arranged hierarchically or work in concert to achieve optimal information processing has been raised repeatedly in the literature (Carrasco, 2011). The 'feature-integration theory' describes the roles of feature-based and location-based selection mechanisms and contains two stages of information processing. Simple features are initially processed in parallel to create feature maps separately for each feature dimension (e.g. color; orientation), whereas subsequent binding of features to objects at specific locations requires serial scanning of the

single feature conjunctions (Treisman & Gelade, 1980). Consequently, only the latter process s require spatial attention (Treisman, 1988; Treisman & Gelade, 1980). This suggests that simple feature detection can be achieved in parallel, independent of the number of items, whereas searching for feature conjunctions involves serial scanning of single item until the target is found (Treisman & Gelade, 1980). Therefore, feature integration theory is a hierarchical model with a superior role for spatial selection.

However, the specific type of feature conjunction appears to be an important factor. Thus, there is evidence for a parallel search mode during certain feature conjunction search tasks, contradicting pure feature integration mechanisms (Wolfe et al., 1989). According to the 'guided search model' early parallel processing involves the creation of feature maps that include both location information and the behavioral saliency of each feature (Wolfe et al., 1989). Thus, the model assumes that behaviorally relevant features may guide the transfer of information from the first to the second stage of information processing in order to facilitate selection. The main difference to feature integration therefore is the possibility of early attentional engagement during search in guided search (Wolfe et al., 1989).

4.1.2 Neuronal mechanisms of feature-based attention

The neuronal characteristics of spatial attention, i.e. enhanced responses of neurons preferentially processing attended locations (Carrasco, 2011), have been studied extensively in past studies and probably contributed to the special role that locations are granted in attentional research (Driver, 2001). However, several studies could show that attention to a certain feature increases neuronal responses in brain regions processing that feature irrespective of stimulus location. Thus, neurons in extrastriate cortical regions respond more strongly to a spatially ignored stimulus if its features match the currently attended feature, both when attending to colors and to motion direction (Saenz et al., 2002). Such global feature-based attention effects are in line with the 'feature-similarity gain model' (Treue & Martinez Trujillo, 1999). The

model assumes that the response gain evoked by attention depends on the correspondence between a neuron's preferred feature and the currently attended feature (Treue & Martinez Trujillo, 1999). In contrast to object-based attention, selection based on features initiates both neuronal enhancement of attended features and suppression of simultaneously presented ignored features (Polk et al., 2008; Wegener et al., 2008). For example, attending to two stimulus apertures at different hemifields reveals both neuronal response enhancement and suppression mechanisms. Thus, behavioral performance is better when the same feature is attended to in both apertures than during attention to opposing features (e.g. attention to green among red stimuli in one hemifield and red among green stimuli in the other hemifield; (Saenz et al., 2003). This is generally in line with the biased competition model described previously. Biased competition refers to competitive interactions of stimuli within a neuron's receptive field, where attention to one stimulus enhances its response gain and simultaneously suppresses the gain of the unattended stimulus (Desimone, 1998). In addition, biased competition assumes parallel competitive interactions of all stimuli in the visual field, whereas feature integration is based on spatially constrained effects of feature-based attention (Corchs & Deco, 2004). Previous studies have shown that attention to a certain feature in a multi-feature stimulus enhances neuronal responses to a level comparable to responses when the feature is presented in isolation (Treue & Maunsell, 1996). A comparison of these models using recordings in monkey area MT suggests that the feature-similarity gain model more accurately explains empirically found feature-based attentional mechanisms (Daliri et al., 2009). Moreover, it accounts for global effects of feature-based attention that are not considered within the feature integration model or the guided search model (Daliri et al., 2009).

4.1.3 Objectives of experiment II

In experiment II, feature-based attention was combined with the same flanker task used in experiment I. Cues predicted the color of flanker stimuli either correctly (valid cueing) or incorrectly (invalid cueing) or contained no predictive value (neutral cueing). Analogous to

experiment I, fMRI and EEG data were collected and analyzed in an fMRI-constrained source analysis.

Like spatial attention, attending to features leads to activity in frontoparietal structures of the brain (Greenberg et al., 2010; Liu et al., 2011). Therefore, a possible observation might be an activity pattern that is analogous to that found in experiment I. However, spatial and feature-based attention differ on a temporal level. Contrary to experiment I, it is thus likely that both manipulations (attention and interference control) operate at different processing stages. Accordingly, additive effects would be expected on a behavioral level (Sternberg, 1966). However, as feature-based attention and flanker congruency both exert effects around 250ms (selection negativity and N200 respectively; (Eimer, 1997; Larson et al., 2014), an alternative observation may be an early interaction of both factors which might also be evident in the behavioral data analysis.

4.2 Material and methods

4.2.1 Study participants

EEG and MRI data were obtained from 21 healthy and right-handed (median = 100%; range=77% - 100% according to the Edinburgh Inventory; (Oldfield, 1971) volunteers (10 male; mean age = 24.9 years; SD = 3) with normal or corrected-to-normal vision. No participant showed signs of color-blindness according to a modified version of the Ishihara Test (Ishihara, 1917) including the colors used in the present experiment. Every participant took part in a training session, an EEG experiment and an MRI experiment on separate days (time between EEG and fMRI sessions: median = 1 day; range = 1 – 9).

4.2.2 Data protection, data security, and legal framework

The study protocol was in line with the Helsinki Declaration of the World Medical Association (Rickham, 1964) and approved by the local ethics committee of the University of Bremen (see Appendix D). Participants were informed about data collection, data protection, and data security of all experimental and personal data, including the pseudonymization procedure. The potential risk factors of the MRI scanner were highlighted and no participant was measured who showed one or more of the exclusion criteria (see Appendix E). Based on this procedure, all participants gave written and informed consent before participating in the study (see Appendices F and G) and they were allowed to quit the experiment at any time without giving reasons. All participants received 30€ or were given course credits.

4.2.3 Data analysis

4.2.3.1 Behavioral data

The same analysis procedure was used as in experiment I. Only correct trials were included in the analysis of RTs. For RT analysis, a repeated-measures ANOVA with factors *method (EEG/fMRI) x cue validity (valid/neutral/invalid) x flanker congruency (CON/INC)*. Error rates (percentage of incorrect trials and misses per condition) were analyzed using Friedman tests.

The significance level was set $\alpha=0.05$ for all behavioral and electrophysiological analyses. Greenhouse Geisser corrected epsilon values are reported if the assumption of sphericity was violated (Mauchly´s Test). Significant effects were further investigated using post hoc paired t-tests (with Bonferroni-Holm correction when required) and Wilcoxon tests for RTs and error rates respectively.

4.2.3.2 (f)MRI data

As in experiment I, the functional scans were temporally resliced, coregistered to the structural scan and smoothed, and both function and structural data were normalized to the standard MNI space. Motion parameters were estimated and used as regressors in a fixed-effects analysis using the correct trials of all six conditions and the cue period, the ISI and the ITI as separate regressors. Group-specific activation of all 21 participants was analyzed with a random-effects analysis using a full factorial design with the factors *cue validity (valid/neutral/invalid)* and *congruency (CON/INC)*. Post hoc paired t-tests were performed on the INC > CON contrast pooled over cue validity levels and separately for each cue validity level. Moreover, conjunction analyses (Nichols et al., 2005) were computed over the INC > CON contrasts with valid and invalid, valid and neutral as well as invalid and neutral cueing to identify those regions showing congruency effects throughout different cueing conditions. For all contrasts, the significance threshold was set to $p<.001$ (uncorrected) with an extent threshold of $k\geq10$ voxels.

The localizers were separately preprocessed. They were realigned to the 5th volume of the whole brain scan (reslice option: mean image), coregistered to the anatomical scan, (source: mean image of whole brain scan), normalized to the standard MNI space with 4th degree B-spline interpolation and resampling to 2 mm³ isotropic voxels, and smoothed with a $4mm^3$ FWHM Gaussian kernel. A fixed-effects design was set up with separate regressors for chromatic and achromatic blocks and the fixation period. The thresholds varied between participants hemispheres in order to obtain clusters of comparable sizes.

The MNI coordinates of all peaks and sub-peaks were transformed into Talairach space (‘mni2tal.m’; http://imaging.mrc-cbu.cam.ac.uk/imaging/MniTalairach) and their anatomical locations were derived from the ‘Talairach Daemon Client’ software (http:// http://www.talairach.org/daemon.html) and the automated anatomical labeling toolbox (‘AAL‘; http://www.gin.cnrs.fr/AAL-217?lang=en).

4.2.3.3 ERP data

In line with experiment I, the EEG data were filtered (high-pass filter 0.05; Notch filter 50Hz) and interpolated (spherical spline interpolation; mean = 2 channels ±2, maximum = 5 channels) or defined as bad (mean = 0.5 channels ±1, maximum = 3 channels) when necessary. Correct trials were averaged stimulus-locked from -200ms to 900ms (mean = 89 trials; 70-100 trials) per condition and participant.

Identical to experiment I, separate repeated-measures ANOVAs with the factors *cue validity (valid/neutral/invalid)* x *flanker congruency (CON/INC)* x *frontality (F/C/P/PO)* x *laterality (left/midline/right)* were conducted on the mean amplitude in 5 consecutive time windows between 200-300ms. Post hoc paired t-tests were computed for significant main and interaction effects using Bonferroni-Holm corrected threshold values.

4.2.3.4 fMRI-constrained source analysis

The same procedure as reported for experiment I was applied for fMRI constrained source analysis in experiment II. Peak coordinates were derived from fMRI contrasts of the conjunction analyses (see Nichols et al., 2005) of CON and INC stimuli pooled over validity levels and contrasted against the ITI ($p<.005$ uncorrected, $k\geq10$ voxels). The resulting 27 distinct peak coordinates were transformed into Talairach space (‘mni2tal.m’;http://imaging. mrc-cbu.cam.ac.uk/downloads/MNI2tal/) and clustered (minimal distance = 30mm; (e.g. Miedl et al., 2014). As in experiment I, the maximally allowed distance between the derived coordinates and their original peaks was 25mm. The resulting coordinates were used to seed

RSs in the source analysis of the grand average ERP waveform of all participants and conditions. This created a source model, which was subsequently applied to the individual ERP data. The source model was checked for potential source sensitivity problems (see Appendix M for the single source sensitivity plots). Finally, BCa bootstrap 95% confidence intervals were computed on the RMS of each source waveform. Only epochs of ≥20ms were considered to reflect meaningful differences between conditions.

4.3 Results

4.3.1 Behavioral data

Behavioral data were analyzed using a repeated-measures ANOVA with the within-subject factors *method (EEG/fMRI)* x *cue validity (valid/neutral/invalid)* x *flanker congruency (CON/INC)*. All factors demonstrated significant main effects (*cue validity*: $F_{[2;40]} = 7$, $p < .005$; *congruency*: $F_{[1;20]} = 47.8$, $p < .001$; *method*: $F_{[1;20]} = 71.6$, $p < .001$) and the factors *congruency* and *method* interacted ($F_{[1;20]} = 5.8$, $p<.05$; see Table 5).

Table 5: Summary of the mean reaction times (RTs) and error rates (top and bottom respectively) with standard deviations (SD) of the six conditions during the EEG (left) and the fMRI session (right). N = 21.

		EEG			fMRI		
	condition	**congruent**	**incongruent**	**total EEG**	**congruent**	**incongruent**	**total fMRI**
RTs [ms] ± SD	**valid**	511.4 ± 79.8	544.6 ± 71	573.3	577 ± 73.6	605.4 ± 63.8	601.9
	neutral	522 ± 78.9	553.5 ± 74.9		591.1 ± 75.4	616.4 ± 71.3	
	invalid	530.3 ± 84	562.3 ± 83.2		598.7 ± 84.9	622.5 ± 75.8	
error rates [%] ± SD	**valid**	3.5 ± 3	3.8 ± 3.2	4.0	3.7 ± 3	4.4 ± 2.8	4.9
	neutral	3.2 ± 2.6	4.5 ± 2.6		3.8 ± 2.5	4.6 ± 3.3	
	invalid	3.6 ± 3.6	5.6 ± 4.7		8.3 ± 4.7	4.8 ± 3.9	

Bonferroni-Holm corrected post hoc paired t-tests showed that valid trials yielded significantly faster RTs than invalid trials ($t_{[20]} = -3.7$, $p < .005$). The *congruency* effect was characterized by higher RTs during INC trials ($t_{[20]} = -6.9$, $p < .001$; see Figures 8 and 9). Finally, RTs were generally faster during EEG measurements as compared to MRI sessions ($t_{[20]} = -8.5$, $p < .001$). Analysis of the error rates with the factors *method* x *cue validity* x *congruency* yielded significant differences between conditions (Friedman test: $\chi_{[11]} = 39.8$, $p < .001$). Post hoc Wilcoxon tests demonstrated significantly higher error rates on invalidly cued trials compared to trials with valid or neutral cueing ($Z= -3.1$; $p<.005$ and $Z= 2.1$; $p<.05$ respectively). Error rates were higher during MRI measurements ($Z= -2.3$; $p<.05$).

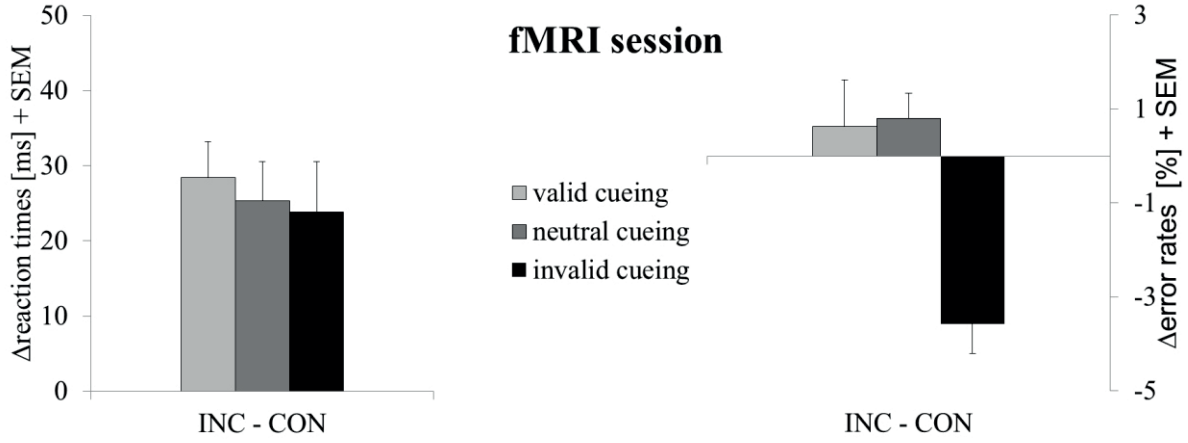

Figure 8: fMRI session: Differences (Δ) of the reaction times (left) and percent error rates (right) between incongruent (INC) and congruent (CON) flanker conditions during valid (light grey), neutral (medium grey), and invalid cueing (black). Error bars show standard error of the mean (SEM). N = 21.

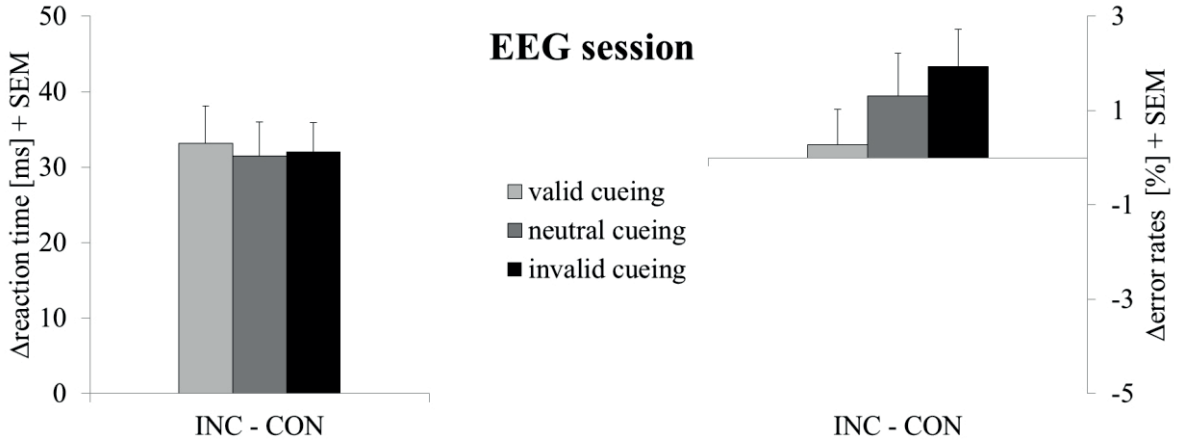

Figure 9: EEG session: Differences (Δ) of the reaction times (left) and percent error rates (right) between incongruent (INC) and congruent (CON) flanker conditions during valid (light grey), neutral (medium grey), and invalid cueing (black). Error bars show standard error of the mean (SEM). N = 21.

4.3.2 fMRI data

Analysis of the fMRI data showed significant activation clusters for the contrast INC > CON located in left frontal (MFG; precentral gyrus/SFG), cingulate (cingulate gyrus; ACC/supplementary motor area (SMA)), parietal (precuneus/SPL), and occipital regions (superior/middle occipital gyri; SOG/MOG) as well as right SFG/SMA and ACC. Post hoc

analyses of the congruency effect (INC > CON) separately for each cue validity level revealed a broad network of activity with valid cueing (see Table 6 and Figure 10). Structures bilaterally activated included IPL, SMG, lingual gyri, SOG/MOG, and ACC/SMA. In the left hemisphere, there was also activation in frontal (SFG/precentral gyrus; MFG), parietal (SPL/precuneus), and insular cortices (insula/operculum), and right hemispheric clusters were significant in angular gyrus, STG, and occipital cortex (IOG; cuneus). The congruency effect with invalid cueing led to activation in bilateral orbitofrontal cortices, left MOG, middle cingulate gyrus/SMA, and right SFG.

Table 6: Talairach peak coordinates of significant activation clusters for the comparison of incongruent (INC) and congruent (CON) flanker conditions pooled over validity levels (top) and for the conjunction of valid and invalid trials (p<.001, k≥10 voxels). BA = Brodmann area; L = left; r = range of nearest grey matter (mm); R = right. N = 21.

contrast	cluster size	t-value	r	peak coordinates (Talairach space)			side	anatomical region (BA)
INC > CON (all validities)	1216	4.9	5	-42	-73	20	L	Middle Temporal Gyrus (39)
		4.8	4	-40	-80	2	L	Middle Occipital Gyrus (19)
		4.7	0	-30	-82	21	L	Middle Occipital Gyrus (19)
	771	4.6	0	-30	-7	56	L	Middle Frontal Gyrus (6)
		4.1	0	-22	-12	63	L	Precentral Gyrus (6)
		3.9	2	-48	-21	54	L	Postcentral Gyrus (1)
	357	4.4	0	-4	-2	42	L	Cingulate Gyrus (24)
		3.9	4	-12	0	33	L	Cingulate Gyrus (24)
		3.9	3	-10	-23	45	L	Cingulate Gyrus(31)
	26	4.1	1	-53	4	33	L	Precentral Gyrus (6)
	19	3.8	0	-26	-52	-24	L	Culmen
	47	3.7	2	0	47	9	L/R	Anterior Cingulate (32)
	58	3.7	1	-18	-57	60	L	Superior Parietal Lobule (7)
	18	3.7	3	28	55	8	R	Superior Frontal Gyrus (10)
	23	3.5	0	26	-48	-21	R	Culmen
		3.4	0	26	-57	-17	R	Declive
	10	3.4	2	18	3	61	R	Medial Frontal Gyrus (6)
INC > CON valid & invalid)	20	3.7	5	-42	-73	20	L	Middle Temporal Gyrus (39)
	14	3.3	0	-2	-13	43	L	Paracentral Lobule (31)

A conjunction analysis (Nichols et al., 2005) was computed over the validly and invalidly cued INC > CON contrasts to identify those regions showing congruency effects in both cueing conditions (p<.001; k≥ 10). This led to suprathreshold activation clusters in left MOG and

middle cingulate gyrus/SMA with a peak in paracentral lobule. With neutral cueing, only the bilateral caudate bodies showed suprathreshold activation, and separate conjunction analyses with the valid and the invalid INC > CON contrasts yielded no significant clusters.

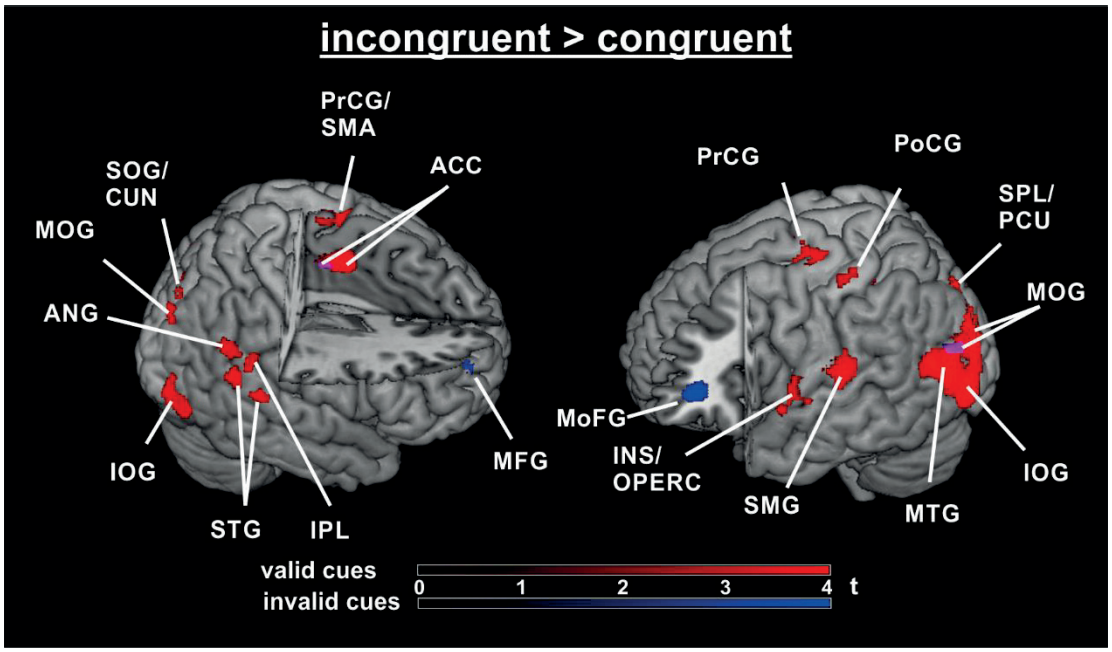

Figure 10: Overlay of activation clusters derived from the contrasts incongruent > congruent with valid (red) and invalid cueing (blue) thresholded at p<.001, k≥10. N = 21.

Labels:
ACC = anterior cingulate gyrus
ANG = angular gyrus
CUN = cuneus
INS = insula
IOG = inferior occipital gyrus
IPL = inferior parietal lobule
MFG = middle frontal gyrus
MoFG = middle orbitofrontal gyrus
MOG = middle occipital gyrus
MTG = middle temporal gyrus
OPERC = operculum
PCU = precuneus
PoCG = postcentral gyrus
PrCG = precentral gyrus
SMA = supplementary motor are
SMG = supramarginal gyrus
SOG = superior occipital gyrus
STG = superior temporal gyrus

4.3.3 ERP data

To analyze the N200 component, the mean amplitude values of INC and CON trials for each cue validity level were examined between 200-300ms. For this purpose, separate repeated-measures ANOVAs with the factors *frontality (F/C/P/PO)* x *laterality (left/midline/right)* x *cue validity (valid/neutral/invalid)* x *flanker congruency (CON/INC)* were computed in consecutive time bins of 20ms each. In general, the difference waves (INC > CON) were characterized by

an early relative negativity of INC stimuli at bilateral parietooccipital electrode sites. In addition, there was a simultaneous frontocentral relative positivity.

From 200ms-220ms, the factor *congruency* demonstrated no main effect or any interaction effect with the other factors. In the time windows from 220ms-240ms, 240-260ms, and 260-280ms, *congruency* interacted with both *frontality* ($F_{[1.3;26.2]}$ = 8.2, p<.01, $F_{[1.3;26.5]}$ = 20.8, p<.001, and $F_{[1.4;27.6]}$ = 12.8; p< .001 respectively) and *laterality* ($F_{[2;40]}$ = 3.8, p<.05, $F_{[2;40]}$ = 8.3, p<.005, and $F_{[2;40]}$ = 3.8; p< .05 respectively). Post hoc t-tests between 220-240ms yielded significant congruency effects at electrodes Cz ($t_{[20]}$ = -3.5; p<.005), C4 ($t_{[20]}$ = -3.2; p<.01) and PO7 ($t_{[20]}$ = 4.0; p<.005; see Figure 11 and Appendix I1 – I3).

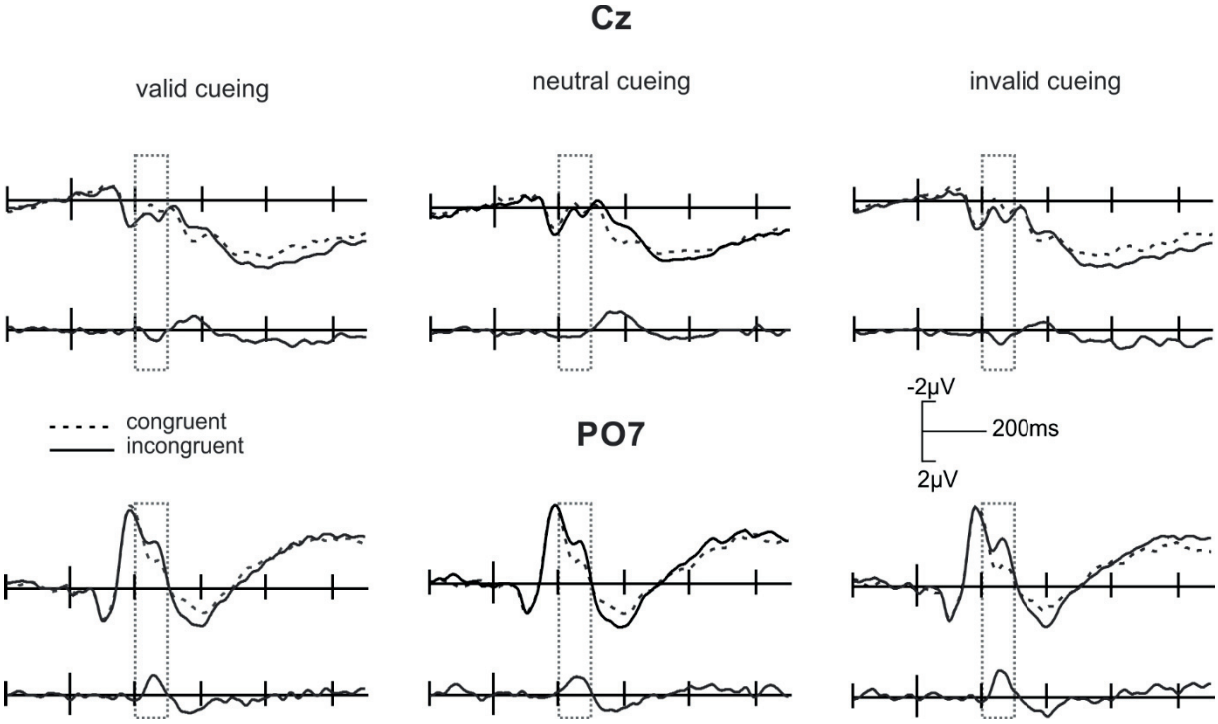

Figure 11: Group ERPs and difference waves during flanker processing at electrodes Cz and PO7: ERPs (stimulus-locked grand average: -200ms to 900ms) of congruent and incongruent conditions with valid (left), neutral (center) and invalid (right) cueing; difference waves (incongruent > congruent) are plotted below the grand averages. N = 21.

From 240-260ms post hoc tests showed significant differences between congruency conditions at electrodes Fz ($t_{[20]}$ = -3.5; p<.005), F4 ($t_{[20]}$ = -4.8; p<.001), C3 ($t_{[20]}$ = -3.3; p<.005), Cz ($t_{[20]}$ = -4.7; p<.001), C4 ($t_{[20]}$ = -4.5; p<.001), P3 ($t_{[20]}$ = 3.4; p<.005), P4 ($t_{[20]}$ = 3.2; p<.01), PO7

($t_{[20]}$ = 7.0; p<.001) and PO8 ($t_{[20]}$ = 3.8; p<.005). In the time window from 260-280ms, post hoc tests demonstrated a *congruency* effect at electrodes F4 ($t_{[20]}$ = -3.4; p<.005), P4 ($t_{[20]}$ = 2.9; p<.01), PO7 ($t_{[20]}$ = 5.6; p<.001) and PO8 ($t_{[20]}$ = 3.3; p<.005).

In the last window from 280ms – 300ms, there was a three-way interaction of flanker *congruency*, *validity* and *laterality* ($F_{[4;80]}$ =3.1; p<.05). A post hoc t-test yielded only sub-threshold differences between the single conditions at left, middle and right electrode sites.

4.3.4 fMRI-constrained source analysis

4.3.4.1 Clustering of fMRI peak coordinates

Sources were derived from clustering of the fMRI peak coordinates (in Talairach space), analogous to experiment I and described in more detail in Bledowski and colleagues (2006). The resulting 10 RSs were situated in left precentral gyri (two RSs), parietal lobe (white matter), cerebellum, and ACC, as well as in right postcentral gyrus, cerebellum, MFG, precuneus, and ACC (see Table 7).

One of the precentral gyrus sources was close to a source derived in experiment I with clustering (distance = 17.6mm). The latter was assumed to reflect activity in left IFG in experiment I because it was in close proximity to a homologous source in right IFG. Due to the similarity of these sources between experiments and given that the source in experiment II was based on peak coordinates including left IFG and postcentral gyrus, this precentral gyrus RS was considered to reflect source activity originating in left IFG. Furthermore, in line with experiment I the cerebellar sources were excluded from further analyses (see also Galashan et al., 2015). Each explained <1% of the overall variance.

A PCA of the residual signal that remained after seeding of the eight fMRI-constrained RSs yielded two principle components explaining 8.1% and 1.4% of the residual variance between 50ms and 150ms respectively. As in experiment I, these components were assumed to reflect

perceptual processing of the visual stimulus properties. Due to the emphasis on stimulus color in experiment II, two RSs were seeded based on the mean of the individual peak coordinates found in the checkerboard localizer (see Table 8) that best matched the coordinates of color-sensitive regions found in the literature (MNI coordinates: ±32 / -82 / -29; according to (van Leeuwen et al., 2014). The color localizers were situated in the bilateral lingual gyri (BA18) and were in close proximity to the additional RSs that were fitted in experiment I (distance = 4.6mm and 7.6mm for left and right RSs respectively). The resulting source model was saturated based on PCA of the residual variance (<1% residual variance of all components) with a Goodness of Fit of 97.9% ±0.9%.

Table 7: Left: Talairach peak coordinates of significant activation clusters when contrasting all congruent trials against the ITI (CON) and all incongruent trials against the ITI (INC) pooled over validity levels respectively (p<.005, k≥10). Right: Labels of regional sources and their locations in Talairach space, resulting from averaging of the corresponding peak coordinates on the left side that were within a distance of 30mm each other. RSs in italics were not included in the final source model. BA = Brodmann area; conj = conjunction; r = range of nearest grey matter (mm); RS = regional source; WM = white matter (no grey matter within 5mm distance). N = 21.

conj	region (BA)	r	peak coordinates (Talairach space)			RS region (BA)	RS coordinates (Talairach space)		
			X	Y	Z		X	Y	Z
CON / INC	Inferior Frontal Gyrus (9)	2	-57	7	31	Precentral Gyrus (6)	-56	-5	39
CON	Postcentral Gyrus (1)	0	-55	-17	44				
INC	Postcentral Gyrus (1)	1	-44	-18	58				
CON / INC	Precentral Gyrus (6)	0	-32	-16	65	Precentral Gyrus (6)	-33	-12	62
CON	Middle Frontal Gyrus (6)	0	-30	-5	61				
INC	Superior Frontal Gyrus (6)	0	-26	-7	63				
CON	Culmen	0	-38	-56	-26				
CON	Culmen	0	-38	-44	-30	*Culmen*	*-32*	*-44*	*-28*
CON	*	0	-26	-38	-28				
INC	*	*	-32	-58	8		-27	-50	22
CON / INC	Parahippocampal Gyrus (30)	4	-30	-50	4				
CON	Angular Gyrus (39)	6	-28	-53	34	WM (Parietal Lobe)			
INC	Caudate Tail	4	-20	-40	15				
CON	Caudate Tail	5	-18	-40	15				
CON / INC	ACC (24)	0	-4	2	39	ACC (24)	-4	2	39
CON / INC	Postcentral Gyrus (43)	4	57	-16	21	Postcentral Gyrus (43)	57	-16	21
CON / INC	Culmen	0	38	-56	-24				
CON / INC	Culmen	0	34	-42	-30	*Culmen*	*33*	*-47*	*-18*
INC	Hippocampus	2	32	-41	0				
CON / INC	Culmen	0	28	-48	-19				
INC	Middle Frontal Gyrus (6)	0	30	-3	61	Middle Frontal Gyrus (6)	30	-3	61
CON / INC	Precuneus (7)	0	16	-59	55	Precuneus (7)	16	-59	55
CON / INC	Medial Frontal Gyrus (10)	2	20	45	11				
INC	Inferior Frontal Gyrus (47)	5	20	35	-2	ACC (24)	10	31	4
CON / INC	ACC (24)	4	4	23	1				
INC	Caudate Body	1	-6	20	6				
	RS seeded (coordinates based on color localizer)					Lingual Gyrus (18)	-28	-73	-9
	RS seeded (coordinates based on color localizer)					Lingual Gyrus (18)	29	-70	-7

Table 8: Individual MNI peak coordinates resulting from the chromatic > achromatic contrast of the checkerboard color localizer using individually defined thresholds for the left and right hemisphere respectively. Distances were computed between each peak coordinate and reference coordinates reported in the literature (see main text). The bottom row shows the mean coordinates over all participants separately for each hemisphere, which were subsequently transformed into Talairach space and used as seed coordinates for the source analysis. ID = participant identity; NaN = definition of color-sensitive region not possible; sub = sub-peak. N = 21.

	left hemisphere (MNI space)					right hemisphere (MNI space)				
subject ID	**cluster size**	**x**	**y**	**z**	**distance (mm)**	**cluster size**	**x**	**y**	**z**	**distance (mm)**
AG21	32	-20	-80	-18	12.3	38	28	-78	-8	13.3
AK36	30	-28	-80	-2	18.5	35	22	-72	-14	15.4
BZ45	31	-22	-78	-14	12.3	36	28	-78	-12	9.8
CU78	34	-24	-68	-14	17.2	37	28	-72	-16	11.5
DH71	sub	-34	-78	-18,0	4.9	33	26	-64	-12	20.6
EQ89	32	-20	-80	-14	13.6	33	30	-74	-16	9.2
FW67	33	-24	-82	-14	10.0	24	30	-72	-8	15.7
GC67	35	-34	-76	-18	6.6	33	26	-80	-14	8.7
HS89	32	-30	-70	-14	13.6	30	34	-68	-18	14.3
IN02	NaN	NaN	NaN	NaN	NaN	NaN	NaN	NaN	NaN	NaN
JB80	36	-30	-68	-14	15.4	33	36	-64	-14	19.4
JH84	30	-22	-74	-16	13.4	31	30	-78	-16	6.0
JX81	31	-32	-80	-14	6.3	33	26	-82	-16	7.2
KW00	30	-30	-80	-18	3.5	30	32	-68	-16	14.6
LO92	37	-28	-74	-16	9.8	30	30	-72	-12	13.0
NT99	30	-36	-76	-18	7.5	32	30	-74	-2	19.8
OY02	40	-26	-68	-10	18.2	30	26	-70	-14	14.7
SZ37	36	-34	-68	-10	17.3	35	32	-80	-12	8.2
TF79	38	-32	-66	-16	16.5	37	30	-66	-14	17.2
VS56	31	-26	-72	-14	13.1	39	26	-70	-14	14.7
WG60	29	-32	-72	-18	10.2	28	26	-66	-12	18.9
group		-28	-75	-15	10		29	-72	-13	12.3

4.3.4.2 Comparison with RSs in experiment I

Several of the RSs in experiment II that were identified using clustering were also evident in experiment I. Thus, the RSs in left precentral gyrus demonstrated identical coordinates across studies. As reported above, a RS derived from peak coordinates in IFG and postcentral gyrus (experiment II) was near a RS that was assigned to left IFG in experiment I (distance = 17.6mm). Moreover, sources in left ACC (both experiments) were located in close proximity (distance = 5.1mm), as were sources in right postcentral gyrus (experiment II) and right IPL (experiment I; distance = 20.9mm). In addition, the sources seeded in bilateral lingual gyri in experiment II demonstrated coordinates adjacent to the RSs that were fitted based on PCA in experiment I (distances: left lingual gyrus RS= 4.6mm; right lingual gyrus RS = 7.6mm).

Finally, a RS located in left parietal lobe in experiment II showed similar coordinates to a RS in left MTG in experiment I (distance = 16.8mm).

4.3.4.3 Source waveform data

Within each cue validity level, source waveforms of INC and CON trials were statistically compared using BCa bootstrap 95%-confidence intervals (Efron & Tibshirani, 1993; see Figure 12 and Table 9 as well as Appendices N, O, and P).

The RS in left IFG showed early congruency effects with invalid cueing overlapping in time with the N200 time window and differences during later stimulus processing. There were no significant epochs within the other cueing conditions. The RS in right precentral gyrus demonstrated early differences between INC and CON when cues were neutral. Additionally, there were source waveform differences arising in bilateral ACC and precentral gyrus with valid and neutral cueing in later phases of the analyzed time window. Invalidly cued trials yielded late source activity differences between INC and CON stimuli in right ACC and precentral gyrus. Furthermore, frontal and parietal RSs were sensitive to stimulus congruency during early stimulus presentation with valid (IPL) and invalid (MFG; IPL) cueing and during later phases with all cue validity types. The postcentral gyrus RS demonstrated early congruency effects when cues were valid or invalid. The precuneus source yielded early congruency effects with neutral cueing and late effects irrespective of cue validity level. Finally, the sources in the lingual gyri contributed to source waveform differences between INC and CON stimuli during early stimulus processing (valid and neutral cueing) and at later phases (valid and invalid cueing).

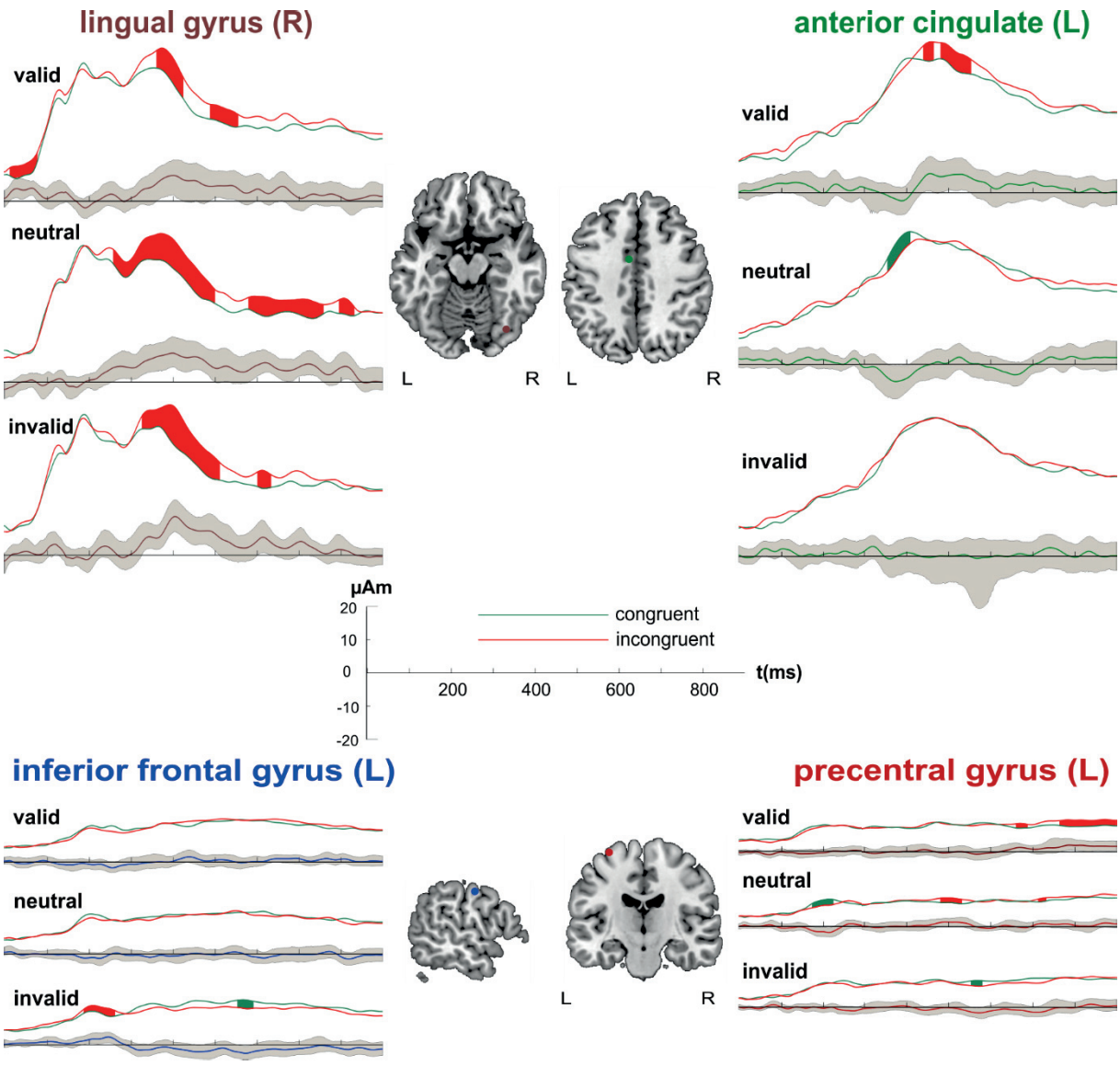

Figure 12: Group source waveforms and BCa bootstrap 95%-confidence intervals. Central column: positions of the regional sources in right lingual gyrus, left anterior cingulate gyrus, left inferior frontal gyrus and left precentral gyrus projected onto the MNI brain. For each regional source, the corresponding root mean square source waveform time course is shown (0-900ms). Green source waveforms indicate congruent conditions; incongruent conditions are presented in red. Difference waves (incongruent > congruent) are depicted in the respective color of the regional source below the source waveforms. The grey area surrounding the difference waves represents the 95%-confidence interval. Epochs deviating from zero for a period of at least 20ms are presented in green (congruent > incongruent) and red (incongruent > congruent). L = left hemisphere; R = right hemisphere. N = 21.

Table 9: Significant time epochs (ms) in which the BCa bootstrap 95%-confidence interval for the difference between incongruent and congruent trials did not include zero for at least 20ms separately for each validity level (left = valid cueing; middle = neutral cueing; right = invalid cueing). N = 21.

Regional Source	valid cueing [ms]	invalid cueing [ms]	neutral cueing [ms]
left Inferior Frontal Gyrus			183-261
			553-589
right Postcentral Gyrus	69-89		0-30
left Anterior Cingulate Gyrus	439-466	355-408	96-164
	479-553		
left Precentral Gyrus	661-689	172-225	553-580
	763-900	476-533	
		712-734	
left Inferior Parietal Lobule	4-50	563-600	0-17
	84-111	853-900	117-135
	446-516		157-170
	534-576		228-260
	582-617		291-329
	622-670		555-711
			718-757
right Middle Frontal Gyrus	475-540	300-326	168-200
	618-664	470-581	797-857
right Precuneus	371-417	126-148	300-427
	500-603	343-467	433-474
	632-667		600-680
			711-764
			815-845
right Anterior Cingulate Gyrus	469-507	26-67	
	517-684	93-130	
	690-719	800-825	
left Lingual Gyrus	348-369		500-644
			670-784
			862-900
right Lingual Gyrus	11-76	256-500	325-510
	360-423	580-757	601-635
	487-554	796-830	

4.4 Discussion

4.4.1 Behavioral data

In the behavioral data analysis significant RT effects were evident for the factors *flanker congruency* (CON < INC), *cue validity* (valid < invalid) and *method* (EEG<fMRI), and more errors were committed on invalid compared to valid and neutral trials.

This pattern of results was also found in experiment I with spatial cueing and was discussed in section 3.4.1 with respect to experimental design differences between the present study and those found in the literature. The similarity between the present studies appears to contradict existing accounts arguing that spatial and feature-based attentional modes differ with regard to underlying mechanisms and temporal patterns (e.g. Liu et al., 2011; Theeuwes, 2010). Thus, a basic claim of the 'stimulus-driven selection theory' states that the initial (preattentive) stimulus processing stage is completely determined by external stimulation, i.e. bottom-up-driven, so that factors such as stimulus saliency guide the initial attentional capture (Theeuwes, 2010). According to the theory, feature-based attentional selection does not occur before 150ms after stimulus onset so that the most salient object involuntarily captures attention. Spatially directed attention on the other hand can affect the preattentive stage because it restricts the region that is analyzed to the attended location. This implies that attentional capture by salient objects can be prevented by spatially directed attention but not by non-spatial top-down mechanisms (e.g. Theeuwes, 2010). Evidence from recordings in color-sensitive are V4 neurons supports this view, as firing rates are identical for the initial ~150ms during a feature-based visual search task, regardless of whether the task is to search for a color or a shape singleton (Ogawa & Komatsu, 2004). Likewise, while the earliest ERP effect distinguishing between attended and unattended locations occurs at ~80-100ms (Mangun, 1995), the selection negativity as a marker of feature-based attention does not occur before ~200ms (Eimer, 1995).

These findings are in contrast to the observed results patterns. With regard to the present experiments, spatially orienting attention to the correct target location should have reduced the flanker effect more than preparing for the correct stimulus color. However, the size of the overall flanker effects (INC > CON) was comparable across experiments (mean ±SD: spatial cueing = 40 ±18ms; feature-based cueing: 29 ±19ms) and neither of the studies showed interactions between cue validity and flanker congruency.

A likely influential factor might be the unpredictable stimulus onset due to a jittered ISI between cues and stimuli. Thus, abrupt target onsets are more likely to capture attention than saliency information alone (Jonides & Yantis, 1988). The sudden onsets of the flanker stimuli in the present studies may have caused a shift of the attentional focus, which interfered with a global search mode generally associated with feature-based experiment (e.g. Liu & Mance, 2011; Störmer & Alvarez, 2014). In the spatial experiment, shifts were discussed in the context of invalidly cued trials, where attention had to switch from the cued to the target location. Attentional redirection may provide sufficient time to solve conflicts so that beneficial effects of validly directed attention (i.e. reduced interference effects) would be shadowed in comparison to invalid trials. This could be shown for spatial shifts of attention in the literature (Fan et al., 2002). Therefore, it is possible that the same explanation applies to violations of feature-based attention in general: Abrupt stimulus onsets potentially captured attention on all trials, similar to invalidly cued trials in experiment I, and when the stimulus color additionally deviated from the expected color (invalid cueing) recalibration mechanisms became necessary (Greenberg et al., 2010). Similar to spatial shifting between locations, the time required to update the attentional task set potentially sufficed for conflict resolution in experiment II, leading to comparable flanker effects on valid and invalid trials.

In sum, comparison of the behavioral data across studies suggests that similar results patterns were observed despite different search modes due to attentional switch mechanisms elicited by

distinct processes. In experiment I, invalid cueing probably led to attentional shifts, and this potentially masked longer response selection times on INC trials compared to those with valid cueing because the conflict could be processed during the shift on invalid trials. In experiment II, attentional captures potentially interrupted a global feature-based search mode on valid and invalid trials. Unexpected color presentations on invalid trials yielded additional attentional recalibration mechanisms, with the same consequence as in experiment I, i.e. a masked reduction of the flanker effect on valid trials.

4.4.2 Neurophysiological data

Brain regions involved in flanker conflict processing partly overlapped between experiments. In addition, there were several analogous RSs evident in both source models, suggesting that similar networks were recruited with both attention types.

In the main fMRI contrast INC > CON, left SPL/precuneus and MFG were active both with spatial cueing (x/y/z Talairach peak coordinates: SPL/precuneus = -24/-56/49; MFG = -26/-8/41) and with feature-based cueing (SPL/precuneus = -18/-57/60; MFG = -30/-7/56). These clusters were also evident in the subset of validly cued trials, where the same regions showed significant activation clusters in the spatial (SPL/precuneus = -24/-58/53; MFG = -24/-4/43) and the feature-based cueing experiment (SPL/precuneus = -14/-63/51; MFG = -26/-2/44; see Figure 13). No similarities were evident between experiments with invalid or neutral cueing. Therefore, the clusters in SPL and MFG might represent general conflict processing mechanisms under the influence of top-down control, because they were activated during correctly directed attention with regard to location (experiment I) as well as color (experiment II). In line with this suggestion, both regions are also elements of the dFPN (Corbetta & Shulman, 2002) which is responsible for top-down attentional orienting processes and active during endogenous attentional cueing (Petersen & Posner, 2012).

Comparing invalid trials between experiments, there were no suprathreshold clusters in experiment I, and in experiment II the observed clusters were distinct from those with valid cueing. As both study designs involved violations of expectations on invalidly cued trials (experiment I: unexpected location; experiment II: unexpected color), invalidly cued trials may generally have activated both SPL and MFG (Corbetta & Shulman, 2002). Consequently, there were presumably no INC > CON clusters in SPL with invalid cueing. With spatial cueing, goal adjustments may have been implemented by shifting the attentional window, while during feature-based attention the attentional task set, i.e. the target color was updated. This points towards a ceiling effect of activity in SPL and MFG, which may have shadowed additional activity increases during processing of INC flanker stimuli compared to CON trials in frontoparietal brain regions.

Experiment II was more similar to neutrally cued trials in the spatial cueing task with respect to location shifts, because participants received no spatial information about the upcoming target. However, the fMRI data pattern still more closely resembles that of spatially cued rather than neutral trials in experiment I with valid cueing, possibly because of early attentional capture mechanisms interrupting a global search mode (Neo & Chua, 2006). In line with similar behavioral data patterns across the present studies, this suggests that the same regions were recruited in order to adjust the attentional goal in response to flanker interference on valid trials.

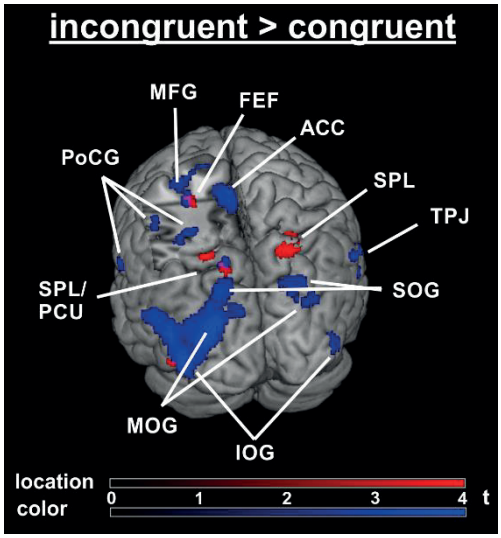

Figure 13: Overlay of activation clusters derived from the contrasts incongruent > congruent with valid spatial cueing (red) and with valid feature-based cueing (blue) thresholded at p<.001, k≥10. N = 19 (experiment I); N = 21 (experiment II).

Labels:
ACC = anterior cingulate gyrus
FEF = frontal eye field
IOG = inferior occipital gyrus
MFG = middle frontal gyrus
MOG = middle occipital gyrus
PCU = precuneus
PoCG = postcentral gyrus
SOG = superior occipital gyrus
SPL = superior parietal lobule
TPJ = temporoparietal junction

SPL/precuneus and MFG may represent domain-independent cortical regions for the execution of attentional shifts, as they show common activation during shifts of attention both with spatial and feature-based attention (shifts between locations or between colors (Greenberg et al., 2010). Thus, SPL/precuneus and MFG not only respond to spatial orienting but also are more generally involved when the currently maintained attentional goal needs to be updated (Greenberg et al., 2010). The fact that the discussed frontoparietal structures demonstrated higher BOLD signals during INC than CON trials with valid cueing in both experiments hints at enhanced efforts to overcome conflict on valid trials. Similar to experiment I, there was possibly an early perceptual mismatch detection between flankers and targets. As a result, spatial focusing mechanisms potentially increased in both experiments, so that validly cued INC trials yielded higher activation levels than CON trials in frontoparietal structures. Conversely, when trials were invalidly cued SPL was probably generally active to mediate goal updates, thus shadowing additional recruitment on INC trials, similar to experiment I.

In line with the suggested involvement of MFG in attentional orienting mechanisms, the peak coordinates of the activated MFG clusters are close to putative area FEF (x/y/z: -30/-4/49 in (Luna et al., 1998); distances: 10mm and 8mm for experiment I and experiment II respectively). Like SPL, FEF is part of the dFPN (Corbetta & Shulman, 2002) and involved in trial-by-trial top-down control processes to adjust the attentional focus (Macaluso & Doricchi, 2013). This is possibly implemented through connections to visual cortical regions (Ruff et al., 2008) in order to establish and continuously update a priority map coding the saliency of each location (Serences et al., 2005). Consistent with the current interpretation, enhanced activity in FEF on validly cued INC trials in experiment II suggests that spatial attentional mechanisms were involved due to attentional captures despite an initial feature-based search mode (see Greenberg et al., 2010).

The congruency contrast (INC > CON) with valid and invalid cueing yielded an additional cluster in experiment II located in bilateral occipital (including lingual) gyri. This may result from a generally enhanced recruitment of visual regions in experiment II, which is corroborated by findings showing that feature-based attention leads to higher activity in visual regions processing the attended feature dimension (Schoenfeld et al., 2007). Accordingly, there is stronger activation in response to distractors with target colors than those in irrelevant colors in visual regions that retinotopically corresponded to the distractor locations (Serences et al., 2005). This finding suggests that attention was captured by the flankers, which were always presented in the target color, introducing higher levels of saliency. Likewise, task-irrelevant color cues capture attention and thus activate the vFPN (Corbetta & Shulman, 2002) when they match with the color of a subsequent target stimulus, even when stimulus color is not response-relevant (Natale et al., 2010). Therefore, color cues sharing irrelevant task-set features appear to activate parts of the ventral attention network. In the present study, the distractors appeared in the same color as the target letter and may generally have captured attention in experiment II, especially if color was attended to (valid and invalid trials). Thus, the same occipital region found separately with valid and invalid congruency effects was also significantly active in a conjunction analysis of INC > CON pooled over valid and invalid feature-based trials. Likewise, the ERP data in experiment II demonstrated a parietooccipital negative voltage difference between INC and CON trials during the N200 time window, which is consistent with the ERP data of experiment I. The posterior negativity may originate in occipital brain regions, as there were complementary source waveform differences observable in RSs in lingual gyri in both experiments. Thus, lingual gyrus is part of color-sensitive visual area V4 (Allison et al., 1993; Gallant et al., 2000) and seems to be sensitive to both spatial and feature-based attention (Hayden & Gallant, 2009).

Considering the overlap in SPL and FEF activation in experiment I and II, it is likely that valid cueing initiated comparable attentional control mechanisms with spatial and color cues. A

recent neuro-cognitive framework of attention (Tian et al., 2014) assumes that visual cortical regions such as V4 communicate with both the ventral (TPJ) and the dorsal (SPL) frontoparietal network during attentional orienting. Accordingly, INC > CON clusters with a peak in left STG with valid cueing in experiment I (x/y/z = -40/-48/13) and in right STG in experiment II (x/y/z = 59/-46/19) overlap with posterior TPJ, as indicated by close proximity to TPJ locations reported in the literature (Igelstroem et al., 2015: mean TPJ coordinates = -57/-54/24 and 59/-48/19; distances: experiment I = 21.1mm; experiment II = 2mm). Given the concurrent clusters in left SPL/precuneus and FEF the observed fMRI pattern points towards a simultaneous involvement of two frontoparietal orienting networks in flanker conflict processing with valid cueing. Thus, the vFPN (TPJ) potentially received visual input about the stimulus color and shape (ventral visual stream; (Desimone et al., 1985), while the dFPN (SPL; FEF) probably processed spatial information (dorsal visual stream; Ungerleider & Mishkin, 1982). TPJ activity is generally considered to reflect bottom-up driven orienting reactions to salient and target-related information at unattended locations. Increased connectivity patterns from TPJ to FEF reported in the literature are considered to show that ventral attention regions signal violations of expectations to the dorsal network, which in turn executes reorientation mechanisms (Vossel et al., 2012). Here, TPJ may have been more active on valid INC trials in both experiments due to feedback signals to lingual gyri during detection of the perceptual mismatch on INC trials. Subsequent signals from TPJ to the dorsal network may in turn have initiated increased focusing as reflected in fMRI clusters in SPL and FEF.

Further clusters that were evident in the INC > CON contrast with valid cueing in experiment II were located in left-hemispheric precentral gyrus and insula/operculum, right STG, and in bilateral IPL and bilateral cingulate gyri. Activation of distinct regions between experiments implies that attending to features (experiment II) required a larger network of structures to overcome conflict compared to spatial cueing in addition to an overlapping frontoparietal control network. Some of these structures (insula; operculum; cingulate gyrus) form parts of

the cingulo-opercular network for task-set maintenance and feedback integration (Dosenbach et al., 2008). This hints at increased efforts to maintain the current task set when stimuli transmitted ambiguous information (INC trials). Thus, compared to experiment I, feature-based cueing initially involved globally directed attention promoting the processing of stimuli throughout the visual field including flankers. Given the concurrent clusters in bilateral IPL, parietal cortex might be the source of the feedback signal to cingulum and insula/operculum, as posterior parietal activity is associated with trial-by-trial control signaling (Dosenbach et al., 2008). The left ACC cluster was located in the rostral cingulate zone, which plays a role in response selection in ambiguous situations more generally (Nee et al., 2011). Therefore, it might reflect increased difficulties with regard to response selection or execution. Correspondingly, left ACC also showed a significant cluster in a conjunction analysis of INC > CON with both valid and invalid feature-based cueing, pointing towards similar conflict resolution mechanisms independent of cue validity. The concurrent cluster in precentral gyrus also suggests that response generation was more difficult or prolonged on INC compared to CON trials with feature-based cueing. Similarly, effective connectivity from ACC towards precentral gyrus on valid trials is enhanced during conflict trials, hinting at a role for ACC in facilitating response selection or execution (Fan et al., 2008).

Source waveform data of RSs overlapping anatomically with the fMRI clusters in ACC and precentral gyrus corroborate this assumption. Thus, differences between INC and CON trials started earlier in the RS in ACC (~440ms) than in precentral gyrus (~660ms) when cues were valid in experiment II. As the congruency effect in ACC occurred relatively late during stimulus processing, it may reflects conflict resolution, whereas precentral gyrus probably demonstrated enhanced source waveforms due to competing responses on INC trials. ACC signals were possibly transmitted to precentral gyrus in order to facilitate response selection (Fan et al., 2008).

By contrast, analogous RSs (ACC and precentral gyrus) in experiment I demonstrated a different temporal sequence of source waveform differences. Valid spatial cueing was first associated with INC > CON effects in precentral gyrus and subsequently in both RSs. This pattern was proposed to reflect the initial maintenance of two response alternatives (precentral gyrus) without conflict on validly cued trials due to early focusing mechanisms. Later INC > CON differences in both RSs (precentral gyrus and ACC) were interpreted as a reactivation of both response channels after selection of the correct response when the attentional window broadened.

On the other hand, during invalid trials there were apparently stronger conflict processing signals in experiment I compared with II. Thus, while early source waveform differences in both ACC and precentral gyrus were observable with spatial cueing potentially due to conflict detection, there were only late differences originating in the precentral gyrus RS in the feature-based experiment. This may be caused by control mechanisms coming from IFG, as there was enhanced source activity towards INC stimuli starting relatively early (~180ms). Due to an initial global search mode, the flanker stimuli potentially initiated control signals from IFG to ACC in order to prepare for the conflict. Later effects originating in precentral gyrus may therefore reflect conflict during response selection. In experiment I in turn, increased responses arising in the IFG RS were also observable, but these occurred later than in experiment II, possibly during conflict resolution. Accordingly, ACC and IFG demonstrated simultaneous source waveform differences followed by enhanced activity originating in precentral gyrus in experiment I, which hints at response conflict processing.

4.4.3 Critical reflections

The present experimental designs provide only an indirect comparison between studies due to differing source models. Even though the discussed sources (ACC; precentral gyrus; lingual gyri; IFG) were in close proximity to each other, each RS's waveform pattern is contingent

upon the contribution of all other sources (Scherg, 1990). Hence, additional sources that were not discussed here may have affected the observed source waveform patterns in different ways depending on the respective source model and therefore on the experiments.

Moreover, in the comparison of the present flanker studies with spatial and feature-bases attention, distinct conflict processing styles are postulated. However, the bootstrap 95% confidence interval in the RS in ACC on invalidly cued trials was much larger in experiment II than I, hinting at larger variabilities between individual source waveform patterns. This was particularly evident between 500-600ms, when the RS in precentral gyrus demonstrated congruency effects. Therefore, conclusions based on an absent difference between conditions in ACC cannot be drawn unequivocally. Source waveforms originating in the precentral gyrus RS demonstrated INC > CON differences around 580ms, hinting at a response conflict similar to that observed with valid cueing. It is therefore conceivable that ACC demonstrated simultaneous source waveform differences as well, but only at a subthreshold level due to interindividual differences. ACC appears to be active during strategic adaptations based on previous trial history (Gratton et al., 1992) and is additionally involved in within-trial adjustments (Botvinick et al., 2001). Such on-line modulations are apparently contingent on individual response styles, leading to increased variabilities of signals arising in ACC (Labrenz et al., 2012).

A potential confounding factor that challenges the present interpretations is the use of different numbers of individuals between experiments. Due to high levels of artefacts in the EEG as well as the fMRI data, the final sample size included in experiment I was reduced to 19 participants available in the fMRI analysis and 18 participants for the ERP and source analyses, whereas 21 data sets were included in in all analyses of experiment II. Sample size is a crucial factor influencing the power of statistical tests, which affects the potential to detect differences between conditions (Kähler, 2008). Therefore, the fact that the clusters found in experiment II

during fMRI analysis were larger and more distributed may partly be due to statistical factors and would thus be unrelated to the attentional manipulation per se.

4.4.4 Conclusions

Comparing the effects of different attention modes (spatial; feature-based) on flanker interference processing delivered a similar recruitment of frontoparietal brain structures but distinct conflict processing mechanisms.

Overlapping activity between experiments in the INC > CON contrast with valid cueing in SPL and putative FEF hints at a general dFPN for top-down control of conflict processing. While correct spatial attention probably involved early attentional window adjustments in order to suppress flankers, globally directed feature-based attention may initially have involved attentional captures to the stimulus location followed by similar focusing processes as in experiment I. Flexible window adjustments in both experiments are additionally corroborated by overlapping activity in TPJ, which possibly triggered violations of expectations to FEF both with regard to locations (experiment I) and colors (experiment II). Invalid cueing yielded no congruency effects in SPL or FEF, possibly because activity in these regions was generally enhanced due to attentional reorientation (experiment I) or updating of the attended color (experiment II). This may in turn have shadowed additional activity increases towards INC flanker stimuli, which parallels a postulated ceiling effect on invalid trials in the behavioral data leading to similar flanker effect sizes as on valid trials.

Conflict processing additionally activated ACC and precentral gyrus with valid cueing in experiment II, and source waveform data from these regions hint at a response-based stage of conflict. The reason for this might be more difficult response selection because of enhanced initial activation of competing response channels in experiment II in comparison with experiment I because of an initial global search mode.

5. SPATIAL AND FEATURE-BASED ATTENTION IN THE PRESENT EXPERIMENTS

5.1 Introduction

During flanker task processing in the present experiments, a common network of frontoparietal structures was observable. In order to substantiate the suggested mechanisms exerted during spatial and feature-based attention, it is important to investigate directly which brain regions were recruited during the different attention modes in the present study and to compare their time courses.

5.1.1 Sources of spatial and feature-based attention

Brain regions demonstrating sensitivity to selective attention may be divided into source and target regions. Sources presumably exert attentional control over target regions by modulating their neuronal response patterns (Yantis, 2008). In visual selective attention, these modulations primarily occur in (extra)striate cortices (Yantis, 2008). As discussed previously (see section 4.4.2), several networks of attention have been identified predominantly in frontal and parietal cortices, which regulate various functions including endogenous orienting (FEF; SPL; Macaluso & Doricchi, 2013; Petersen & Posner, 2012), shifts of attention (MFG; IPS; Greenberg et al., 2010), and task set maintenance (cingulum; insula; Dosenbach et al., 2008). Although regions such as FEF or IPS display a topographical organization, i.e. neighboring locations in the visual scene are mapped onto adjacent cells of the cortical surface (Bisley, 2011), they are also active during feature-based attention (Serences & Boynton, 2007; Vossel et al., 2014). This activity pattern hints at a domain-general frontoparietal network for attentional control (Wojciulik & Kanwisher, 1999). However, while bilateral SFG, MFG, and posterior parietal cortex generally demonstrate overlapping activity during cue periods based on location as well as colors, spatial information leads to stronger activity levels in dorsal

portions (SFG; MFG; SPL) contralateral to the cued location (Giesbrecht et al., 2003). This pattern either may suggest a superior role for locations or an additional domain-specific component of both attention types. Thus, higher activity in frontoparietal structures during spatial cueing may reflect domain-specific covert orienting mechanisms as corroborated by a lateralized activation pattern. By contrast, parietal regions overlapping between attention modes are discussed in the context of task-set maintenance with regard to the relevant dimension (location; color (Giesbrecht et al., 2003).

5.1.2 Targets of spatial and feature-based attention

Although spatial and feature-based attention target overlapping regions such as area V4, they have distinct effects on the neuronal population response (Carrasco, 2011). A possible outcome of such a modulation is a response *gain* with generally enhanced responses of those neurons preferentially processing the target item (e.g. vertical lines in area V4), reflecting a multiplicative effect on all stimuli (e.g. all orientations) including those that are non-preferred (Williford & Maunsell, 2006). By contrast, response *tuning* refers to a higher level of selectivity so that responses to non-preferred stimuli including those with similar properties as the target stimulus are suppressed (Ling et al., 2009). Moreover, several studies found attention-induced enhancements of neuronal activity in striate and extrastriate cortices without stimulus presentation, hinting at increased *baseline* levels triggered by attention (Kastner et al., 1998; Luck et al., 1997).

Response patterns during spatial and feature-based attention under different degrees of competition (i.e., presentation of targets among non-preferred items) suggest that in addition to baseline increases (David et al., 2008) spatial selection is based on a response gain, leading to beneficial effects at low levels of competition. Selection of features apparently also initiates involves baseline increases (David et al., 2008) and involves narrower tuning curves leading to better performance when there is a large amount of competing stimuli. Moreover, there appears

to be an additional gain mechanism for all stimuli (Ling et al., 2009; but see White & Carrasco, 2011). The latter is consistent with findings of reduced feature-based attentional benefits in the absence of competition in the literature (Saenz et al., 2003; but see Baldassi & Verghese, 2005; Ling et al., 2009). In line with empirical findings, the feature-similarity gain model postulates bidirectional attentional effects, i.e. both firing rate increases (gain mechanism), but only in response to features preferentially processed by a neuron, and decreases when a non-preferred feature is attended to (tuning mechanism; (Martinez-Trujillo & Treue, 2004). In contrast to pure gain models, feature-similarity gain therefore assumes non-multiplicative modulations (Carrasco, 2011).

5.1.3 Temporal characteristics of spatial and feature-based attention

Gain and competition mechanisms demonstrate distinct time courses, with earlier gain effects and subsequent competition in visual neurons (Maunsell & McAdams, 2001). This pattern possibly reflects gain mechanisms in early visual areas that are fed forward to extrastriate regions where competition occurs due to larger and thus overlapping receptive fields (Andersen & Mueller, 2010). Accordingly, extrastriate visual areas demonstrate larger BOLD signal increases during focused attention than striate cortex (Kastner et al., 1999; Maunsell & Cook, 2002), which may result from accumulated feed-forward signals along the visual stream that are additionally boosted by attention (Carrasco, 2011).

Receptive field size increases from striate to extrastriate cortices may result in temporal differences between both attention types. Spatial attention is restricted to particular locations that are processed by neurons already in early striate regions with small receptive fields processing the currently attended location (Carrasco, 2011). Feature-based attentional benefits are global across the entire visual field and therefore require integration of signals in extrastriate cortical neurons at later stages. Accordingly, spatial and feature-based attentional effects demonstrated additive, i.e. independent effects on areas of the ventral and the dorsal stream in

electrophysiological studies (Saenz et al., 2006; Treue & Martinez Trujillo, 1999), though a small super-additive component in area V4 suggests some degree of interaction (Hayden & Gallant, 2009).

Neuronal enhancement and suppression mechanisms are also visible in the time course of attention reflected in distinct ERP components. Selection based on spatial information yields modulations of early ERP components including a positivity (P1; 80-120ms) and a subsequent negativity (N1; 150-190ms) at contralateral posterior electrodes sites in response to targets at attended locations (Hillyard & Muente, 1984). The P1 is assumedly a sign of active suppression of unattended locations as indexed by decreased amplitude values on invalid compared to neutral trials, whereas the N1 appears to reflect sensory gain mechanisms of neurons processing the attended location given enhanced amplitude values on valid trials (Hillyard et al., 1998).

Enhancement and suppression of unattended material is also evident during feature-based selection, reflected in modulations of the P1 component (Moher et al., 2014) and of neuronal firing rates (Martinez-Trujillo & Treue, 2004). Still, enhancement of attended features evolves later (~220ms) than during spatial attention and precedes suppression (~360ms; Andersen & Mueller, 2010). Furthermore, a selection negativity (SN) was identified for selection based on features (Harter et al., 1982) which demonstrates enhanced negative amplitude values at posterior electrode sites in response to attended compared to unattended features (McGinnis & Keil, 2011). The SN typically peaks between 160-360ms (Hillyard & Muente, 1984), though latencies may vary between feature dimensions (e.g. between color and motion direction; (Anllo-Vento & Hillyard, 1996). Finally, the P300 is also sensitive to attentional manipulations and peaks between 300-800ms (Rugg & Coles, 1997). It occurs after perceptual stimulus analysis and may reflect updating of the internally represented context in response to external stimulation (Donchin & Coles, 1988; Polich, 2007).

5.1.4 Objectives

In both experiments, the same basic task was applied with identical timings and physical stimulations except for the cue words. Here, the effects of spatial and feature-based attention on fMRI and ERP activity patterns were investigated and directly compared with each other. For this purpose, joint analyses of the fMRI and ERP data were conducted. As the source models differed between experiments with several distinct RSs that were active in only one but not the other, a direct comparison of source waveforms was not possible.

Whereas spatial attention has been investigated extensively, leading to the formulation of several neuronal models including the frontoparietal networks (Corbetta & Shulman, 2002; Dosenbach et al., 2008) less is known about the sources of feature-based attention (Mazer, 2011). Here, similar activity patterns were expected for both experiments with regard to the contrasts invalid > neutral and valid > neutral reflecting attentional shifts and facilitation respectively. These assumptions are based on findings in the literature suggesting that similar brain regions may be recruited by both attention types (Greenberg et al., 2010; Liu et al., 2011).

Concerning the ERP data, the SN as well as the P300 component were analyzed. Earlier components such as the P1 or N1 could not be considered, because both require a vast amount of repetitions per condition in order to detect differences between conditions (Luck, 2005b). This could not be realized given the number of conditions included in the present experiments.

5.2 Data analysis

5.2.1 Behavioral data

The RTs of both studies were analyzed in a repeated-measures ANOVA using the within-subject factors *cue validity (valid/neutral/invalid)* x *flanker congruency (CON/INC)* x *method (EEG/fMRI*) and the between-subjects factor *attention mode* (*spatial/feature-based*). Post hoc analyses were conducted using unpaired t-tests (α=0.05; Bonferroni-Holm correction).

5.2.2 fMRI data

To compare spatial and feature-based attention effects in the present studies the single-subject contrasts of the six experimental conditions (three validity levels x two congruency levels) from both experiments (experiment I = 19 participants; experiment II = 21 participants) were analyzed with a random-effects analysis. For this purpose, a full factorial design was set up with the factors *attention mode (spatial/feature-based)*, *cue validity (valid/neutral/invalid)* and *congruency (CON/INC)*. For each attention mode, separate contrasts were defined including attentional switches (invalid > neutral), facilitation (valid > neutral), and a contrast directly comparing these mechanisms (invalid > valid), with all contrasts pooled over congruency levels. Moreover, for each of these comparisons a conjunction analysis over both attention modes was computed. The significance threshold was $p<.001$ (uncorrected) with an extent threshold of $k\geq10$ voxels.

The MNI coordinates of all peaks and sub-peaks were transformed into Talairach space (‘mni2tal.m’; http://imaging.mrc-cbu.cam.ac.uk/imaging/MniTalairach) and their anatomical locations were derived from the ‘Talairach Daemon Client’ software (http:// http://www.talairach.org/daemon.html) and the automated anatomical labeling toolbox (‘AAL‘; http://www.gin.cnrs.fr/AAL-217?lang=en).

5.2.3 ERP data

All analyses were based on mean amplitude values and included the within-subject factors *cue validity (valid/neutral/invalid)* and *flanker congruency (CON/INC)* and the between-subject factor *attention mode (spatial/feature-based)*. Differences between cueing types during the SN were analyzed from 200-300ms with the additional factors *frontality (F/C/P/PO)* and *laterality (left/midline/right).* The P300 was investigated between 300-400ms using the additional factor *frontality (Fz/Cz/Pz)*. In cases where the between-subject factor *attention mode* yielded significant effects, unpaired t-tests were computed on the difference waves between invalid and neutral cueing as well as between valid and neutral cueing. For all other post hoc tests, paired t-tests pooled over the factor *attention mode* were applied. All t-tests were based on a Bonferroni-Holm corrected standard threshold ($\alpha = .05$).

5.3 Results

5.3.1 Behavioral data

A repeated-measures ANOVA was conducted with the within-subject factors *cue validity (valid/neutral/invalid)* x *flanker congruency (CON/INC)* x *method (EEG/fMRI*) and the between-subjects factor *attention mode* (*spatial/feature-based*).

There was a main effect of *method* ($F_{[1; 38]} = 150.3$, $p < 0.001$) with significantly higher RTs in the fMRI compared to the EEG session ($t_{[39]} = 12.4$, $p<.001$; mean ±SD: fMRI = 595 ±71; EEG = 532 ±77ms; see Table 10). The main effect of *cue validity* ($F_{[1.7; 63.2]} = 24.4$, $p<.001$) was reflected in a RT pattern of invalid (576 ±77ms) > neutral (564 ±74ms) > valid (550 ±70ms) trials ($t_{[39]} = 5.5$, $p<.001$, $t_{[39]} = 4.3$, $p<.001$, and $t_{[39]} = 3.5$, $p<.005$ for invalid > valid, neutral > valid, and invalid > neutral trials respectively). The *congruency effect* was also significant ($F_{[1;38]} =136.0$; $p<.001$) with higher RTs in the INC condition ($t_{[39]} = 11.3$, $p<.001$; INC = 580±70ms; CON = 546±76ms; see Figures 14 and 15). Furthermore, the factors *method* and *congruency* significantly interacted ($F_{[1;38]} = 5.4$, $p<.05$). Post hoc paired t-tests showed that this interaction was caused by a larger flanker effect in the EEG sessions compared to the fMRI sessions ($t_{[39]} = 2.4$, $p<.05$; flanker effects: EEG = 36 ±19ms; fMRI = 32 ±22ms). There were no other significant effects and no interactions with the factor *attention mode*.

Table 10: Summary of the mean reaction times (RTs) and error rates (top and bottom respectively) with standard deviations (SD) of the cueing conditions pooled over congruency levels during the EEG (left) and the fMRI session (right). N = 19 (experiment I); N = 21 (experiment II).

		EEG			fMRI		
	condition	**spatial**	**feature-based**	**total EEG**	**spatial**	**feature-based**	**total fMRI**
RTs [ms] ± SD	**valid**	508.2 ± 74.4	528 ± 74.8	518.6 ± 74.3	569.1 ± 71.9	591.2 ± 67.8	580.7 ± 69.8
	neutral	523.7 ± 80.5	537.8 ± 76.2	531.1 ± 77.6	587.9 ± 75.4	603.7 ± 72.2	596.2 ± 73.2
	invalid	544.4 ± 87.9	546.3 ± 83	545.4 ± 84.3	602.9 ± 69.7	610.6 ± 79.5	607 ± 74.2
error rates [%] ± SD	**valid**	4.9 ± 3.2	3.7 ± 2.5	4.3 ± 2.9	4.6 ± 4.5	4 ± 2.4	4.3 ± 3.5
	neutral	4.4 ± 2.4	3.8 ± 2.4	4.1 ± 2.4	3.6 ± 3.3	4.2 ± 2.6	3.9 ± 2.9
	invalid	5.3 ± 2.7	4.6 ± 3.9	4.9 ± 3.4	3.7 ± 3.6	6.5 ± 3.5	5.2 ± 3.8

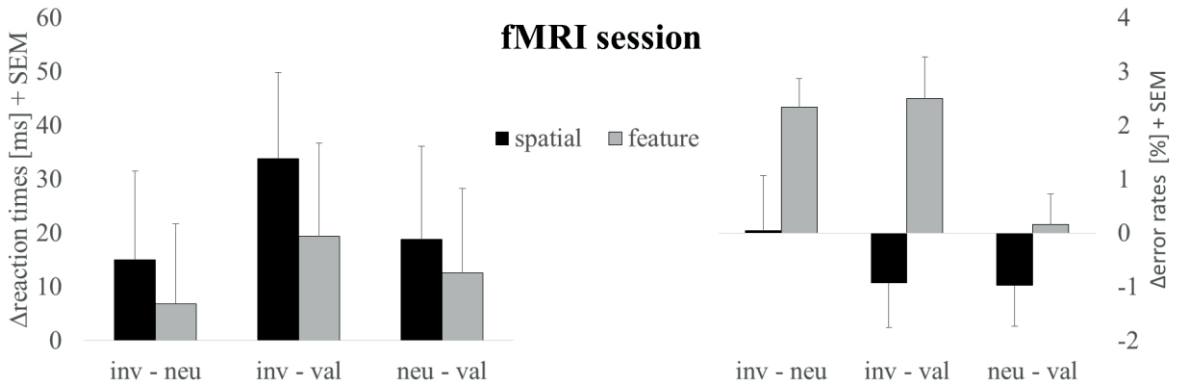

Figure 14: fMRI session: Differences of the reaction times (left) and percent error rates (right) between the single cueing conditions during experiment I (black) and experiment II (medium grey). Error bars show standard error of the mean (SEM). inv = invalid; neu = neutral; val = valid; N = 19 (experiment I); N = 21 (experiment II).

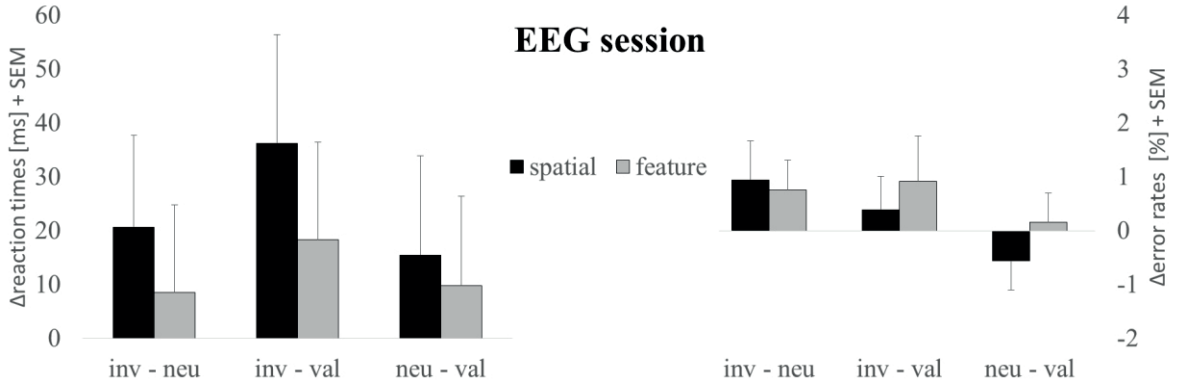

Figure 15: EEG session: Differences of the reaction times (left) and percent error rates (right) between the single cueing conditions during experiment I (black) and experiment II (medium grey). Error bars show standard error of the mean (SEM). inv = invalid; neu = neutral; val = valid; N = 19 (experiment I); N = 21 (experiment II).

5.3.2 fMRI data

In the spatial attention mode, contrasting invalid > valid activated clusters in bilateral IFG and IPL, left MFG (including precentral gyrus), SPL (including precuneus), STG/MTG, and SMA, as well as right SFG, MFG, and MOG. The invalid > valid clusters with feature-based attention spread over SFG, SMA, IFG, and IPL of the right hemisphere (see Table 11). There were no overlapping clusters between these contrasts in a conjunction analysis.

Table 11: Talairach peak coordinates of significant activation clusters for the comparisons of invalid > neutral and valid > neutral conjunct over both attention modes and pooled over congruency levels and for the comparison of invalid > valid separately for each attention mode. r = range of nearest grey matter (mm); BA = Brodmann area; (p<.001, k≥10 voxels). N = 19 (experiment I); N = 21 (experiment II).

contrast	cluster size	t-value	r	peak coordinates (Talairach space)			side	anatomical region (BA)
invalid > neutral (conjunction)	392	5.4	2	10	16	56	R	Superior Frontal Gyrus (6)
		4	0	2	20	49	R	Superior Frontal Gyrus (8)
	513	5.2	1	50	15	-2	R	Inferior Frontal Gyrus (47)
		4.2	1	40	25	-6	R	Inferior Frontal Gyrus (47)
	17	3.7	1	48	8	46	R	Middle Frontal Gyrus (6)
	24	3.6	0	63	-39	31	R	Inferior Parietal Lobule (40)
	51	3.5	2	-53	-45	37	L	Inferior Parietal Lobule (40)
valid > neutral (conjunction)	94	3.6	1	57	18	2	R	Inferior Frontal Gyrus (45)
		3.6	2	49	8	4	R	Superior Temporal Gyrus (22)
		3.6	0	42	14	-2	R	Insula (13)
invalid > valid (spatial)	306	5.1	1	-34	2	50	L	Middle Frontal Gyrus (6)
	165	4.8	0	-8	-50	47	L	Precuneus (7)
	383	4.3	1	-50	19	21	L	Inferior Frontal Gyrus (9)
		4.1	0	-44	21	30	L	Middle Frontal Gyrus (9)
		4	1	-46	17	-1	L	Inferior Frontal Gyrus (47)
	230	4.1	3	-53	-46	19	L	Superior Temporal Gyrus (13)
		3.3	4	-44	-49	26	L	Superior Temporal Gyrus (39)
	60	4.1	1	-4	16	54	L	Superior Frontal Gyrus (6)
	93	3.9	1	53	-47	32	R	Supramarginal Gyrus (40)
		3.4	2	46	-45	32	R	Supramarginal Gyrus (40)
		3.3	1	63	-45	28	R	Supramarginal Gyrus (40)
	40	3.5	0	44	11	34	R	Middle Frontal Gyrus (9)
	10	3.4	3	24	1	50	R	Sub-Gyral (6)
	14	3.4	0	-24	-48	43	L	Precuneus
	31	3.4	1	32	-70	33	R	Precuneus
	10	3.4	3	-36	-39	33	L	Supramarginal Gyrus (40)
invalid > valid (feature-based)	115	4.5	2	10	16	56	R	Superior Frontal Gyrus (6)
		3.6	2	8	22	45	R	Medial Frontal Gyrus (8)
	15	3.9	1	18	58	25	R	Superior Frontal Gyrus (10)
	47	3.6	0	-16	-36	-23	L	*
	21	3.6	0	34	29	-10	R	Inferior Frontal Gyrus (47)
	21	3.5	2	57	-51	36	R	Inferior Parietal Lobule (40)

To distinguish correctly directed top-down attention from bottom-up reorientation, valid and invalid trials were separately contrasted against neutral trials. Correctly directed spatial attention (valid > neutral) was associated with significant BOLD signal increases in bilateral SFG, IFG (pars opercularis), SPL (including precuneus), SMA, and IPL, in left precentral gyrus as well as STG, and in right MFG. Validly cued feature-based trials showed suprathreshold

activation in right IFG (pars opercularis) and insula. The same cluster were evident in a conjunction over both attention modes for the valid > neutral contrast (see Figure 16).

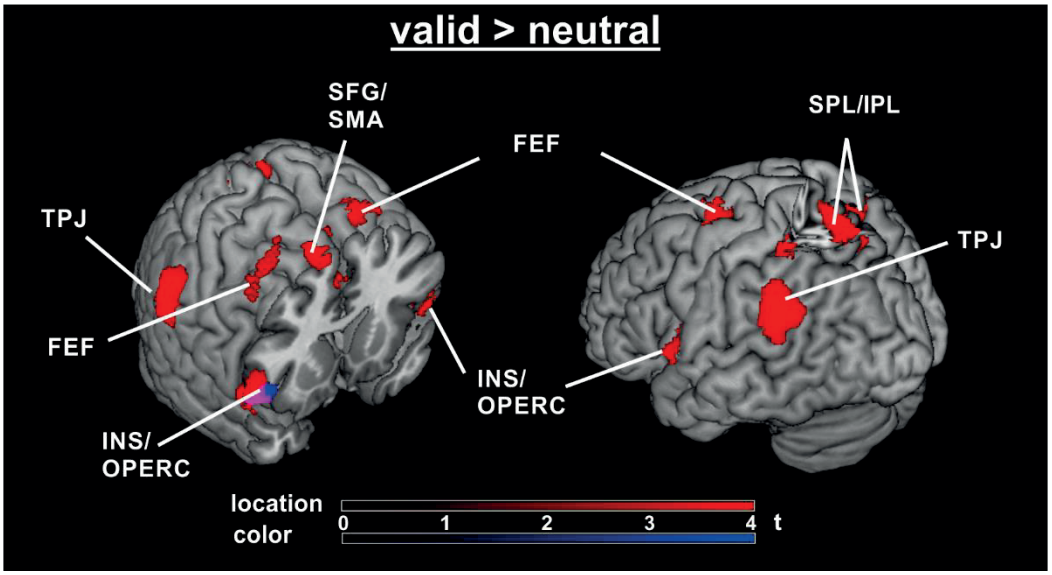

Figure 16: Overlay of activation clusters derived from the contrasts valid > neutral with spatial (red) and feature-based cueing (blue) thresholded at p<.001, k≥10. N = 19 (experiment I); N = 21 (experiment II).

Labels:
FEF = frontal eye field
INS = insula
IPL = inferior parietal lobule
OPERC = operculum
SFG = superior frontal gyrus
SMA = supplementary motor are
SPL = superior parietal lobule
TPJ = temporoparietal junction

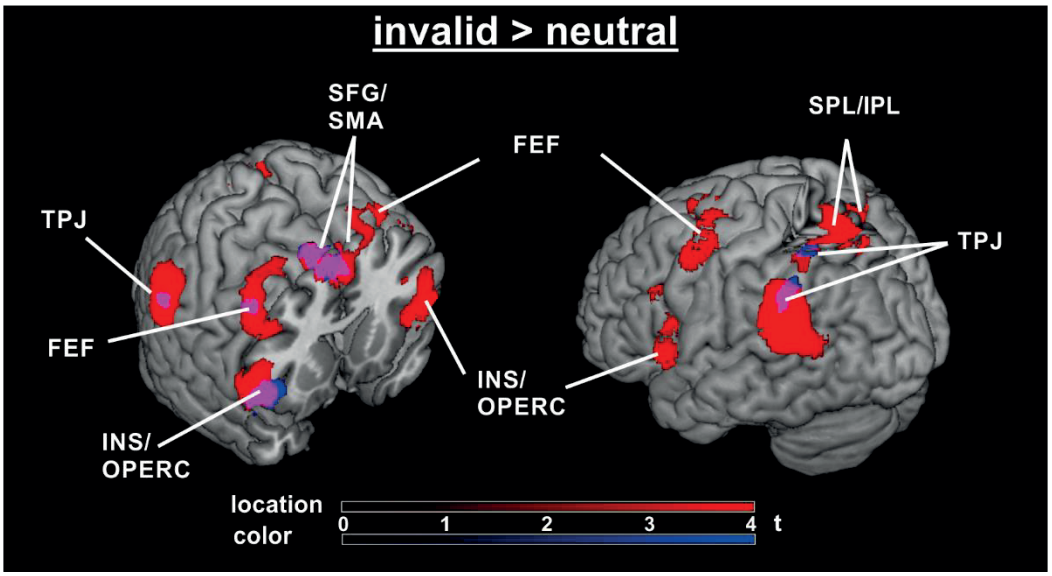

Figure 17: Overlay of activation clusters derived from the contrasts invalid > neutral with spatial (red) and feature-based cueing (blue) thresholded at p<.001, k≥10. N = 19 (experiment I); N = 21 (experiment II).

Switching attention to the correct location (invalid > neutral) mainly activated a frontoparietal network with clusters in bilateral SFG, MFG (including precentral gyri), IFG (pars opercularis), SMA, SPL (including precuneus), IPL, and MOG, as well as left insula, MTG, and SOG, and right STG. Attentional recalibration during invalidly cued feature-based trials led to activation in bilateral MFG (including precentral gyri), IFG, insula, SMA, and IPL, in left-hemispheric SPL, and in right MTG. A conjunction over both contrasts showed that these structures partly overlapped namely in bilateral SMA and IPL as well as right IFG, insula, and MFG (including precentral gyrus; see Figure 17).

5.3.3 ERP data

The present ERP analyses are based on mean amplitude values and include the repeated measures ANOVA within-subject factors *cue validity (valid/neutral/invalid)* and *flanker congruency (CON/INC)* and the between-subject factor *attention mode (spatial/feature-based)*.

During the SN, the within-subject factor *cue validity* interacted with electrode site *(cue validity x laterality x frontality*: $F_{[5.5;202.9]} = 2.2$, $p<.05$). The difference waves of invalid > neutral and valid > neutral both demonstrated enhanced positive amplitude values at central electrodes and a concurrent negativity at parietooccipital sites. Paired t-tests on these difference waves per electrode yielded significant results at electrodes C3 (invalid > neutral: $t_{[38]} = 4.1$, $p<.005$; valid > neutral: $t_{[38]} = 4.4$, $p<.005$), Cz (invalid > neutral: $t_{[38]} = 5.53.1$, $p<.005$; valid > neutral: $t_{[38]} = 3.3$, $p<.005$), and PO8 (valid > neutral: $t_{[38]} = -3.6$, $p<.005$).

During the P300 time window there was a main effect of the factor *validity* ($F_{[2;74]} = 20.2$, $p<.005$, and this interacted with *attention mode* ($F_{[2;74]} = 11.4$, $p<.005$). Paired t-tests confirmed significantly higher amplitude values during invalid as well as valid cueing compared to neutral cueing ($t_{[38]} = 5.3$, $p<.001$ and $t_{[38]} = 3.9$, $p<.001$ respectively). Unpaired t-tests on these difference waves with *attention mode* as between-subject factor showed only subthreshold results (see Figure 18 and Appendices Q and R).

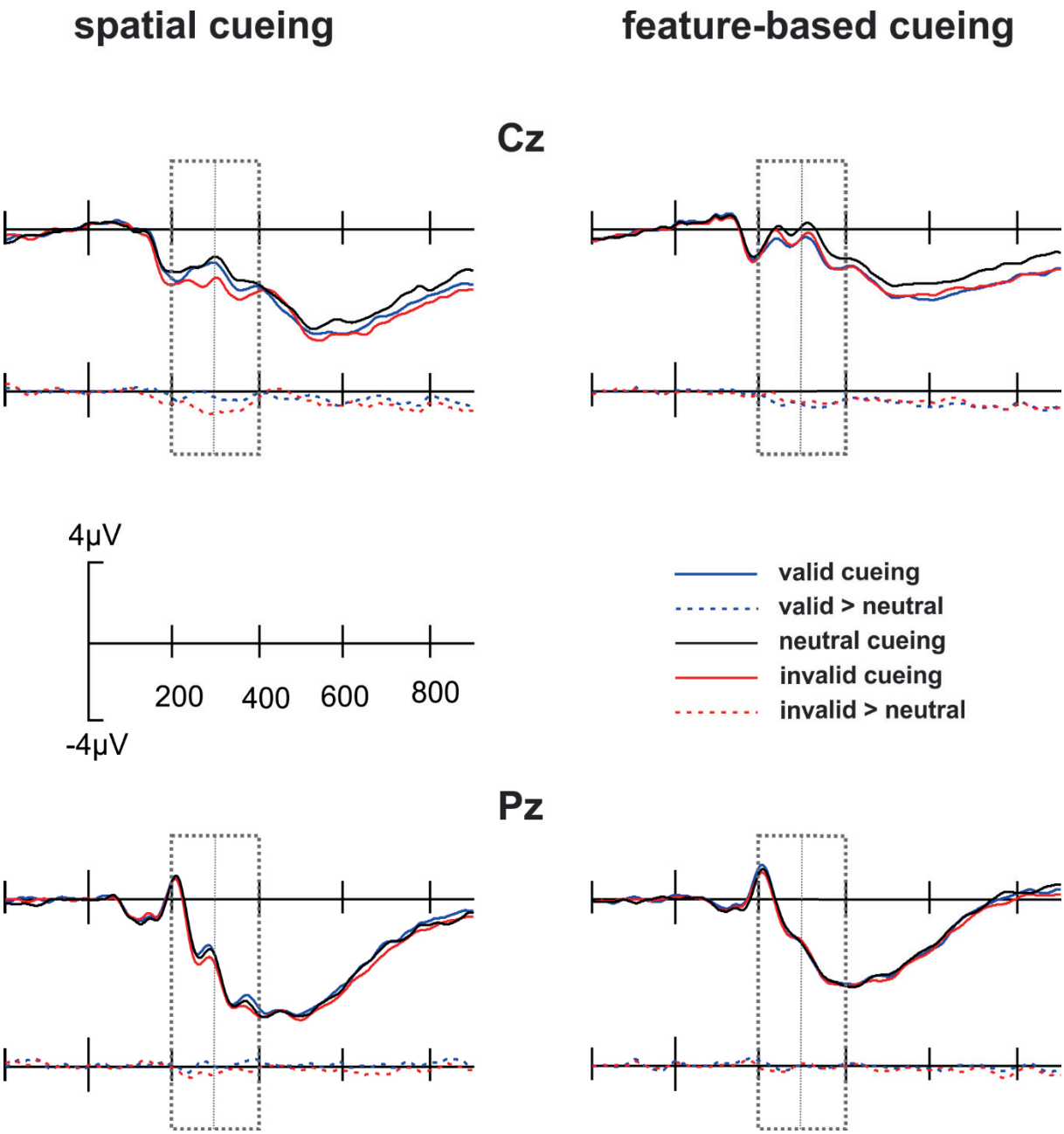

Figure 18: Group ERPs (solid lines) and difference waves (dotted lines) during different attentional processing states: ERPs (stimulus-locked grand average: -200ms to 900ms) of valid (blue), neutral (black), and invalid (red) trials with spatial (left) and feature-based cueing (right) at electrode positions Cz (top) and Pz (bottom). Difference waves during facilitation (valid > neutral) and reorientation (invalid > neutral) are plotted below the grand averages. Boxes indicate analyzed time windows (left = SN; right = P300 respectively). N = 18 (experiment I); N = 21 (experiment II).

5.4 Discussion

5.4.1 Behavioral data

In the RT analysis of the present studies, there were significant reorientation (invalid > neutral) as well as top-down facilitation effects (valid < neutral). These results confirm that the neutral cueing manipulation was indeed uninformative and did not differ perceptually or conceptually from valid or invalid cues. Thus, when introducing a baseline condition in order to separate beneficial effects from response costs, it should not differ from the conditions of interest (valid and invalid cueing respectively) in terms of confounding factors such as alertness levels, frequency of appearance or perceptual properties; (see Chica et al., 2014). These findings strengthen the conclusions drawn from the neurophysiological data analyses with regard to reorientation and facilitation mechanisms.

Comparing the present experiments, the behavioral indices did not significantly differ between spatial and feature-based attention. Both studies led to comparable amounts of attention effects. This is in line with previous findings of comparable cueing effects between both attention types (Egner et al., 2008), though feature cueing effects might be restricted to those locations currently attended to (Stoppel et al., 2007), as opposed to findings of global feature-based attention (Liu & Mance, 2011; Störmer & Alvarez, 2014). In general, there are discrepant findings in the literature with regard to feature-based attentional influences on performance, as putative beneficial effects (e.g. Baldassi & Verghese, 2005) may alternatively be explained by the guidance of spatial attention based on attended features (Shih & Sperling, 1996). When controlling for such spatial confounding factors, Liu et al. (2007) identified location-independent effects of feature cues and separable time courses. Thus, spatially directed attention improved performance already 300ms after cue presentation, whereas feature-based cueing benefits showed up around 500ms, though with the same magnitude as spatial cueing. Similarly, when cueing the color of objects presented above or below fixation in red or green (as in the

present study) and associating each location primarily with one of the colors so that cues simultaneously also predict the likely location, performance is better for invalid colors at the location associated with the precued color. This was interpreted as a selection mechanism based on color information rather than location (Lambert & Corban, 1992). However, in displays with more possible target locations selection probably occurs by spatial information, though feature-based attention may initially guide attention to locations containing a cued feature (Vierck & Miller, 2008).

A further finding in the behavioral data pattern is the fact that attention effects were significant despite equal cue probabilities. The present study thus confirms that cues can be effective even when they are statistically uninformative. Equal frequencies of valid and invalid trials are particularly relevance because they allow an independent analysis of reorienting mechanisms (invalid > neutral) without violations of expectations due to oddball effects (Macaluso & Doricchi, 2013). Such reorientation effects may be ascribed to pure reflexive orienting without volitional control (Ristic et al., 2006). However, Hommel et al. (2001) could show that both arrow cues and semantic cues ('left'; 'right') that are uninformative lead to facilitation in a way that is consistent with attentional control processes rather than unintentional orienting. Moreover, uninformative arrows involuntarily cause a shift of attention when they are presented in the target color, suggesting an influence of top-down selection (task-set, Pratt & Hommel, 2003). However, none of these studies directly manipulated attention to features as an independent variable. The present results therefore add to existing knowledge about attentional mechanisms by showing that uninformative feature cues lead to comparable attention effects as spatial cues. It is nevertheless important to consider the underlying spatial and temporal response patters generated in the brain, because such data may be more sensitive to attentional processes and can therefore complement conclusions based on RTs (Wilkinson & Halligan, 2004)

5.4.2 Neurophysiological data

Comparing spatial and feature-based cueing effects in a joint fMRI analysis revealed common as well as distinct effects of the different validity levels. Reorienting of attention after invalid cues seems to rely on largely overlapping structures independent of attention mode, and valid and invalid cueing both seem to activate a common network for the detection of the attended stimulus attribute. However, feature-based attentional direction probably involved additional spatial attentional captures by stimulus locations. In both experiments, there were similar temporal courses of activity, as demonstrated by similar attention effects irrespective of attention mode during the SN and P300 time windows.

In experiment I (spatial attention), there were fMRI clusters located in structures of the frontoparietal networks during reorientation on invalid trials as well as during attentional facilitation on valid trials (both compared to neutral cueing), including bilateral SFG, MFG, precentral gyri, SPL (dorsal network), IFG, and IPL (ventral network). In the literature, structures of the dorsal network demonstrate enhanced activity in response to repeated distraction, whereas ventral structures show the reverse pattern (stronger activity with low distraction frequencies, Casey et al., 2000). This might reflect distinct contributions of the networks to adjust the attentional window, with the dorsal network triggering a narrower focus and the ventral network initiating a more global search mode (Casey et al., 2000). The present results pattern in the spatial cueing study corroborates this claim, because both valid and invalid trials probably involved attentional adjustments compared to neutral trials. As previously suggested (see sections 3.4.2 and 4.4.2), validly cued trials either may have led to a narrower (INC flanker stimuli) or a broader focus of attention (CON flanker stimuli). As the clusters were pooled over congruency levels, there processes may together account for activity in the dorsal and ventral networks respectively. Moreover, invalid spatial cueing initially required reorientation to the target location, potentially activating ventral structures during bottom-up captures (ventral network) followed by a location shift (dorsal network).

Vossel and colleagues (2014) suggest an interactive involvement of both networks in top-down and bottom-up attentional processing. Thus, during focused attention (valid cueing) connections from dorsal to ventral structures were found to inhibit processing of distracting information that is not target-related (DiQuattro et al., 2014), whereas distractors that carry target-relevant information do elicit ventral frontoparietal activity (Geng & Mangun, 2011). Likewise, in experiment I of the present studies spatially directed attention possibly enhanced activity in dorsal structures, leading to initial inhibition of the ventral network in order to focus attention on the target location. However, shortly after stimulus onset ventral regions probably showed activity due to the saliency of the flanker stimuli both on valid and invalid trials, with an additional signal enhancement in ventral and dorsal regions on invalid trials as attention shifted to the correct target location (Corbetta et al., 2008; Kincade et al., 2005). Consequently, invalid cueing should lead to stronger BOLD signal increases during stimulus processing than valid cueing in frontoparietal structures. Indeed, clusters in the comparison invalid > valid largely overlapped with the contrast invalid > neutral in the dorsal network (bilateral MFG, left SPL, right SFG) and in ventral regions (bilateral IFG and IPL). Stronger activation in frontoparietal regions towards reorientation on invalidly cued trials than to attentional facilitation on valid trials are also reported in the literature (Corbetta & Shulman, 2011).

In the feature-based cueing experiment (II), attentional recalibration mechanisms (invalid > neutral) yielded activation clusters in similar frontoparietal regions as in experiment I (bilateral MFG, IFG, and IPL, left SPL). A conjunction over both studies showed an overlap in bilateral IPL as well as right IFG and MFG. In keeping with these results, findings in the literature suggest that reorientation to unattended locations (spatial attention) and attentional recalibration mechanisms (feature-based attention) recruit partly overlapping frontoparietal structures, including SPL, FEF, and MFG (Greenberg et al., 2010; Liu et al., 2011). In the present study, overlapping clusters between attention modes in right MFG/precentral gyrus (invalid > neutral) were located in putative area FEF (x/y/z: conjunction = 48/8/46; Luna et al., 1998: 34/-3/47;

distance = 18mm). In addition, structures located in bilateral TPJ showed common activation among spatial and feature-based reorienting of attention (conjunction between spatial and feature-based attention in the contrast invalid > neutral = -53/-45/37 and 63/-39/31; (Igelstroem et al., 2015: -57/-54/24 and 59/-48/19; distances = 16mm and 16mm respectively). Whereas FEF is topographically organized (Bisley, 2011) with feedback connections to extrastriate cortical regions (Serences et al., 2005), TPJ is not spatially selective (Vossel et al., 2014). Still, FEF activity was reported even during attention to the ipsilateral hemifield, suggesting a more general role in attentional processing beyond spatial selection (Egner et al., 2008).

In the present analyses, the observed early ERP deflections during the SN further suggest that this frontoparietal activity may have served to adjust the attentional focus via feedback projections to visual brain regions. Thus, there were ERP deflections at central and parietooccipital sites between 200-300ms during valid as well as invalid compared to neutral cueing in both experiments. Both attention types probably involved similar early mechanisms in order to redirect attention (invalid > neutral) as well as during facilitation (valid > neutral). In accordance with this finding, the posterior SN has a putative generator in visual brain regions reflecting enhanced stimulus processing (Lange et al., 1998).

The overlap of clusters in TPJ and FEF between experiments during invalid trials fits with a common involvement of both frontoparietal networks in attentional control processes after violations of expectation (Kincade et al., 2005). Moreover, this overlap hints at a more general role of TPJ activity beyond spatial reorienting, perhaps as a circuit breaker when unexpected events elicit bottom-up attentional adjustment processes (Chang et al., 2013). Many studies found enhanced TPJ activity towards invalidly cued locations (Doricchi et al., 2010; Kincade et al., 2005; Natale et al., 2010), and TPJ also responds to non-spatial violations of expectation (Asplund et al., 2010; Shomstein et al., 2012). Interrupt signals from TPJ to dorsal frontoparietal

structures (FEF) possibly serve to update the current task goal and adjust to a new task context (Shomstein et al., 2012).

In the present study, TPJ and FEF demonstrated a hierarchical activity pattern during spatial attention depending on cue validity (invalid > valid; invalid > neutral; valid > neutral), leading to a pattern of invalid > valid > neutral. By contrast, there were no significant clusters in these regions when comparing valid > neutral in experiment II. As previously suggested (see section 4.4.2), without spatially directed attention (experiment II), there were probably attentional captures by the stimulus position that interrupted an initial global search mode on all trials. These spatial attentional captures may have been signaled by TPJ to FEF (Shomstein et al., 2012). As spatial attention generally yields larger BOLD signals than feature-based attention (Greenberg et al., 2010), additional activation of TPJ and FEF on valid compared to neutral trials was possibly shadowed in experiment II due to a ceiling effect. Thus, the valid > neutral contrast rather delivered clusters in opercular parts of IFG and insula in experiment II. The same clusters were also significantly active in the conjunctions of the invalid > neutral as well as of the valid > neutral contrast over both experiments respectively. This means that insulo-opercular structures were generally active during directed attention (valid; invalid) irrespective of attention mode. Insula and operculum respond to transient events such as errors (Neta et al., 2015) and saliency processing (Seeley et al., 2007). A shared feature of directed attention (valid; invalid) compared to neutral trials in both experiments may therefore be the detection of the attended stimulus attribute (location and color respectively), yielding saliency signals originating in insulo-opercular structures (Seeley et al., 2007).

In line with TPJ activation during bottom-up reorienting and top-down facilitation, there were ERP differences between cue conditions during the P300 time window. The P300 is the ERP component that is most closely associated with TPJ activity (Geng & Mangun, 2011). It occurs after perceptual stimulus analysis and may reflect updating of the internally represented context

in response to external stimulation (Donchin & Coles, 1988; Polich, 2007). This also corroborates the idea that in the present study TPJ activity was not restricted to attentional captures due to violations of expectations but more generally triggered a contextual update to dorsal frontoparietal structures in order to meet dynamically changing task requirements (Geng & Mangun, 2011). In addition, there were no significant differences between attention modes with respect to the invalid > neutral or valid >neutral difference waves. This is in line with the overlapping fMRI clusters in TPJ during both attention types.

5.4.3 Critical reflections

Comparison of spatial and feature-based attention in the present studies corresponds to results from previous studies. These suggest that both attention-types recruit a domain-general network during attentional redirections in response to invalidly attended locations or features (Greenberg et al., 2010). However, shifts of attention after invalid cueing involve several processes including captures by the target stimulus, disengagement and shift of attention, and subsequent focusing (Posner, 1980). With the present study designs, these sub-processes cannot be isolated using fMRI, as the slow nature of the hemodynamic response particularly impedes the measurement of transient processes (Chica et al., 2014; Hahn et al., 2006). Even though EEG has a high temporal resolution, assigning different ERP components to the single attentional processes would be arbitrary. Moreover, these processes have been largely studied in the context of spatial attention and may not be transferable to feature-based processes. It is generally questionable at what stage of stimulus processing attentional captures by stimulus locations interfered with a globally directed feature search. Consequently, similarities between both studies might be more closely related to analogous spatial orienting and focusing processes than to a domain-general attention mechanism.

Concerning temporal comparisons between experiments, another limitation of the present experiments is the fact that early components such as P1 or N1 could not be analyzed due an

insufficient amount of trials per condition. Therefore, early spatial attentional effects may have been present but could not be detected with the observed data.

Amongst others, frontoparietal activity overlapped between experiments in SPL and IPL. However, activity originating in the intersection of these regions in IPS cannot be explicitly assumed based on the present analyses, as this requires additional techniques such as functional localization (Scolari et al., 2015). Confirming activity in IPS during both valid and invalid trials irrespective of attention mode would corroborate the present interpretations, because IPS has previously been discussed with regard to independent non-spatial attention effects (Egner et al., 2008; Liu et al., 2011). Moreover, IPS appears to be a crucial juncture between volitional attention direction and stimulus-driven orienting, i.e. between the dorsal and the ventral network (Corbetta & Shulman, 2002). Thus, there are bidirectional connections between IPS and TPJ, which may be responsible for switches between networks. Together, they possibly serve as a relay station negotiating between external stimulation and internal states (Geng & Mangun, 2011).

5.4.4 Conclusions

In the present flanker studies, spatial and feature-based attention recruited similar frontoparietal as well as insulo-opercular brain regions depending on cue validity. The observed temporal activity patterns additionally suggest that these regions exerted similar effects on visual areas.

According to the observed fMRI data patterns, resolving invalidly directed attention generally led to activity in dorsal and ventral frontoparietal structures including putative FEF, SPL, and TPJ. In experiment I, this probably reflects spatial reorientations, whereas experiment II potentially involved task-set updates to direct attention to the correct color. Comparable ERP deflections during the SN time window suggest that these processes targeted visual brain regions with similar temporal courses. During valid cueing, dorsal frontoparietal recruitment

may have derived from focus adjustments (narrow or broad) due to different flanker congruency levels in experiment I.

Both contrasts (invalid > neutral; valid > neutral) overlapped between attention modes (spatial; feature-based) in TPJ and insulo-opercular structures, hinting at saliency signals upon detection of the task-relevant stimulus attribute (location; color). Assuming that there were additional involuntary captures towards stimulus positions in the feature-based experiment on all trials, a ceiling effect could explain why TPJ activity was not observable in the valid > neutral contrast in experiment II. In accordance with TPJ activity, there were comparable attention effects between experiments in the analysis of the P300 component, which reflects contextual updating processes and may have originated in TPJ in the present studies.

6. GENERAL DISCUSSION

6.1 An integrative perspective on the results

Despite a long history of research in the field of attention, important questions remain unanswerable. Theories based on factors such as 'perceptual-load' (Lavie, 1995), 'dilution by visual interference' (Benoni & Tsal, 2010) or 'occasional slippages' (Gaspelin et al., 2014) ultimately all aim at determining at what stage of stimulus processing attentional influences may be effective. In a related debate, the dichotomy between top-down and bottom-up factors serves to separate complete volitional control from pure stimulus-driven effects on information processing (Theeuwes, 2010), and these processes have been linked with anatomical structures in frontoparietal parts of the brain (Corbetta & Shulman, 2002; Dosenbach et al., 2008). However, with the help of neuroimaging and more sophisticated task designs it becomes increasingly clear that a strict separation between internally and externally driven processes may not be adequate (Katsuki & Constantinidis, 2014). The present studies addressed these issues by contrasting spatial and feature-based attention in the same task design and by comparing their individual influences during interference processing. The results hint at a common network of control mechanisms and furthermore suggest that these interact at various stages of information processing.

In the present experiments certain brain regions were active in response to various experimental manipulations, e.g. parts of the dFPN responded to incorrectly cued stimuli (invalid > neutral) as well as to flanker processing (INC > CON) in both experiments (spatial; feature-based). The associated cognitive operations leading to activity during the different contrasts that were investigated in the present experiments may be sorted into distinct categories. These potentially include *expectation-based responses* depending on cue validity (confirmation/violation of expectation) and *attentional captures* by salient stimulus information (location; color)

irrespective of validity, *control of the attentional window* (broad/narrow) as well as *conflict processing* (INC > CON), both depending on flanker congruency.

Concerning *expectation-based* responses, the valid > neutral and invalid > neutral contrasts mainly seem to reflect enhanced recruitment of resources dedicated to facilitation (confirmation of expectation) and reorientation/recalibration (violation of expectation) respectively. The structures involved in these processes lie in dorsal and ventral frontoparietal brain regions (e.g. Greenberg et al., 2010; Kincade et al., 2005), which is generally consistent with the respective clusters found in both experiments. Dorsal and ventral structures (including FEF and TPJ) may have initiated attentional switches (experiment I) and recalibrations (experiment II) on invalid trials, suggesting a domain-general control mechanism (Greenberg et al., 2010) which altered activity in visual brain regions through feedback projections (Serences et al., 2004). Accordingly, both spatial and feature-based attention lead to enhanced activity in the same visual regions (Maunsell & Treue, 2006), and their effects appear to be independent and at comparable time courses (McAdams & Maunsell, 2000). Furthermore, the results pattern of a past study suggests that the same regions might control both attention types independently using different types of interspersed neurons (Egner et al., 2008). These neurons are probably topographically arranged for spatial attention (Bisley, 2011) in order to signal shifts to the correct location on invalid trials, whereas invalidly cued features possibly recruit neurons specialized in updating the task goal held in working memory (Hopfinger et al., 2001).

The present results further hint at a graded activation of frontoparietal brain regions. Thus, a pattern of invalid > valid > neutral trials was observable in experiment I with regard to dorsal and ventral frontoparietal activation. This means that reorientation after invalid cues resulted in higher activity levels than focus adjustments of attention on valid trials. Similarly, Posner (2014) reported higher behavioral cost effects when attention had to be reoriented after invalid spatial cueing than during orienting after previously unfocused attention. Reorientation

involves disengagement from a previously attended location before shifting to the target stimulus (Posner, 1980) and activates both dorsal and ventral frontoparietal regions (Ruff et al., 2008). By contrast, attentional captures appear to trigger the detection of salient information and activate parts of the ventral attention network ((Uddin, 2015), including TPJ, insula, and operculum. These structures were identified as core regions for saliency signals (Kucyi et al., 2012). Clusters in TPJ, insula, and operculum overlapped in both contrasts (invalid > neutral; valid > neutral) of both experiments, suggesting that *attentional captures* represent a common element of spatial and feature-based attention beyond spatial orienting. A shared characteristic of valid and invalid trials in both experiments may be the detection of the attended stimulus dimension (location; color), leading to capture effects. TPJ and insulo-opercular structures are nonspecifically active during many different cognitive operations such as target detection or response generation and may hence represent a superordinate task-control unit (Sestieri et al., 2014).

However, the contrast valid > neutral delivered no TPJ cluster in experiment II. This may be caused by a ceiling effect of activity in TPJ. Thus, without previous information about the target location, *attentional captures* by stimulus locations were probably generally present in experiment II, potentially leading to activation of TPJ on all trials (DiQuattro et al., 2014; Shomstein et al., 2012). As suggested above (see section 5.4.2), attentional captures by locations lead to larger BOLD signal increases than feature-based captures (Greenberg et al., 2010). As a result, the valid > neutral contrast possibly delivered only subthreshold results because of similar activity levels in TPJ that were primarily driven by spatial captures. By contrast, the invalid > neutral contrast possibly yielded suprathreshold activation in TPJ because invalid trials involved both spatial captures and attentional recalibration mechanisms because of an incorrectly attended color. This idea is supported by the graded activation pattern in experiment I (invalid > valid > neutral), which suggests that invalidly cued trials generally involved higher levels of activity in these regions than valid or neutral trials.

Activity in frontoparietal brain regions was also observable during flanker conflict processing INC > CON) on validly cued trials. This potentially reflects modulations of the *attentional window* depending on flanker congruency in both experiments and may have been driven by increased efforts to focus on the central target letter on INC trials. Control signals to induce a narrower focus mainly draw on dorsal frontoparietal parts of the brain (Casey et al., 2000). Accordingly, these structures demonstrated suprathreshold activation in the INC > CON contrast in both experiments during validly cued trials. To achieve this, feedback signals from FEF to occipital structures including lingual gyri potentially led to increased spatial focusing in order to suppress INC flanker stimuli. Thus, FEF shows connections to visual cortical regions (Ruff et al., 2008), and neurons in area V4 are sensitive to top-down influences from frontoparietal network (Zhou & Desimone, 2011). Likewise, there were INC > CON fMRI clusters in occipital brain regions in both experiments on validly cued trials, which were compatible with a posterior relative negativity during the N200 component. Source waveform differences between INC and CON trials originating in lingual gyri in both experiments further suggest that these findings from fMRI and ERP analyses reflect the same underlying mechanism of early focus adjustments triggered by frontoparietal cortices.

Even though flanker interference processing showed overlapping activity patterns in frontoparietal brain regions, the resulting effects on *conflict processing* differed. Early increased activity in cingulate and precentral gyrus on INC trials was evident in the fMRI data of experiment II with valid cueing but not experiment I. This hints at a higher degree of conflict when top-down modulations were based on feature-based compared with spatial information. A past study suggested that response conflict is more likely when early selection is not possible, leading to ACC activation because of late response competition (Kanwisher & Wojciulik, 2000). Likewise, those source waveforms originating in the ACC and precentral gyrus RSs overlapping between experiments showed distinct temporal patterns between experiments. There were INC vs. CON differences of source waveforms arising in ACC around 440ms and

in precentral gyrus around 660ms during validly directed feature-based attention. This pattern hints at a response-based conflict. In addition, source waveform differences of INC vs. CON in precentral gyrus started much earlier but without concurrent ACC activity in experiment I, potentially reflecting the active maintenance of both response alternatives before response selection. By contrast, conflict experience was apparently stronger during spatially invalid cueing, as reflected by early activity differences in both ACC and precentral gyrus, which was possibly a sign conflict detection.

However, in the present experiments the size of the behaviorally observable flanker effect differed neither between experiments nor between cue validity levels. Thus, validly directed spatial attention did not reduce captures of spatial attention by the flanker stimuli as predicted by the 'slippage theory' of attention (Gaspelin et al., 2014) and valid feature-based cueing resulted in comparable amounts of interference. By contrast, a past study reported smaller interference effects when cueing the target location or the color of a uniquely colored target letter (Wilson et al., 2011). However, studies finding top-down cueing effects on flanker processing often used circular arrays with higher location uncertainty, yielding larger benefits for correctly cued locations (McCarley & Mounts, 2008; Yantis & Johnston, 1990). In these studies, attentional captures by task-relevant flankers were probably more likely than in the present study where stimulus position was fixed to two possible locations. This also suggests that the observed flanker effects in the present studies may not have been caused by attentional slippages to the flankers positions. Due to equal frequencies of valid and invalid cues, spatial attentional resources were possibly not entirely concentrated on the cued stimulus location in general in experiment I, and in experiment II spatial attention was potentially globally directed at the visual field or divided between both stimulus locations. Participants possibly adopted a flexible attentional adjustment mode in order to be able to react adequately to both flanker congruency and cue validity (both experiments) as well as to attentional captures by stimulus

position (experiment II). The dual-task requirements may thus have promoted processing of the flanker stimulus positions by default.

Corroborating these assumptions, the comparison between studies hints at a common activation of the top-down dFPN irrespective of attention mode (spatial; feature-based) which responded to *expectation-based processing* as well as during the *control of the attentional window*. In the literature, dorsal frontoparietal brain regions (SPL; MFG) also demonstrate overlapping activity between top-down spatial attentional control and conflict processing (Fan et al., 2007) even though these processes were mainly found to yield independent activity (Fan et al., 2005). In the present studies, spatial attentional mechanisms apparently played a dominant role. Thus, a narrower spatial focus of attention probably facilitated responding to INC flanker stimuli in both experiments.

However, this overlap was restricted to validly cued trials in both experiments. There were no clusters in dorsal frontoparietal brain regions during flanker conflict processing with invalid cues. This was possibly due to high levels of activity in these regions in order to reorient attention (experiment I) or update the task set (experiment II), which may have shadowed further activity increases in response to INC flanker stimuli.

6.2 Final conclusions

The present thesis aimed at identifying intersections between different attention-related processes. One topic of interest concerned the question whether spatially directed attention could prevent attentional slippages to locations containing distracting information. For the second issue, the same experiment was repeated using non-spatial cues. This allowed a comparison between focused spatial attention (experiment I) and globally directed attention (experiment II) with respect to the amount of interference. Finally, both attention types were contrasted with each other in order to reveal the spatio-temporal activity patterns leading to these putative alterations of interference processing. The results suggest that both attentional modulations as well as flanker processing recruit similar structures because of analogous control mechanisms. There were expectation-based responses observable in frontoparietal brain regions during attentional adjustments on invalid trials (both attention modes) and on trials with valid spatial allocation of attention. The observed hierarchical activity pattern (invalid > valid > neutral) is in line with increased efforts during invalid trials due to attentional disengagement processes preceding attentional focusing mechanisms, which are both controlled by overlapping frontoparietal brain structures.

Attentional captures were probably generally present during directed attention (valid; invalid) in both experiments upon detection of the attended stimulus attribute (location; color). The observed comprehensive activity in TPJ and insulo-opercular structures over experiments hints at a superordinate ventral control network processing salient task-relevant information. In experiment II, additional attentional captures by stimulus position possibly prevented suprathreshold activity in TPJ during validly directed attention.

Flanker congruency effects assumedly evoked modulations at different stages of processing. First, on an early perceptual level the mismatch between letters on INC trials may have evoked a mismatch detection response, which resulted in focus adjustments triggered by dorsal

frontoparietal cortices to visual areas. This process probably interacted with expectation-based adjustments in response to different validity levels. Thus, invalidly directed spatial attention possibly postponed the suggested focusing process, leading to enhanced conflict signals relative to valid spatial cueing. Moreover, attention mode also affected conflict processing, as a response conflict was evident with feature-based cueing in general and with invalid spatial cueing. All of these conditions required attentional shifts during which flanker processing may have been enhanced. Finally, experiment II demonstrated additional recruitment of brain regions relative to experiment I, possibly in order to achieve comparable performance levels as in experiment I.

In sum, the present thesis suggests that similar control mechanisms are involved during spatial and non-spatial attention with distinct effects on conflict processing.

6.3 Suggestions for future research

While the idea of a frontoparietal network of attention has become indisputable in the literature, the interplay of its numerous nodes is still a matter of debate. Moreover, there are many different and partly inconsistent definitions of these sub-components and their precise functions. With the help of modern imaging techniques, the characteristics of these networks may be uncovered. The present studies used fMRI-constrained source analyses to reveal the temporal dynamics of brain activity during flanker processing under the influence of different attention types. Magnetoencephalography provides an alternative way to inform about spatio-temporal activity patterns. The method can more directly link anatomical structures with the respective time courses because both data sets are simultaneously acquired within one session (Cohen & Cuffin, 1983). By contrast, the fMRI-constrained source analyses applied in the present studies necessarily required separate measurement sessions and timing differences between the designs in the EEG compared to the fMRI session. The data sets may therefore differ with regard to task-unrelated factors (e.g. repetition effects or strategic differences due to a slower timing in the scanner). Moreover, fMRI is generally less sensitive to transient signal fluctuations (Huettel et al., 2004) so that certain underlying mechanisms may be visible in the ERP but not the fMRI data (Chica et al., 2014). This raises a potential problem because transient and sustained processes are both carried out by the frontoparietal networks (Dosenbach et al., 2008). Therefore, magnetoencephalography may provide an alternative way to investigate top-down influences on interference processing.

In order to achieve genuine selection by color and not by space, future studies addressing feature-based attentional effects on interference processing should carefully avoid the possibility of a spatial strategy especially during early stimulus processing. Instead of spatially separated stimuli, two superimposed stimulus apertures could be used that differ in an irrelevant dimension such as color (e.g. red vs. green) of which one aperture is cued in advance (e.g. red).

One aperture might contain target-relevant stimuli (e.g. characters) whereas the other might contain distractors that belong to the stimulus set but are not currently response-relevant (non-target characters drawn from the stimulus set). In order to inform participants which stimulus is to be responded to per trial, they could be informed about another task-irrelevant feature that tags a stimulus as being the current target. For example, the characters in the apertures may alternate between vowels and consonants. A vowel in the attended aperture may signal a switch to the other aperture if the previously attended aperture contained a consonant. Otherwise, the attended aperture must be responded to. Thus, on any current trial, the character within the attended aperture must be analyzed with regard to this criterion before deciding whether to switch to the other stimulus aperture or not. If feature-bases attention affects early stages of stimulus processing before conflict detection, the distracting information in the unattended aperture should have minor influences on performance. Spatially directed attention would not be helpful in reducing distraction in such a design.

Lateralized stimulus designs are particularly useful to separate spatial and feature-based attentional effects. While the dorsal attention system appears to respond to attentional manipulations bilaterally (Egner et al., 2008), reports of ventral activation are more frequently restricted to the right hemisphere irrespective of presentation side (Chang et al., 2013). By contrast, in the present studies with stimulation varying only along the vertical line, activity in TPJ was found bilaterally. This may suggest either that TPJ shows lateralized effects during stimulation of one hemifield or that both hemispheres were recruited in order to meet the task requirements. This should be tested in future studies.

Furthermore, it would be interesting to apply the present task design to neglect patients who have difficulties shifting attention to the contralesional hemifield (usually to the left). Neglect symptoms are often linked with lesions to SPL or TPJ, which were both omnipresent in almost

all contrasts ranging from attentional captures (invalid cueing) to flanker conflict processing, suggesting a domain-general role for TPJ independent of spatial shifts of attention.

The debate about control systems in the human brain is also of high clinical relevance. Various mental disorders are apparently linked with reduced or malfunctioning activity patterns in core brain regions for cognitive control, and an intact control system apparently serves as a protective factor against mental diseases (Cole et al., 2014). The attentional network test (Fan et al., 2002; Fan et al., 2005) has become a well-established means for testing populations demonstrating reduced resilience (e.g. children or elderly) on spatial orienting, interference processing, and alertness. The present experimental designs share similarities with the attentional network test and further introduce a non-spatial component. Therefore, it may be suitable to test clinical populations.

References

References

Allison, T., Begleiter, A., McCarthy, G., Roessler, E., Nobre, A. C., & Spencer, D. D. (1993). Electrophysiological studies of color processing in human visual cortex. *Electroencephalography and Clinical Neurophysiology, 88*(5), 343-355.

Allport, D. A. (1971). Parallel encoding within and between elementary stimulus dimensions. *Perception & Psychophysics, 10*(2), 104-108.

Andersen, S. K., & Mueller, M. M. (2010). Behavioral performance follows the time course of neural facilitation and suppression during cued shifts of feature-selective attention. *Proceedings of the National Academy of Sciences of the United States of America, 107*(31), 13878-13882.

Anllo-Vento, L., & Hillyard, S. A. (1996). Selective attention to the color and direction of moving stimuli: Electrophysiological correlates of hierarchical feature selection. *Perception & Psychophysics, 58*(2), 191-206.

Asplund, C. L., Todd, J. J., Snyder, A. P., & Marois, R. (2010). A central role for the lateral prefrontal cortex in goal-directed and stimulus-driven attention. *Nature Neuroscience, 13*(4), 507-512.

Baldassi, S., & Verghese, P. (2005). Attention to locations and features: Different top-down modulation of detector weights. *Journal of Vision, 5*(6), 556-570.

Bartholow, B. D., Pearson, M. A., Dickter, C. L., Sher, K. J., Fabiani, M., & Gratton, G. (2005). Strategic control and medial frontal negativity: Beyond errors and response conflict. *Psychophysiology, 42*(1), 33-42.

Benoni, H., & Tsal, Y. (2010). Where have we gone wrong? perceptual load does not affect selective attention. *Vision Research, 50*(13), 1292-1298.

Birbaumer, N., & Schmidt, R. F. (2010). *Biologische Psychologie.* (7., vollst. überarb. u. ergänzte Auflage ed.). Berlin/ Heidelberg: Springer.

Bisley, J. W. (2011). The neural basis of visual attention. *The Journal of Physiology, 589*(1), 49-57.

Bledowski, C., Cohen Kadosh, K., Wibral, M., Rahm, B., Bittner, R. A., Hoechstetter, K., Scherg, M., Maurer, K., Goebel, R., & Linden, D. E. (2006). Mental chronometry of working memory retrieval: A combined functional magnetic resonance imaging and event-related potentials approach. *The Journal of Neuroscience: The Official Journal of the Society for Neuroscience, 26*(3), 821-829.

Bledowski, C., Linden, D. E., & Wibral, M. (2007). Combining electrophysiology and functional imaging - different methods for different questions. *Trends in Cognitive Sciences, 11*(12), 500-502.

Bocquillon, P., Bourriez, J. L., Palmero-Soler, E., Molaee-Ardekani, B., Derambure, P., & Dujardin, K. (2014). The spatiotemporal dynamics of early attention processes: A high-resolution electroencephalographic study of N2 subcomponent sources. *Neuroscience, 271*, 9-22.

Botvinick, M. M., Braver, T. S., Barch, D. M., Carter, C. S., & Cohen, J. D. (2001). Conflict monitoring and cognitive control. *Psychological Review, 108*(3), 624-652.

Botvinick, M. M., Cohen, J. D., & Carter, C. S. (2004). Conflict monitoring and anterior cingulate cortex: An update. *Trends in Cognitive Sciences, 8*(12), 539-546.

Broadbent, D. E. (1958). *Perception and communication*. Oxford: Oxford University Press.

Bunge, S. A., Hazeltine, E., Scanlon, M. D., Rosen, A. C., & Gabrieli, J. D. (2002). Dissociable contributions of prefrontal and parietal cortices to response selection. *NeuroImage, 17*(3), 1562-1571.

Burle, B., Spieser, L., Servant, M., & Hasbroucq, T. (2014). Distributional reaction time properties in the Eriksen task: Marked differences or hidden similarities with the Simon task? *Psychonomic Bulletin & Review, 21*(4), 1003-1010.

Carrasco, M. (2011). Visual attention: The past 25 years. *Vision Research, 51*(13), 1484-1525.

Carrasco, M., Loula, F., & Ho, Y. X. (2006). How attention enhances spatial resolution: Evidence from selective adaptation to spatial frequency. *Perception & Psychophysics, 68*(6), 1004-1012.

Carter, C. S., & van Veen, V. (2007). Anterior cingulate cortex and conflict detection: An update of theory and data. *Cognitive, Affective & Behavioral Neuroscience, 7*(4), 367-379.

Casey, B. J., Thomas, K. M., Welsh, T. F., Badgaiyan, R. D., Eccard, C. H., Jennings, J. R., & Crone, E. A. (2000). Dissociation of response conflict, attentional selection, and expectancy with functional magnetic resonance imaging. *Proceedings of the National Academy of Sciences of the United States of America, 97*(15), 8728-8733.

Chang, C. F., Hsu, T. Y., Tseng, P., Liang, W. K., Tzeng, O. J., Hung, D. L., & Juan, C. H. (2013). Right temporoparietal junction and attentional reorienting. *Human Brain Mapping, 34*(4), 869-877.

Chao, H. F. (2011). Active inhibition of a distractor word: The distractor precue benefit in the Stroop color-naming task. *Journal of Experimental Psychology: Human Perception and Performance, 37*(3), 799-812.

Chelazzi, L., Duncan, J., Miller, E. K., & Desimone, R. (1998). Responses of neurons in inferior temporal cortex during memory-guided visual search. *Journal of Neurophysiology, 80*(6), 2918-2940.

Chica, A. B., Martin-Arevalo, E., Botta, F., & Lupianez, J. (2014). The spatial orienting paradigm: How to design and interpret spatial attention experiments. *Neuroscience and Biobehavioral Reviews, 40*, 35-51.

Cohen, D., & Cuffin, B. N. (1983). Demonstration of useful differences between magnetoencephalogram and electroencephalogram. *Electroencephalography and Clinical Neurophysiology, 56*(1), 38-51.

Cole, M. W., Repovs, G., & Anticevic, A. (2014). The frontoparietal control system: A central role in mental health. *The Neuroscientist: A Review Journal Bringing Neurobiology, Neurology and Psychiatry, 20*(6), 652-664.

Corbetta, M., Patel, G., & Shulman, G. L. (2008). The reorienting system of the human brain: From environment to theory of mind. *Neuron, 58*(3), 306-324.

Corbetta, M., & Shulman, G. L. (2002). Control of goal-directed and stimulus-driven attention in the brain. *Nature Reviews Neuroscience, 3*(3), 201-215.

Corbetta, M., & Shulman, G. L. (2011). Spatial neglect and attention networks. *Annual Review of Neuroscience, 34*, 569-599.

Corchs, S., & Deco, G. (2004). Feature-based attention in human visual cortex: Simulation of fMRI data. *NeuroImage, 21*(1), 36-45.

Correa, A., Rao, A., & Nobre, A. C. (2009). Anticipating conflict facilitates controlled stimulus-response selection. *Journal of Cognitive Neuroscience, 21*(8), 1461-1472.

Cutrone, E. K., Heeger, D. J., & Carrasco, M. (2014). Attention enhances contrast appearance via increased input baseline of neural responses. *Journal of Vision, 14*(14): 16, 1-14.

Daliri M. R., Kozyrev, V., & Treue, S. (2009). Evaluating the Feature Similarity Gain and Biased Competition Models of Attentional Modulation. Conference Abstract: Bernstein Conference on Computational Neuroscience*, Goettingen: Germany*.

Danielmeier, C., Wessel, J. R., Steinhauser, M., & Ullsperger, M. (2009). Modulation of the error-related negativity by response conflict. *Psychophysiology, 46*(6), 1288-1298.

David, S. V., Hayden, B. Y., Mazer, J. A., & Gallant, J. L. (2008). Attention to stimulus features shifts spectral tuning of V4 neurons during natural vision. *Neuron, 59*(3), 509-521.

de Haas, B., Schwarzkopf, D. S., Anderson, E. J., & Rees, G. (2014). Perceptual load affects spatial tuning of neuronal populations in human early visual cortex. *Current Biology: CB, 24*(2), R66-67.

Della-Maggiore, V., Chau, W., Peres-Neto, P. R., & McIntosh, A. R. (2002). An empirical comparison of SPM preprocessing parameters to the analysis of fMRI data. *NeuroImage, 17*(1), 19-28.

Desimone, R. (1998). Visual attention mediated by biased competition in extrastriate visual cortex. *Philosophical Transactions of the Royal Society B: Biological Sciences, 353*(1373), 1245-1255.

Desimone, R., & Duncan, J. (1995). Neural mechanisms of selective visual attention. *Annual Review of Neuroscience, 18*, 193-222.

Desimone, R., Schein, S. J., Moran, J., & Ungerleider, L. G. (1985). Contour, color and shape analysis beyond the striate cortex. *Vision Research, 25*(3), 441-452.

Deutsch, J. A., & Deutsch, D. (1963). Attention: Some theoretical considerations. *Psychological Review, 70*, 80-90.

DiQuattro, N. E., Sawaki, R., & Geng, J. J. (2014). Effective connectivity during feature-based attentional capture: Evidence against the attentional reorienting hypothesis of TPJ. *Cerebral Cortex, 24*(12), 3131-3141.

Donchin, E., & Coles, M. G. H. (1988). Is the P300 component a manifestation of context updating? *Behavioral and Brain Sciences, 11*(03), 357-374.

Doricchi, F., Macci, E., Silvetti, M., & Macaluso, E. (2010). Neural correlates of the spatial and expectancy components of endogenous and stimulus-driven orienting of attention in the Posner task. *Cerebral Cortex, 20*(7), 1574-1585.

Dosenbach, N. U., Fair, D. A., Cohen, A. L., Schlaggar, B. L., & Petersen, S. E. (2008). A dual-networks architecture of top-down control. *Trends in Cognitive Sciences, 12*(3), 99-105.

Dosenbach, N. U., Fair, D. A., Miezin, F. M., Cohen, A. L., Wenger, K. K., Dosenbach, R. A., Fox, M. D., Snyder, A: Z., Vincent, J. L., Raichle, M. E., Schlaggar, B. L., & Petersen, S. E. (2007). Distinct brain networks for adaptive and stable task control in humans. *Proceedings of the National Academy of Sciences of the United States of America, 104*(26), 11073-11078.

Dosenbach, N. U., Visscher, K. M., Palmer, E. D., Miezin, F. M., Wenger, K. K., Kang, H. C., Burgund, E. D., Grimes, A. L., Schlaggar, B. L., & Petersen, S. E. (2006). A core system for the implementation of task sets. *Neuron, 50*(5), 799-812.

Driver, J. (2001). A selective review of selective attention research from the past century. *British Journal of Psychology, 92*(1), 53-78.

Duncan, J. (1984). Selective attention and the organization of visual information. *Journal of Experimental Psychology: General, 113*(4), 501-517.

Efron, B., & Tibshirani, R. J. (1993). *An introduction to the bootstrap*. New York: Chapman & Hall.

Egner, T., Monti, J. M., Trittschuh, E. H., Wieneke, C. A., Hirsch, J., & Mesulam, M. M. (2008). Neural integration of top-down spatial and feature-based information in visual search. *The Journal of Neuroscience: The Official Journal of the Society for Neuroscience, 28*(24), 6141-6151.

Eimer, M. (1995). Event-related potential correlates of transient attention shifts to color and location. *Biological Psychology, 41*(2), 167-182.

Eimer, M. (1997). An event-related potential (ERP) study of transient and sustained visual attention to color and form. *Biological Psychology, 44*(3), 143-160.

Engel, S. A., Glover, G. H., & Wandell, B. A. (1997). Retinotopic organization in human visual cortex and the spatial precision of functional MRI. *Cerebral Cortex, 7*(2), 181-192.

Eriksen, B. A., & Eriksen, C. W. (1974). Effects of noise letters upon the identification of a target letter in a nonsearch task. *Perception and Psychophysics, 16*, 143-149.

Facoetti, A. (2001). Facilitation and inhibition mechanisms of human visuospatial attention in a non-search task. *Neuroscience Letters, 298*(1), 45-48.

Fan, J., Flombaum, J. I., McCandliss, B. D., Thomas, K. M., & Posner, M. I. (2003). Cognitive and brain consequences of conflict. *NeuroImage, 18*(1), 42-57.

Fan, J., Hof, P. R., Guise, K. G., Fossella, J. A., & Posner, M. I. (2008). The functional integration of the anterior cingulate cortex during conflict processing. *Cerebral Cortex, 18*(4), 796-805.

Fan, J., Kolster, R., Ghajar, J., Suh, M., Knight, R. T., Sarkar, R., & McCandliss, B. D. (2007). Response anticipation and response conflict: An event-related potential and functional magnetic resonance imaging study. *The Journal of Neuroscience: The Official Journal of the Society for Neuroscience, 27*(9), 2272-2282.

Fan, J., McCandliss, B. D., Fossella, J., Flombaum, J. I., & Posner, M. I. (2005). The activation of attentional networks. *NeuroImage, 26*(2), 471-479.

Fan, J., McCandliss, B. D., Sommer, T., Raz, A., & Posner, M. I. (2002). Testing the efficiency and independence of attentional networks. *Journal of Cognitive Neuroscience, 14*(3), 340-347.

Fehr, T., Wiechert, J., & Erhard, P. (2014). Variability in color-choice Stroop performance within and across EEG and MRI laboratory contexts. *Attention, Perception & Psychophysics, 76*(8), 2495-2507.

Folstein, J. R., & Van Petten, C. (2008). Influence of cognitive control and mismatch on the N2 component of the ERP: A review. *Psychophysiology, 45*(1), 152-170.

Fournier, L. R., & Shorter, S. (2001). Is evidence for late selection due to automatic or attentional processing of stimulus identities? *Perception & Psychophysics, 63*(6), 991-1003.

Fox, E. (1995). Pre-cuing target location reduces interference but not negative priming from visual distractors. *The Quarterly Journal of Experimental Psychology A, Human Experimental Psychology, 48*(1), 26-40.

Galashan, D., Fehr, T., & Herrmann, M. (2015). Differences between target and non-target probe processing - combined evidence from fMRI, EEG and fMRI-constrained source analysis. *NeuroImage, 111*, 289-299.

Gallant, J. L., Shoup, R. E., & Mazer, J. A. (2000). A human extrastriate area functionally homologous to macaque V4. *Neuron, 27*(2), 227-235.

Gaspelin, N., Ruthruff, E., & Jung, K. (2014). Slippage theory and the flanker paradigm: An early-selection account of selective attention failures. *Journal of Experimental Psychology: Human Perception and Performance, 40*(3), 1257-1273.

Geng, J. J., & Mangun, G. R. (2011). Right temporoparietal junction activation by a salient contextual cue facilitates target discrimination. *NeuroImage, 54*(1), 594-601.

Giesbrecht, B., Woldorff, M. G., Song, A. W., & Mangun, G. R. (2003). Neural mechanisms of top-down control during spatial and feature attention. *NeuroImage, 19*(3), 496-512.

Gratton, G., Coles, M. G., & Donchin, E. (1992). Optimizing the use of information: Strategic control of activation of responses. *Journal of Experimental Psychology: General, 121*(4), 480-506.

Greenberg, A. S., Esterman, M., Wilson, D., Serences, J. T., & Yantis, S. (2010). Control of spatial and feature-based attention in frontoparietal cortex. *The Journal of Neuroscience: The Official Journal of the Society for Neuroscience, 30*(43), 14330-14339.

Hahn, B., Ross, T. J., & Stein, E. A. (2006). Neuroanatomical dissociation between bottom-up and top-down processes of visuospatial selective attention. *NeuroImage, 32*(2), 842-853.

Harter, M. R., Aine, C., & Schroeder, C. (1982). Hemispheric differences in the neural processing of stimulus location and type: Effects of selective attention on visual evoked potentials. *Neuropsychologia, 20*(4), 421-438.

Hayden, B. Y., & Gallant, J. L. (2009). Combined effects of spatial and feature-based attention on responses of V4 neurons. *Vision Research, 49*(10), 1182-1187.

Hillyard, S. A., & Muente, T. F. (1984). Selective attention to color and location: An analysis with event-related brain potentials. *Perception & Psychophysics, 36*(2), 185-198.

Hillyard, S. A., Vogel, E. K., & Luck, S. J. (1998). Sensory gain control (amplification) as a mechanism of selective attention: Electrophysiological and neuroimaging evidence. *Philosophical Transactions of the Royal Society of London: Series B, Biological Sciences, 353*(1373), 1257-1270.

Hommel, B., Pratt, J., Colzato, L., & Godijn, R. (2001). Symbolic control of visual attention. *Psychological Science, 12*(5), 360-365.

Hopf, J. M., Luck, S. J., Boelmans, K., Schoenfeld, M. A., Boehler, C. N., Rieger, J., & Heinze, H. J. (2006). The neural site of attention matches the spatial scale of perception. *The Journal of Neuroscience: The Official Journal of the Society for Neuroscience, 26*(13), 3532-3540.

Hopfinger, J. B., Khoe, W., & Song, A. (2005). Combining electrophysiology with structural and functional neuroimaging: ERP's, PET, MRI, fMRI. In T. C. Handy (Ed.), *Event-related Potentials. A methods handbook* (pp. 345-379). Cambridge: MA: MIT Press.

Hopfinger, J. B., Woldorff, M. G., Fletcher, E. M., & Mangun, G. R. (2001). Dissociating top-down attentional control from selective perception and action. *Neuropsychologia, 39*(12), 1277-1291.

Huettel, S. A., Song, A. W., & McCarthy, G. (2004). *Functional magnetic resonance imaging.* Sunderland, Maas: Sinauer.

Igelstroem, K. M., Webb, T. W., & Graziano, M. S. (2015). Neural processes in the human temporoparietal cortex separated by localized independent component analysis. *The Journal of Neuroscience: The Official Journal of the Society for Neuroscience, 35*(25), 9432-9445.

Ishihara, S. (1917). Tests for colour-blindness. Handaya, Tokyo, Hongo Harukicho.

James, W. A. (1950). *The principles of psychology*. New York: Dover Publications, Inc.

Johnstone, T., Ores Walsh, K. S., Greischar, L. L., Alexander, A. L., Fox, A. S., Davidson, R. J., & Oakes, T. R. (2006). Motion correction and the use of motion covariates in multiple-subject fMRI analysis. *Human Brain Mapping, 27*(10), 779-788.

Jonides, J., & Yantis, S. (1988). Uniqueness of abrupt visual onset in capturing attention. *Perception & Psychophysics, 43*(4), 346-354.

Kähler, W. (2008). *Statistische Datenanalyse: Verfahren verstehen und mit SPSS gekonnt einsetzen*. Wiesbaden: Vieweg.

Kanwisher, N., & Wojciulik, E. (2000). Visual attention: Insights from brain imaging. *Nature Reviews Neuroscience, 1*(2), 91-100.

Kastner, S., De Weerd, P., Desimone, R., & Ungerleider, L. G. (1998). Mechanisms of directed attention in the human extrastriate cortex as revealed by functional MRI. *Science, 282*(5386), 108-111.

Kastner, S., Pinsk, M. A., De Weerd, P., Desimone, R., & Ungerleider, L. G. (1999). Increased activity in human visual cortex during directed attention in the absence of visual stimulation. *Neuron, 22*(4), 751-761.

Kastner, S., & Ungerleider, L. G. (2000). Mechanisms of visual attention in the human cortex. *Annual Review of Neuroscience, 23*, 315-341.

Katsuki, F., & Constantinidis, C. (2014). Bottom-up and top-down attention: Different processes and overlapping neural systems. *The Neuroscientist: A Review Journal Bringing Neurobiology, Neurology and Psychiatry, 20*(5), 509-521.

Kincade, J. M., Abrams, R. A., Astafiev, S. V., Shulman, G. L., & Corbetta, M. (2005). An event-related functional magnetic resonance imaging study of voluntary and stimulus-driven orienting of attention. *The Journal of Neuroscience: The Official Journal of the Society for Neuroscience, 25*(18), 4593-4604.

Klemen, J., Verbruggen, F., Skelton, C., & Chambers, C. D. (2011). Enhancement of perceptual representations by endogenous attention biases competition in response selection. *Attention, Perception & Psychophysics, 73*(8), 2514-2527.

Kornblum, S., Hasbroucq, T., & Osman, A. (1990). Dimensional overlap: Cognitive basis for stimulus-response compatibility--a model and taxonomy. *Psychological Review, 97*(2), 253-270.

Koski, L., & Paus, T. (2000). Functional connectivity of the anterior cingulate cortex within the human frontal lobe: A brain-mapping meta-analysis. *Experimental Brain Research, 133*(1), 55-65.

Kucyi, A., Hodaie, M., & Davis, K. D. (2012). Lateralization in intrinsic functional connectivity of the temporoparietal junction with salience- and attention-related brain networks. *Journal of Neurophysiology, 108*(12), 3382-3392.

Labrenz, F., Themann, M., Wascher, E., Beste, C., & Pfleiderer, B. (2012). Neural correlates of individual performance differences in resolving perceptual conflict. *PloS One, 7*(8), e42849.

Lambert, A. J., & Corban, R. (1992). Spatial attention and expectancy for colour, category and location: Further evidence against the spotlight model. *Acta Psychologica, 81*(1), 39-51.

Lange, J. J., Wijers, A. A., Mulder, L. J., & Mulder, G. (1998). Color selection and location selection in ERPs: Differences, similarities and 'neural specificity'. *Biological Psychology, 48*(2), 153-182.

Larson, M. J., Clayson, P. E., & Clawson, A. (2014). Making sense of all the conflict: A theoretical review and critique of conflict-related ERPs. *International Journal of Psychophysiology: Official Journal of the International Organization of Psychophysiology, 93*(3), 283-297.

Lavie, N. (1995). Perceptual load as a necessary condition for selective attention. *Journal of Experimental Psychology: Human Perception and Performance, 21*(3), 451-468.

Lavie, N., & Tsal, Y. (1994). Perceptual load as a major determinant of the locus of selection in visual attention. *Perception & Psychophysics, 56*(2), 183-197.

Ling, S., Liu, T., & Carrasco, M. (2009). How spatial and feature-based attention affect the gain and tuning of population responses. *Vision Research, 49*(10), 1194-1204.

Liu, T., Hospadaruk, L., Zhu, D. C., & Gardner, J. L. (2011). Feature-specific attentional priority signals in human cortex. *The Journal of Neuroscience: The Official Journal of the Society for Neuroscience, 31*(12), 4484-4495.

Liu, T., & Mance, I. (2011). Constant spread of feature-based attention across the visual field. *Vision Research, 51*(1), 26-33.

Liu, T., Stevens, S. T., & Carrasco, M. (2007). Comparing the time course and efficacy of spatial and feature-based attention. *Vision Research, 47*(1), 108-113.

Luck, S. J. (2005a). *An introduction to the event-related potential technique*. Cambridge, MA: MIT Press.

Luck, S. J. (2005b). Ten simple rules for designing and interpreting ERP experiments. In T. C. Handy (Ed.), *Event-related potentials: A methods handbook* (pp. 17-32). Cambridge: The MIT Press.

Luck, S. J., Chelazzi, L., Hillyard, S. A., & Desimone, R. (1997). Neural mechanisms of spatial selective attention in areas V1, V2, and V4 of macaque visual cortex. *Journal of Neurophysiology, 77*(1), 24-42.

Luck, S. J., & Hillyard, S. A. (1994). Electrophysiological correlates of feature analysis during visual search. *Psychophysiology, 31*(3), 291-308.

Luna, B., Thulborn, K. R., Strojwas, M. H., McCurtain, B. J., Berman, R. A., Genovese, C. R., & Sweeney, J. A. (1998). Dorsal cortical regions subserving visually guided saccades in humans: An fMRI study. *Cerebral Cortex, 8*(1), 40-47.

Lupiáñez, J., Jesús Funes, M. (2005). Peripheral spatial cues modulate spatial congruency effects: Analysing the "locus" of the cueing modulation. *European Journal of Cognitive Psychology, 17*(5), 727-752.

Macaluso, E., & Doricchi, F. (2013). Attention and predictions: Control of spatial attention beyond the endogenous-exogenous dichotomy. *Frontiers in Human Neuroscience, 7*, 685.

Mangun, G. R. (1995). Neural mechanisms of visual selective attention. *Psychophysiology, 32*(1), 4-18.

Martinez-Trujillo, J. C., & Treue, S. (2004). Feature-based attention increases the selectivity of population responses in primate visual cortex. *Current Biology: CB, 14*(9), 744-751.

Mattler, U. (2003). Delayed flanker effects on lateralized readiness potentials. *Experimental Brain Research, 151*(2), 272-288.

Maunsell, J. H., & Cook, E. P. (2002). The role of attention in visual processing. *Philosophical Transactions of the Royal Society of London: Series B, Biological Sciences, 357*(1424), 1063-1072.

Maunsell, J. H., & McAdams, C. J. (2001). Effects of attention on the responsiveness and selectivity of individual neurons in visual cerebral cortex. In J. Braun, C. Koch & J. L. Davis (Eds.), *Visual attention and cortical circuits* (pp. 103-119). Cambridge MA: MIT Press.

Maunsell, J. H., & Treue, S. (2006). Feature-based attention in visual cortex. *Trends in Neurosciences, 29*(6), 317-322.

Mazer, J. A. (2011). Spatial attention, feature-based attention and saccades: Three sides of one coin? *Biological Psychiatry, 69*(12), 1147-1152.

McAdams, C. J., & Maunsell, J. H. (2000). Attention to both space and feature modulates neuronal responses in macaque area V4. *Journal of Neurophysiology, 83*(3), 1751-1755.

McCarley, J. S., & Mounts, J. R. (2008). On the relationship between flanker interference and localized attentional interference. *Acta Psychologica, 128*(1), 102-109.

McGinnis, E. M., & Keil, A. (2011). Selective processing of multiple features in the human brain: Effects of feature type and salience. *PloS One, 6*(2), e16824.

Mechelli, A., Humphreys, G. W., Mayall, K., Olson, A., & Price, C. J. (2000). Differential effects of word length and visual contrast in the fusiform and lingual gyri during reading. *Proceedings of the Royal Society of London B: Biological Sciences, 267*(1455), 1909-1913.

Miedl, S. F., Fehr, T., Herrmann, M., & Meyer, G. (2014). Risk assessment and reward processing in problem gambling investigated by event-related potentials and fMRI-constrained source analysis. *BMC Psychiatry, 14*, 229.

Moher, J., Lakshmanan, B. M., Egeth, H. E., & Ewen, J. B. (2014). Inhibition drives early feature-based attention. *Psychological Science, 25*(2), 315-324.

Munneke, J., Heslenfeld, D. J., Usrey, W. M., Theeuwes, J., & Mangun, G. R. (2011). Preparatory effects of distractor suppression: Evidence from visual cortex. *PloS One, 6*(12), e27700.

Munneke, J., Van der Stigchel, S., & Theeuwes, J. (2008). Cueing the location of a distractor: An inhibitory mechanism of spatial attention? *Acta Psychologica, 129*(1), 101-107.

Natale, E., Marzi, C. A., & Macaluso, E. (2010). Right temporal-parietal junction engagement during spatial reorienting does not depend on strategic attention control. *Neuropsychologia, 48*(4), 1160-1164.

Nee, D. E., Kastner, S., & Brown, J. W. (2011). Functional heterogeneity of conflict, error, task-switching, and unexpectedness effects within medial prefrontal cortex. *NeuroImage, 54*(1), 528-540.

Nee, D. E., Wager, T. D., & Jonides, J. (2007). Interference resolution: Insights from a meta-analysis of neuroimaging tasks. *Cognitive, Affective & Behavioral Neuroscience, 7*(1), 1-17.

Neo, G., & Chua, F. K. (2006). Capturing focused attention. *Perception & Psychophysics, 68*(8), 1286-1296.

Neta, M., Miezin, F. M., Nelson, S. M., Dubis, J. W., Dosenbach, N. U., Schlaggar, B. L., & Petersen, S. E. (2015). Spatial and temporal characteristics of error-related activity in the human brain. *The Journal of Neuroscience: The Official Journal of the Society for Neuroscience, 35*(1), 253-266.

Nichols, T., Brett, M., Andersson, J., Wager, T., & Poline, J. B. (2005). Valid conjunction inference with the minimum statistic. *NeuroImage, 25*(3), 653-660.

Niendam, T. A., Laird, A. R., Ray, K. L., Dean, Y. M., Glahn, D. C., & Carter, C. S. (2012). Meta-analytic evidence for a superordinate cognitive control network subserving diverse executive functions. *Cognitive, Affective & Behavioral Neuroscience, 12*(2), 241-268.

Nieuwenhuis, S., Yeung, N., van den Wildenberg, W., & Ridderinkhof, K. R. (2003). Electrophysiological correlates of anterior cingulate function in a go/no-go task: Effects of response conflict and trial type frequency. *Cognitive, Affective & Behavioral Neuroscience, 3*(1), 17-26.

O'Connor, D. H., Fukui, M. M., Pinsk, M. A., & Kastner, S. (2002). Attention modulates responses in the human lateral geniculate nucleus. *Nature Neuroscience, 5*(11), 1203-1209.

Ogawa, T., & Komatsu, H. (2004). Target selection in area V4 during a multidimensional visual search task. *The Journal of Neuroscience: The Official Journal of the Society for Neuroscience, 24*(28), 6371-6382.

Oldfield, R. C. (1971). The assessment and analysis of handedness: The Edinburgh Inventory. *Neuropsychologia, 9*(1), 97-113.

Paquet, L. (2001). Eliminating flanker effects and negative priming in the flankers task: Evidence for early selection. *Psychonomic Bulletin & Review, 8*(2), 301-306.

Petersen, S. E., & Posner, M. I. (2012). The attention system of the human brain: 20 years after. *Annual Review of Neuroscience, 35*, 73-89.

Polich, J. (2007). Updating P300: An integrative theory of P3a and P3b. *Clinical Neurophysiology: Official Journal of the International Federation of Clinical Neurophysiology, 118*(10), 2128-2148.

Polk, T. A., Drake, R. M., Jonides, J. J., Smith, M. R., & Smith, E. E. (2008). Attention enhances the neural processing of relevant features and suppresses the processing of irrelevant features in humans: A functional magnetic resonance imaging study of the Stroop task. *The Journal of Neuroscience: The Official Journal of the Society for Neuroscience, 28*(51), 13786-13792.

Posner, M. I. (1980). Orienting of attention. *The Quarterly Journal of Experimental Psychology, 32*(1), 3-25.

Posner, M. I. (2014). Orienting of attention: Then and now. *The Quarterly Journal of Experimental Psychology (2006), 67*, 1-12.

Posner, M. I., & Petersen, S. E. (1990). The attention system of the human brain. *Annual Review of Neuroscience, 13*, 25-42.

Pratt, J., & Hommel, B. (2003). Symbolic control of visual attention: The role of working memory and attentional control settings. *Journal of Experimental Psychology: Human Perception and Performance, 29*(5), 835-845.

Rickham, P. P. (1964). Human experimentation. Code of ethics of the world medical association. Declaration of Helsinki. *British Medical Journal, 2*(5402), 177.

Ristic, J., Wright, A., & Kingstone, A. (2006). The number line effect reflects top-down control. *Psychonomic Bulletin & Review, 13*(5), 862-868.

Ro, T., Machado, L., Kanwisher, N., & Rafal, R. D. (2002). Covert orienting to the locations of targets and distractors: Effects on response channel activation in a flanker task. *The Quarterly Journal of Experimental Psychology A, Human Experimental Psychology, 55*(3), 917-936.

Ruff, C. C., Bestmann, S., Blankenburg, F., Bjoertomt, O., Josephs, O., Weiskopf, N., Deichmann, R., & Driver, J. (2008). Distinct causal influences of parietal versus frontal areas on human visual cortex: Evidence from concurrent TMS-fMRI. *Cerebral Cortex, 18*(4), 817-827.

Rugg, M. D., & Coles, M. G. H. (Eds.). (1997). *Electrophysiology of Mind: Event-Related Brain Potentials and Cognition*. Oxford: Oxford University Press.

Saenz, M., Boynton, G. M., & Koch, C. (2006). Combined effects of spatial and feature-based attention in human visual cortex [Abstract]. *Journal of Vision, 6*(6) 599-599.

Saenz, M., Buracas, G. T., & Boynton, G. M. (2002). Global effects of feature-based attention in human visual cortex. *Nature Neuroscience, 5*(7), 631-632.

Saenz, M., Buracas, G. T., & Boynton, G. M. (2003). Global feature-based attention for motion and color. *Vision Research, 43*(6), 629-637.

Scherg, M. (1990). Fundamentals of dipole source potential analysis. *Advances in Audiology, 6*, 40-69.

Scherg, M., & Von Cramon, D. (1986). Evoked dipole source potentials of the human auditory cortex. *Electroencephalography and Clinical Neurophysiology, 65*(5), 344-360.

Schoenfeld, M. A., Hopf, J. M., Martinez, A., Mai, H. M., Sattler, C., Gasde, A., Heinze, H.-J., & Hillyard, S. A. (2007). Spatio-temporal analysis of feature-based attention. *Cerebral Cortex, 17*(10), 2468-2477.

Scolari, M., Seidl-Rathkopf, K. N., & Kastner, S. (2015). Functions of the human frontoparietal attention network: Evidence from neuroimaging. *Current Opinions in Behavioral Sciences, 1*, 32-39.

Seeley, W. W., Menon, V., Schatzberg, A. F., Keller, J., Glover, G. H., Kenna, H., Reiss, A. L., & Greicius, M. D. (2007). Dissociable intrinsic connectivity networks for salience processing and executive control. *The Journal of Neuroscience: The Official Journal of the Society for Neuroscience, 27*(9), 2349-2356.

Serences, J. T., & Boynton, G. M. (2007). Feature-based attentional modulations in the absence of direct visual stimulation. *Neuron, 55*(2), 301-312.

Serences, J. T., Liu, T., & Yantis, S. (2005). Parietal mechanisms of switching and maintaining attention to locations, features, and objects. In L. Itti, G. Rees & J. Tsotsos (Eds.), *Neurobiology of attention* (pp. 35-41). San Diego, CA: Elsevier.

Serences, J. T., Shomstein, S., Leber, A. B., Golay, X., Egeth, H. E., & Yantis, S. (2005). Coordination of voluntary and stimulus-driven attentional control in human cortex. *Psychological Science, 16*(2), 114-122.

Serences, J. T., Yantis, S., Culberson, A., & Awh, E. (2004). Preparatory activity in visual cortex indexes distractor suppression during covert spatial orienting. *Journal of Neurophysiology, 92*(6), 3538-3545.

Sestieri, C., Corbetta, M., Spadone, S., Romani, G. L., & Shulman, G. L. (2014). Domain-general signals in the cingulo-opercular network for visuospatial attention and episodic memory. *Journal of Cognitive Neuroscience, 26*(3), 551-568.

Sheth, S. A., Mian, M. K., Patel, S. R., Asaad, W. F., Williams, Z. M., Dougherty, D. D., Bush, G., & Eskandar, E. N. (2012). Human dorsal anterior cingulate cortex neurons mediate ongoing behavioural adaptation. *Nature, 488*(7410), 218-221.

Shih, S. I., & Sperling, G. (1996). Is there feature-based attentional selection in visual search? *Journal of Experimental Psychology: Human Perception and Performance, 22*(3), 758-779.

Shomstein, S., Kravitz, D. J., & Behrmann, M. (2012). Attentional control: Temporal relationships within the fronto-parietal network. *Neuropsychologia, 50*(6), 1202-1210.

Simon, J. R. (1969). Reactions toward the source of stimulation. *Journal of Experimental Psychology, 81*(1), 174-176.

Sternberg, S. (1966). High-speed scanning in human memory. *Science, 153*(3736), 652-654.

Stoppel, C. M., Boehler, C. N., Sabelhaus, C., Heinze, H. J., Hopf, J. M., & Schoenfeld, M. A. (2007). Neural mechanisms of spatial- and feature-based attention: A quantitative analysis. *Brain Research, 1181*, 51-60.

Störmer, V. S., & Alvarez, G. A. (2014). Feature-based attention elicits surround suppression in feature space. *Current Biology: CB, 24*(17), 1985-1988.

Sturm, W. (2004). Kognitive Kontrolle der Aufmerksamkeitsintensitaet: *Zeitschrift fuer Psychologie, 212*(2), 107-114.

Suwazono, S., Machado, L., & Knight, R. T. (2000). Predictive value of novel stimuli modifies visual event-related potentials and behavior. *Clinical Neurophysiology: Official Journal of the International Federation of Clinical Neurophysiology, 111*(1), 29-39.

Talairach, J., & Tournoux, P. (1988). Co-Planar Stereotaxic Atlas of the Human Brain. Stuttgart, Germany: Georg Thieme Verlag. Theeuwes, J. (1994). The effects of location cuing on redundant-target processing. *Psychological Research, 57*(1), 15-19.

Theeuwes, J. (2010). Top-down and bottom-up control of visual selection. *Acta Psychologica, 135*(2), 77-99.

Tian, Y., Liang, S., & Yao, D. (2014). Attentional orienting and response inhibition: Insights from spatial-temporal neuroimaging. *Neuroscience Bulletin, 30*(1), 141-152.

Treisman, A. (1988). Features and objects: The fourteenth bartlett memorial lecture. *The Quarterly Journal of Experimental Psychology A, Human Experimental Psychology, 40*(2), 201-237.

Treisman, A. M., & Gelade, G. (1980). A feature-integration theory of attention. *Cognitive Psychology, 12*(1), 97-136.

Treue, S., & Martinez Trujillo, J. C. (1999). Feature-based attention influences motion processing gain in macaque visual cortex. *Nature, 399*(6736), 575-579.

Treue, S., & Maunsell, J. H. (1996). Attentional modulation of visual motion processing in cortical areas MT and MST. *Nature, 382*(6591), 539-541.

Uddin, L. Q. (2015). Salience processing and insular cortical function and dysfunction. *Nature Reviews Neuroscience, 16*(1), 55-61.

Ullsperger, M., & von Cramon, D. Y. (2001). Subprocesses of performance monitoring: A dissociation of error processing and response competition revealed by event-related fMRI and ERPs. *NeuroImage, 14*(6), 1387-1401.

Ungerleider, L. G., & Mishkin, M. (1982). Two cortical visual systems. In D. J. Ingle, M. A. Goodale & R. J. W. Mansfield (Eds.), *Analysis of visual behavior* (pp. 549-586). Cambridge, MA: MIT.

van Leeuwen, T. M., Petersson, K. M., Langner, O., Rijpkema, M., & Hagoort, P. (2014). Color specificity in the human V4 complex – an fMRI Repetition suppression study. In D. Papageorgiou, G. I. Christopoulos & S. M. Smirnakis (Eds.), *Advanced brain neuroimaging topics in health and disease - methods and applications* (pp. 275-295). Rijeka, Croatia: InTech.

van Maanen, L., Forstmann, B. U., Keuken, M. C., Wagenmakers, E. J., & Heathcote, A. (2015). The impact of MRI scanner environment on perceptual decision-making. *Behavior Research Methods. doi:10.3758/s13428-015-0563-6 [doi]*

Van Veen, V., & Carter, C. S. (2002). The timing of action-monitoring processes in the anterior cingulate cortex. *Journal of Cognitive Neuroscience, 14*(4), 593-602.

van Veen, V., Cohen, J. D., Botvinick, M. M., Stenger, V. A., & Carter, C. S. (2001). Anterior cingulate cortex, conflict monitoring, and levels of processing. *NeuroImage, 14*(6), 1302-1308.

Vierck, E., & Miller, J. (2008). Precuing benefits for color and location in a visual search task. *Perception & Psychophysics, 70*(2), 365-373.

Vossel, S., Geng, J. J., & Fink, G. R. (2014). Dorsal and ventral attention systems: Distinct neural circuits but collaborative roles. *The Neuroscientist: A Review Journal Bringing Neurobiology, Neurology and Psychiatry, 20*(2), 150-159.

Vossel, S., Weidner, R., Driver, J., Friston, K. J., & Fink, G. R. (2012). Deconstructing the architecture of dorsal and ventral attention systems with dynamic causal modeling. *The Journal of Neuroscience: The Official Journal of the Society for Neuroscience, 32*(31), 10637-10648.

Wegener, D., Ehn, F., Aurich, M. K., Galashan, F. O., & Kreiter, A. K. (2008). Feature-based attention and the suppression of non-relevant object features. *Vision Research, 48*(27), 2696-2707.

Wei, P., Szameitat, A. J., Mueller, H. J., Schubert, T., & Zhou, X. (2013). The neural correlates of perceptual load induced attentional selection: An fMRI study. *Neuroscience, 250*, 372-380.

White, A. L., & Carrasco, M. (2011). Feature-based attention involuntarily and simultaneously improves visual performance across locations. *Journal of Vision, 11*(6): *15*, 1-10.

Wilkinson, D., & Halligan, P. (2004). The relevance of behavioural measures for functional-imaging studies of cognition. *Nature Reviews Neuroscience, 5*(1), 67-73.

Williford, T., & Maunsell, J. H. (2006). Effects of spatial attention on contrast response functions in macaque area V4. *Journal of Neurophysiology, 96*(1), 40-54.

Wilson, D. E., Muroi, M., & MacLeod, C. M. (2011). Dilution, not load, affects distractor processing. *Journal of Experimental Psychology: Human Perception and Performance, 37*(2), 319-335.

Wojciulik, E., & Kanwisher, N. (1999). The generality of parietal involvement in visual attention. *Neuron, 23*(4), 747-764.

Wolfe, J. M., Cave, K. R., & Franzel, S. L. (1989). Guided search: An alternative to the feature integration model for visual search. *Journal of Experimental Psychology: Human Perception and Performance, 15*(3), 419-433.

Yantis, S. (2008). The neural basis of selective attention: Cortical sources and targets of attentional modulation. *Current Directions in Psychological Science, 17*(2), 86-90.

Yantis, S., & Johnston, J. C. (1990). On the locus of visual selection: Evidence from focused attention tasks. *Journal of Experimental Psychology: Human Perception and Performance, 16*(1), 135-149.

Yeung, N., Botvinick, M. M., & Cohen, J. D. (2004). The neural basis of error detection: Conflict monitoring and the error-related negativity. *Psychological Review, 111*(4), 931-959.

Yeung, N., Ralph, J., & Nieuwenhuis, S. (2007). Drink alcohol and dim the lights: The impact of cognitive deficits on medial frontal cortex function. *Cognitive, Affective & Behavioral Neuroscience, 7*(4), 347-355.

Zhang, H. H., Zhang, J., & Kornblum, S. (1999). A parallel distributed processing model of stimulus-stimulus and stimulus-response compatibility. *Cognitive Psychology, 38*(3), 386-432.

Zhou, H., & Desimone, R. (2011). Feature-based attention in the frontal eye field and area V4 during visual search. *Neuron, 70*(6), 1205-1217.

List of Tables

List of Figures

Acknowledgements

First and foremost, I would like to thank my supervisors Prof. Dr. Dr. Manfred Herrmann, who advised and guided me throughout my PhD student time, and Dr. Daniela Galashan without whom the project would not have been possible and who supported me morally as well as scientifically in all respects (including a certain trip to a tropical island).

I am also grateful to Prof. Fahle for reviewing my doctoral thesis and to Prof. Dr. Koch as well as Stephanie Rosemann and David Lüdtke for being willing to survey my dissertation colloquium. My special thanks go to Dr. Thorsten Fehr for the many exhilarating discussions about scientific viewpoints but also off-topic about crucial social matters. As the German Research Foundation financially supported this project, I would also like to express my thanks to this funding organization. Moreover, I am also indebted to all participants who volunteered in the experiments.

Scientific life is often frustrating and nerve-racking; therefore, one needs compensation in order to stay motivated. Several people brightened the grey everyday in the Cognium with occasional coffee breaks in the kitchen, most notably Dr. Rita Korsch and Sascha Clamer who were always ready to sacrifice themselves by eating biscuits with me. Sascha also supported me a lot when technical problems occurred (which happened very often during measurements). I would also like to thank Peter Erhard and Jana Vogelgesang for making the endless measurement sessions endurable. In addition, I would like to thank Davina Biel, Anna Balatsan, Charlotte Herzmann, and Barbara Muntz who helped and supported me in several respects.

Working on a doctoral thesis requires more time than seems to be available. I am deeply thankful to my uncomplaining husband Stefan Siemann who had to endure endless nights of writing sessions and a chaos in the living room (not to mention my fretfulness…). Thank you also to my family who knew when to distract me. My mother often provided me with healthy food during the end of my pregnancy and probably ensured that I gave birth to a healthy child.

My beautiful daughter Fiona Siemann was with me throughout the hot phase of writing and kept me motivated to stay on the ball. In the end, she won the race, but her birth gave me the opportunity to gain distance from the dissertation and offered me a new perspective on things – that of a loving mother who knows now that time is endless, but we are not.

Appendix

Appendix A: Experiment I (spatial cueing): Instruction file presented to participants before the training session. All task-relevant aspects were described in detail including cue validity frequencies and response button allocations (here: H = left; S = right; allocation was counterbalances across participants). The instruction file in experiment II (feature-based cueing) was analogous but with color cues instead of location cues.

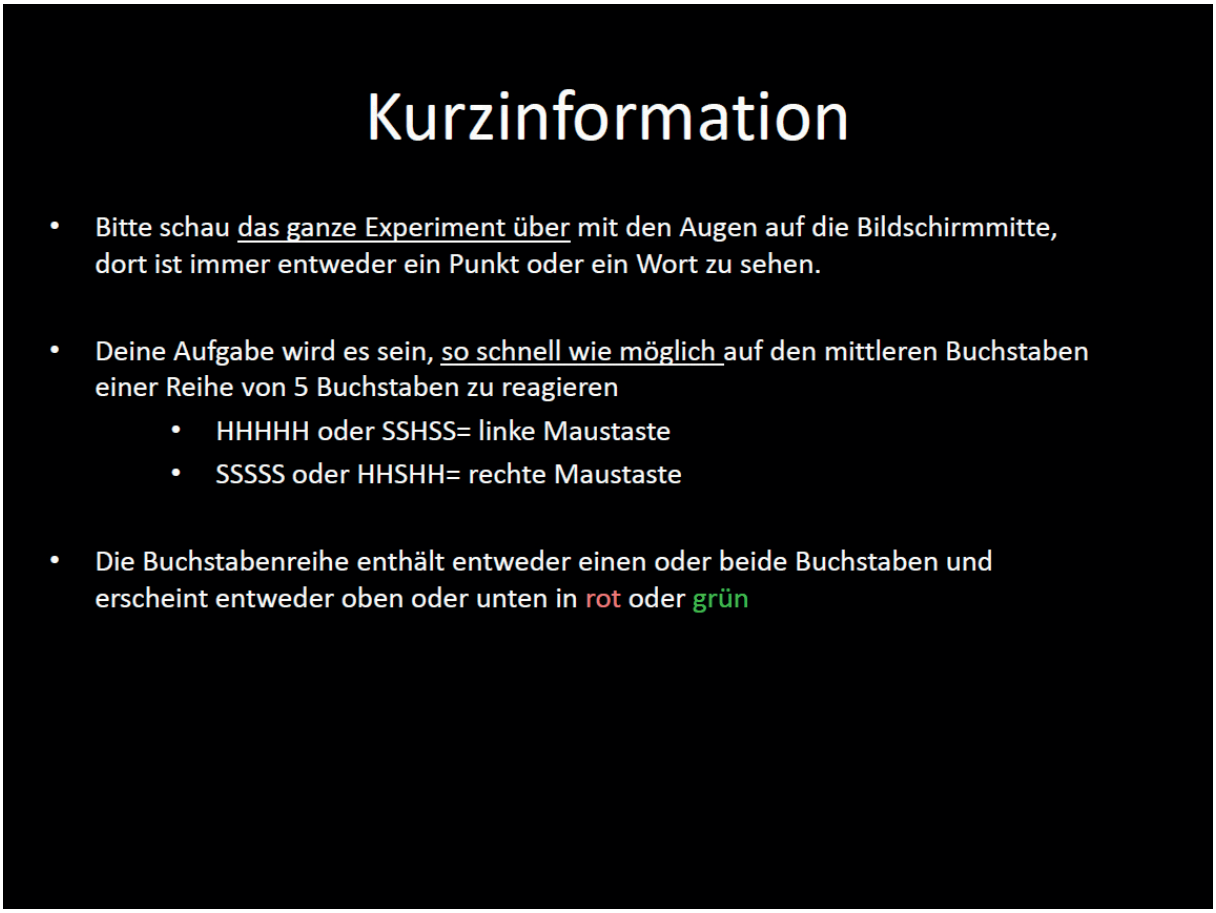

Nun im Detail:
die Erklärung der Aufgabe ist links dargestellt
und rechts ein Beispiel der Reize, die Du sehen wirst.

Es gibt 2 Antworttasten (linke und rechte Maustaste in der rechten Hand),
die mit dem Zeige- und Mittelfinger der rechten Hand gedrückt werden sollen.

- Zunächst siehst Du einen mittig präsentierten Punkt,

- Danach kommt als Hinweis entweder das Wort „oben“ oder „unten“ oder eine Reihe mit „xxxx“
- Konzentriere Dich dann auf die jeweilige Position (oben/unten) und erwarte, dass dort Buchstabenreihe mit dem H oder S in der Mitte erscheint, allerdings OHNE die Augen von der Bildschirmmitte weg zu bewegen.
- Wenn als Hinweis „xxxx“ erscheint, dann sollst Du Deine Aufmerksamkeit auf beide Positionen gleichzeitig ausrichten.

- Für kurze Zeit wird nun wieder der Punkt in der Mitte präsentiert

- Als nächstes erscheint über oder unter dem Punkt, auf den du immer schaust, die Buchstabenreihe in einer der möglichen Farben.
- Hierbei ist es Deine Aufgabe, so schnell und richtig wie möglich die richtige Taste zu drücken, und zwar die linke Maustaste, wenn der mittlere Buchstabe ein „H“ ist und die rechte, wenn es ein „S“ ist
- H = links; S = rechts

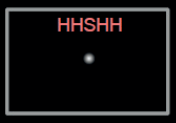

- Der **Hinweisreiz** am Anfang sagt die Position des Zielreizes nicht immer richtig voraus.
- Warum solltest du trotzdem den **Zielreiz** an der Position erwarten, die durch den Hinweisreiz vorgegeben wird?

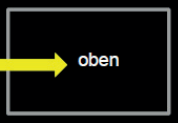

- Wenn du deine Aufmerksamkeit auf diese Position ausrichtest und der Hinweisreiz die richtige Position vorhersagt, bist du am schnellsten.
- Dies trifft auf die Hälfte der Fälle mit dem Hinweisreiz zu, Du kannst also nur dann in der Hälfte der Fälle sehr schnell sein, wenn Du Dich tatsächlich auf die Position einstellst, die dieser ansagt.
- Und genau in diesen Bedingungen sollst Du besonders schnell sein!
- Es ist nicht schlimm, wenn Du dadurch in der Bedingung, in der die Position falsch vorausgesagt wurde, etwas langsamer bist. Versuche auch hier so schnell es geht zu antworten!

Wichtig ist:

- 1.) dass Du Deine Aufmerksamkeit tatsächlich auf die Position ausrichtest, die der Hinweisreiz anzeigt und den Zielreiz in dieser Position erwartest!
- 2.) dass Du immer so schnell wie möglich antwortest, ob in der Mitte des Zielreizes ein „H“ (linke Taste) oder ein „S“ (rechte Taste) aufgetaucht ist!

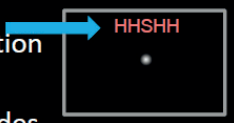

- Zunächst wirst du einen Durchgang machen, in dem du Rückmeldung bekommst („richtig“, „falsch“, „zu langsam“).
- Danach gibt es noch einen Durchgang ohne Rückmeldung.
- Im eigentlichen Experiment werden 5 Durchgänge OHNE Rückmeldung präsentiert. Zwischen den Durchgängen gibt es Pausen, in denen Du Dich erholen und bei Bedarf etwas essen oder trinken kannst.

- Um zu bestimmen, wie gut du es schaffst, immer mit den Augen auf die Bildschirmmitte zu schauen, werden Deine Augenbewegungen mittels einer Infrarotkamera aufgezeichnet
- So können wir dir Rückmeldung geben, falls dein Blick sich zu weit von der Bildschirmmitte entfernt

➔ Obwohl deine **Augen** die Mitte fixieren, kannst und sollst du deine **Aufmerksamkeit** auf die Position richten, die der Hinweisreiz vorgibt

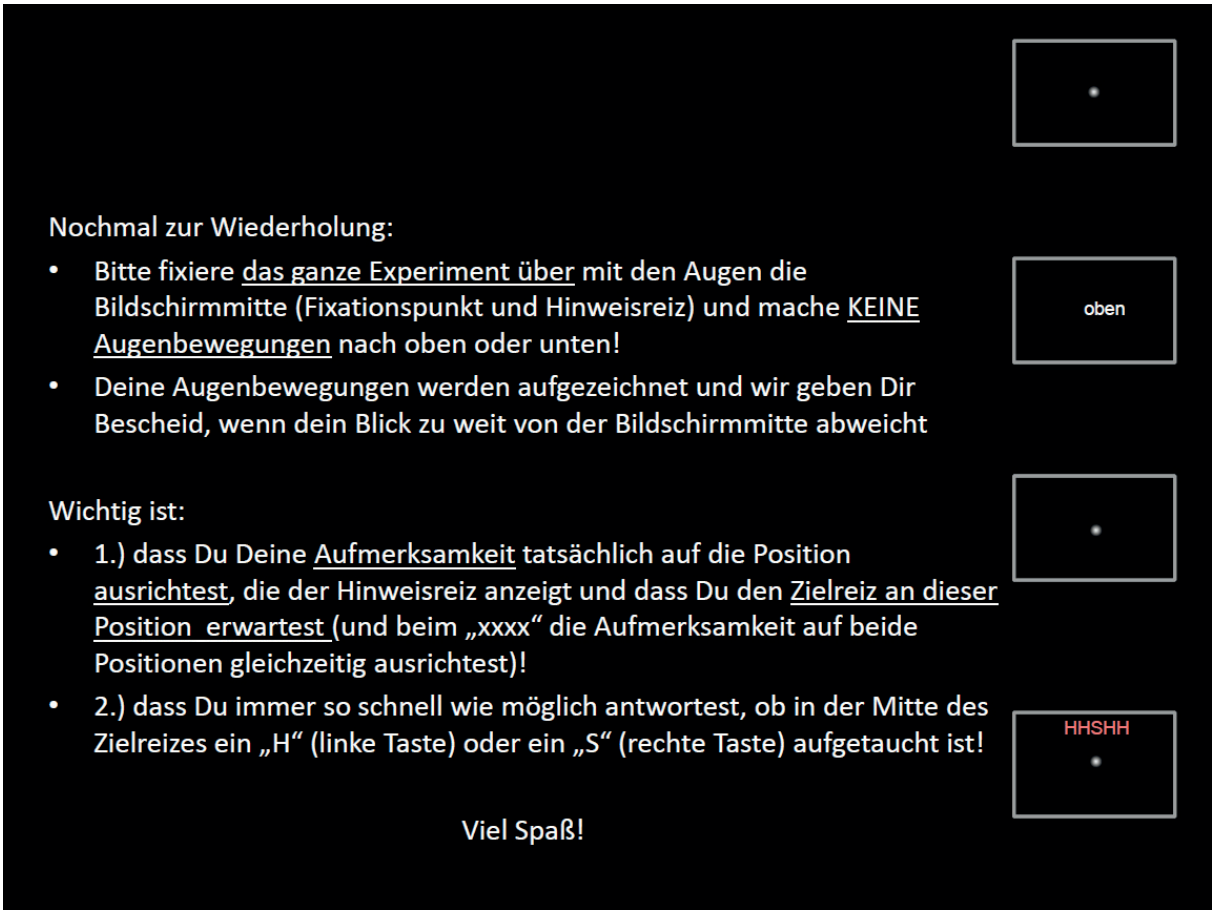
Nochmal zur Wiederholung:
• Bitte fixiere das ganze Experiment über mit den Augen die Bildschirmmitte (Fixationspunkt und Hinweisreiz) und mache KEINE Augenbewegungen nach oben oder unten!
• Deine Augenbewegungen werden aufgezeichnet und wir geben Dir Bescheid, wenn dein Blick zu weit von der Bildschirmmitte abweicht
oben
Wichtig ist:
• 1.) dass Du Deine Aufmerksamkeit tatsächlich auf die Position ausrichtest, die der Hinweisreiz anzeigt und dass Du den Zielreiz an dieser Position erwartest (und beim „xxxx“ die Aufmerksamkeit auf beide Positionen gleichzeitig ausrichtest)!
• 2.) dass Du immer so schnell wie möglich antwortest, ob in der Mitte des Zielreizes ein „H“ (linke Taste) oder ein „S“ (rechte Taste) aufgetaucht ist!
HHSHH
Viel Spaß!

Appendix B: Parameters and example images of the color localizers. The first localizer was made up of the letters presented during the main experiment, the second localizer consisted of a 3 x 3 checkerboard. In both cases, there were blocks of varying colors (chromatic) and blocks with matching shades of grey (achromatic). The colors flickered at 8Hz and were presented in alternating blocks of chromatic and achromatic with a fixation period before each switch. In order to maintain a constant level of attention, participants were asked to count occasional switches of the central fixation plus to a cross.

Stimulus Localizer

Checkerboard localizer

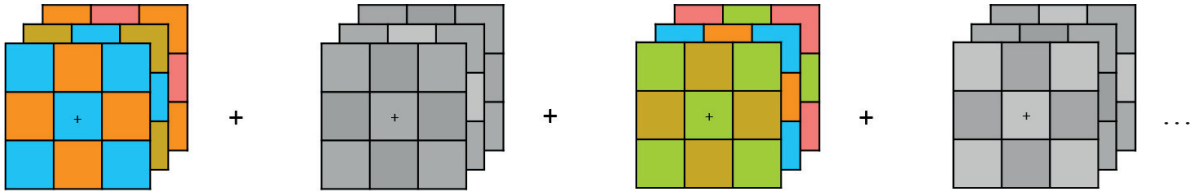

Appendix C: Additional image presented during the Ishihara test with colors in the red and green colors used in the experiments. This ensured that the colors used in the experiment could be distinguished. Participants were asked to trace the red line with their index finger.

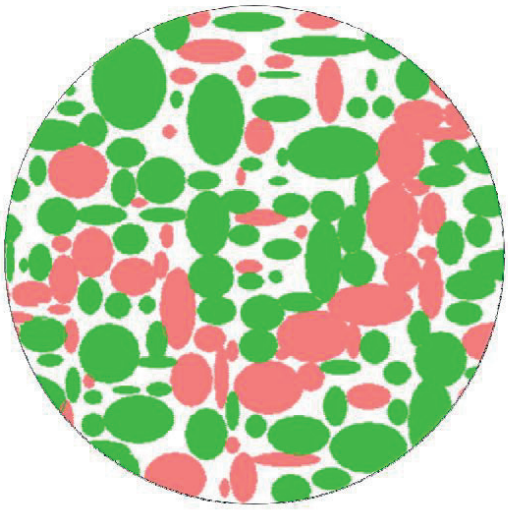

Appendix D: Written confirmation of the local ethics committee that was obtained before measurements.

Universität Bremen

Ethikkommission

Der Vorsitzende
Prof. Dr. jur. Robert Francke

Universität Bremen Referat 06 Bibliothekstraße 1, D-28359 Bremen

Dr. Daniela Galashan
Universität Bremen
Abteilung für Neuropsychologie und Verhaltensneurobiologie
Zentrum für Kognitionswissenschaften (ZKW)
Center for Advanced Imaging (CAI) – Bremen
Hochschulring 18

28359 Bremen

Rechtsstelle der Universität
Ansprechpartnerin: Frau Brüning
ibruening@uni-bremen.de
Tel.: 0421-218-60213
Fax.: 0421-218-98-60213
http://www.ethikkommission.uni-bremen.de/

30. Juni 2011

Ihr Forschungsvorhaben:

Zeitlich-räumliche Charakterisierung neuronaler Konflikt-Verarbeitungsprozesse unter dem Einfluss räumlicher und eigenschaftsbasierter Aufmerksamkeitsausrichtung

Sehr geehrte Frau Dr. Galashan,

die Ethik-Kommission der Universität Bremen hat Ihren Forschungsantrag geprüft. Die Prüfung der Kommission hat sich auf folgende Unterlagen bezogen:

Forschungsvorhaben: Zeitlich-räumliche Charakterisierung neuronaler Konflikt-Verarbeitungsprozesse unter dem Einfluss räumlicher und eigenschaftsbasierter Aufmerksamkeitsausrichtung (Stand: Juni 2011)

Die Ethikkommission der Universität Bremen hat festgestellt, dass auf der Grundlage der zur Beratung vorgelegten Unterlagen nach dem gegenwärtigen Stand wissenschafts- und berufsethische Bedenken gegen die Durchführung der geplanten Studie nicht bestehen. Das heißt, Sie erhalten hiermit ein positives Votum der Ethikkommission.

Bitte beachten Sie freundlicherweise folgende Hinweise:

Bei Änderung des Studiendesigns sollte der Antrag erneut vorgelegt werden.

Über alle schwerwiegenden oder unerwarteten und unerwünschten Ereignisse, die während der Studie auftreten, muss die Kommission umgehend benachrichtigt werden.

Hilfreich wäre es, wenn Sie nach Abschluss des Projektes einen sehr knappen Bericht übersenden würden, aus dem der Erfolg/Misserfolg der Studie ersichtlich wird und der Angaben darüber enthält, ob die Studie

abgebrochen oder geändert wurde und ob Regressansprüche geltend gemacht wurden.

Die wissenschaftliche, ärztliche und juristische Verantwortung des Leiters der Untersuchung bleibt entsprechend der Beratungsfunktion der Ethik-Kommission durch unsere Stellungnahme unberührt.

Ihrer Arbeit wünsche ich guten Erfolg.

Mit freundlichen Grüßen

R. Francke

(Prof. Dr. Robert Francke)

Appendix E: Written information file, questionnaire with exclusion criteria, and consent form for fMRI measurements.

Code: .....

Informationsblatt für Probanden

Sehr geehrte Untersuchungsteilnehmerin, sehr geehrter Untersuchungsteilnehmer,

vielen Dank für Ihr Interesse an einer Studie, bei der die Aktivität im Gehirn unter Ruhe und beim Lösen von Aufgaben untersucht werden soll. Wir möchten Sie zunächst über den Ablauf informieren, um Ihnen einen Überblick über die geplanten Messungen zu ermöglichen und Ihnen das Ziel der Untersuchungen zu erklären.

Die Untersuchungen werden mit einem Magnetresonanztomographen (kurz MRT) durchgeführt, der uns Messungen der Durchblutung im Gehirn schmerzfrei und ohne zusätzliche Gabe von Medikamenten ermöglicht.

Ziele und Ablauf der Untersuchung

In dieser Studie soll die Aktivität des Gehirns während der Darbietung visueller Reize bestimmt werden. In einigen Versuchsteilen ist es nötig, die Augenbewegungen zu kontrollieren. Daher kann gegebenenfalls eine Video-Überwachung mittels Infrarot-Beleuchtung der Augen (Eye-Tracking) erfolgen. In einigen Untersuchungen ist außerdem eine Reaktion auf den gezeigten Reiz erforderlich, die per Tastendruck gegeben wird. Die Art der Aufgabe wird Ihnen vor der Messung ausführlich vom Versuchsleiter erklärt.

Im Fall der aktuellen Studie wird zunächst die Augen-Messanlage individuell eingestellt, dann folgt das eigentliche Experiment (ca. 35 Minuten). Anschließend werden zwei kurze Messungen (jeweils 5 Minuten) aufgenommen, um später die Lokalisation bestimmter Areale im Gehirn zu ermöglichen. Als letztes wird die Anatomie des Gehirns aufgezeichnet.

Was ist eine Magnetresonanztomographie?

Im Rahmen der Studie ist eine funktionelle Magnetresonanztomographie des Gehirns vorgesehen. Mit Hilfe dieser Methode ist es möglich, die Durchblutung in Ihrem Gehirn zu messen und daraus Rückschlüsse auf die bei der Aufgabe beteiligten Bereiche zu ziehen. Hierbei treffen Radiowellen, die in dem Magnetfeld erzeugt worden sind, auf den Körper, der Signale zurückschickt. Diese Echosignale werden von speziellen Antennen aufgefangen und in einem Computer ausgewertet.

Ein Kontrastmittel ist **n i c h t** erforderlich. Es werden **k e i n e** Röntgenstrahlen eingesetzt.

Wie läuft die Untersuchung ab?

Vor der Untersuchung werden Sie vom Untersuchungsleiter ausführlich über die für den Tag geplanten Messungen und Ziele informiert. Auch im Verlauf der Untersuchung werden Sie vom Untersucher jederzeit gehört. **Sie haben das Recht, ohne Angabe von Gründen jederzeit die Teilnahme an der Messung abzulehnen bzw. abzubrechen.**

Für die Untersuchung legen Sie sich auf eine Liege, wo Ihr Kopf in einer Kopfspule positioniert wird. Anschließend werden Sie langsam in die Öffnung des Magnetresonanztomographen geschoben. Dort befinden Sie sich während der gesamten Untersuchung. Während der Messungen sind sehr laute Klopfgeräusche zu hören, die völlig normal sind und von den schnell geschalteten Magnetfeldgradienten verursacht werden. Um Ihrem Gehör nicht zu schaden, müssen Sie einen geeigneten Hörschutz (Ohrstöpsel oder Schallschutz'hörer') tragen. Für die Qualität der Messungen ist es wichtig, während der Untersuchung möglichst ruhig liegen zu bleiben. Um dies zu erleichtern, werden Kopf, Arme und Beine mit Polstern und anderen Hilfsmitteln schmerzfrei und bequem gelagert.

1

Die Aufgaben, die Sie während der Untersuchung bearbeiten sollen, werden Ihnen über einen an der Kopfspule angebrachten Spiegel oder Kopfhörer dargeboten.

Mögliche Risiken der Methode:

Im Magnet des Magnetresonanztomographen herrscht mit 3Tesla (T) ein Magnetfeld, das in etwa 62.500-mal stärker als das Erdmagnetfeld in Mitteleuropa ist. Dieser Magnet wird nie ausgeschaltet und zieht mit sehr starker Kraft alle magnetischen und magnetisierbaren Gegenständen an, welche in seine Nähe geraten. Die größte Gefahr geht von Unfällen mit solchen Gegenständen aus, die angezogen werden und mit sehr großer Geschwindigkeit in den Magneten fliegen und anschließend an ihm „festkleben". Deshalb wird mit größter Sorgfalt darauf geachtet, dass keine magnetischen oder magnetisierbaren Gegenstände in die Nähe des Magneten geraten.

Der Magnetresonanztomograph hält alle für die Sicherheit des Betriebes und insbesondere die Sicherheit der Probanden/Patienten erforderlichen Grenzwerte ein. Er wurde vom TÜV einer Sicherheitsprüfung unterzogen und wird darüber hinaus in den vorgeschriebenen Intervallen überprüft. Dennoch müssen folgende Punkte beachtet werden.

1. ***Magnetische und magnetisierbare* Gegenstände *dürfen nicht in den Messraum gelangen.***

   Auf Gegenstände, die Eisen oder Nickel enthalten, wie z.B. Messer, Schraubenzieher, Kugelschreiber, Münzen, Haarspangen, etc., wird im Bereich des Magneten eine starke Anziehungskraft ausgeübt. Dadurch werden die Gegenstände mit großer Geschwindigkeit in den Magneten gezogen und können Personen gegebenenfalls lebensgefährlich verletzten. Metallkörper (Metallplatten etc.) und andere Fremdkörper wie Geschossteile können ebenfalls ferromagnetisch sein und durch magnetische Kräfte ihre Position im Körper verändern, die dann innere Verletzungen hervorrufen.
   Kleine Metallsplitter im Auge können durch magnetische Kräfte bewegt oder gedreht werden und das Auge verletzen.

2. Personen mit Chochlea-Implantaten, Defibrillatoren oder Pumpensystemen dürfen nicht einem starken Magnetfeld ausgesetzt werden, da es auch in diesen Fällen zu Risiken durch magnetische Kräfte kommen kann.

3. ***Personen mit Herzschrittmachern dürfen nicht an Untersuchungen teilnehmen.*** Herzschrittmacher können im Magnetfeld ihre Funktionsfähigkeit verlieren Zumindest ist es sehr wahrscheinlich, dass diese in einen Grundzustand („Reset") versetzt werden.

4. Bei der Messung mit dem Magnetresonanztomographen kommt es zur Abstrahlung von hochfrequenter elektromagnetischer Strahlung, wie sie z.B. bei Radiosendern und Funktelefonen auftritt. Dies kann zu einer geringfügigen Erwärmung des untersuchten Gewebes führen, wird aber sowohl geräte- als auch steuerungstechnisch kontrolliert.

5. ***Bei allen Messungen müssen entweder schallabsorbierende Kopf'hörer' oder Lärmschutzstopfen getragen werden, die wir zur Verfügung stellen.*** Das Schalten der Magnetfeldgradienten führt in Teilen des Gradientensystems zu mechanischen Verformungen, die Geräusche mit Lautstärken über 100 dB erzeugen können. Bei Einhaltung dieser Vorsichtsmaßnahmen kann eine Schädigung des Hörsystems ausgeschlossen werden.

6. Manche Menschen erleben enge Räume als bedrohlich. Sie berichten über Unwohlsein z.B. in Fahrstühlen oder in großen Menschenansammlungen. Obwohl diese Angstgefühle meist über die Anamnese ausgeschlossen werden können, ist ein erstmaliges Auftreten während der Messung im Magnetresonanztomographen möglich. Der Untersucher ist bei der Messung anwesend; bei dem Auftreten von Symptomen kann der Proband über Sprechkontakt bzw. über eine Notklingel jederzeit auf sich aufmerksam machen, so dass eine rasche Intervention bei Symptomen gewährleistet ist.

Zufallsbefunde

Obwohl die Messungen an einem klinisch üblichen Magnetresonanztomographen stattfinden, handelt es sich bei den Messungen **um keine medizinische Untersuchung**. Die Messungen sind daher auch nicht dazu geeignet, pathologische Veränderungen zu entdecken. Auch werden die Daten nicht von fachkundigen Neuroradiologen oder Neurologen begutachtet. Deshalb können keine Rückschlüsse auf den gesundheitlichen Status gezogen werden. Trotzdem besteht die Möglichkeit, dass sich in den aufgezeichneten MRT-Bildern strukturelle Anomalien, sog. Zufallsbefunde, finden lassen. Im Falle eines Zufallsbefundes oder eines Verdachts auf einen Zufallsbefund werden in der Regel repräsentative Bilder einem fachkundigen Arzt vorgelegt, um eine erste Einschätzung einzuholen. Falls der Verdacht auf einen Zufallsbefund weiterhin vorliegt, wird Ihnen die Vorstellung bei einem Facharzt empfohlen. In jedem Fall werden wir Ihnen diese Beobachtung mitteilen.

Ihr Einverständnis dazu ist Voraussetzung dafür, an der Untersuchung teilnehmen zu können.

Code: ....

Fragebogen zur Teilnahme an Magnetresonanzuntersuchungen

Beantworten Sie bitte folgende Fragen zu möglichen Gegenanzeigen für Ihre Teilnahme an der Untersuchung (Zutreffendes bitte ankreuzen):

Tragen Sie einen *Herzschrittmacher* oder ein anderes elektrisches/medizinisches Gerät (z.B. *Insulinpumpe*)?	**o** ja	**o** weiß nicht	**o** nein
Besitzen Sie *metallische Implantate* (z.B. Zahnschrauben, Zahnspangen, Metallplatten, Katheder, Stent o.ä. oder mechanische, metallische *Verhütungsmittel*)?	**o** ja	**o** weiß nicht	**o** nein
Befinden sich in Ihrem Körper andere *metallische Fremdkörper* wie Metallplatten, Geschosssplitter o.ä.?	**o** ja	**o** weiß nicht	**o** nein
Leiden Sie unter *Raum- oder Platzangst*?	**o** ja	**o** weiß nicht	**o** nein
Sind bei Ihnen oder in Ihrer Familie Anfallsleiden (*Epilepsie*, *Fallsucht*) aufgetreten?	**o** ja	**o** weiß nicht	**o** nein
Besteht die Möglichkeit, dass Sie *schwanger* sind?	**o** ja		**o** nein
Sind Sie Brillenträger/in?	**o** ja	**o** weiß nicht	**o** nein
Tragen Sie Kontaktlinsen?	**o** ja	**o** weiß nicht	**o** nein
Haben Sie Tätowierungen?	**o** ja	**o** weiß nicht	**o** nein
Wurden Sie schon einmal operiert? Art der Operation / welches Jahr ______________________	**o** ja	**o** weiß nicht	**o** nein
Wurde bei Ihnen eine Gefäßoperation durchgeführt?	**o** ja	**o** weiß nicht	**o** nein

Erklärung:
Ich habe alle Fragen auf dieser Seite wahrheitsgemäß und nach bestem Wissen beantwortet.

_________________ _____________ ___________________________________

Ort Datum Unterschrift

✂ • ✂

Persönliche Daten:

Name ....

Adresse ....

Händigkeit .... Geschlecht ....

Geburtsdatum ....

Telefonnummer...

Email ....

Beruf: ....

5

Code: .....

Einwilligungserklärung

Über Art und Durchführung der geplanten MRT-Untersuchung im Rahmen dieser wissenschaftlichen Studie hat mich Frau / Herr ..... in einem Aufklärungsgespräch ausführlich informiert. Das Informationsblatt für Probanden ist mir ausgehändigt worden. Ich konnte alle mir wichtig erscheinenden Fragen, z.B. über spezielle Risiken und mögliche Komplikationen sowie Neben- und Folgemaßnahmen stellen, die zur Vorbereitung oder während der Untersuchung erforderlich sind. Die mir erteilten Informationen habe ich verstanden.

Ich erkläre mich hiermit bereit, an der im Informationsblatt beschriebenen freiwilligen Untersuchung im Rahmen der oben genannten wissenschaftlichen Studie teilzunehmen und gebe meine Einwilligung, dass bei mir im Rahmen der wissenschaftlichen Studie eine MRT-Untersuchung des Gehirns durchgeführt wird. Mir ist bekannt, dass ich die Einwilligung zur Teilnahme an der Studie jederzeit und ohne Angaben von Gründen widerrufen und die Untersuchung abbrechen kann.

Ich erkläre mich damit einverstanden, dass die im Rahmen der Magnetresonanzuntersuchungen erhobenen Daten in verschlüsselter Form (pseudonymisiert) auf elektronischen Datenträgern gespeichert und verarbeitet werden dürfen. Ich bin auch damit einverstanden, dass die Untersuchungsdaten in anonymer Form veröffentlicht werden. Ich habe davon Kenntnis genommen, dass nach Auswertung und Abschluss der Studie, die personenbezogenen Daten gelöscht werden und so keine Zuordnung der erhobenen Untersuchungsdaten zu meiner Person mehr möglich sein wird. Die anonymisierten Untersuchungsdaten werden spätestens zehn Jahre nach Abschluss der Studie vollumfänglich gelöscht (im Jahre 2024).

Ich erkläre mich damit einverstanden, dass die in dem „Fragebogen zur Teilnahme an Magnetresonanzuntersuchungen“ erhobenen persönlichen Daten in einer der Öffentlichkeit nicht zugänglichen Datenbank erfasst werden. Die Speicherung dieser personenbezogenen Daten dient ausschließlich der Möglichkeit einer erneuten Kontaktaufnahme durch das Institut und der Zuordnung der pseudonymisierten Untersuchungsergebnisse zu meiner Person für den Fall, dass ich meine Einwilligung zurückziehe und die Löschung der Daten verlange.

Mir ist bekannt, dass es sich bei der an mir vorzunehmenden magnetresonanztomographischen Untersuchung um keine medizinische Untersuchung handelt und ich daher keine Rückschlüsse auf meinen gesundheitlichen Status ziehen kann. Im Falle eines Zufallsbefundes oder eines Verdachts auf einen Zufallsbefund möchte ich informiert werden.

Mir ist bekannt, dass ich meine Einwilligung in die Datenverarbeitung jederzeit und ohne Angabe von Gründen widerrufen kann und die Löschung der Daten verlangen kann.

Ort, Datum	Unterschrift Untersuchungsteilnehmer/in	Unterschrift Untersucher

6

Appendix F: Written information file for EEG measurements.

Universität Bremen

Untersuchung von Aufmerksamkeitsprozessen - Studie 1

Dr. D. Galashan, Abt. für Neuropsychologie und Verhaltensneurobiologie

---

Informationsblatt für Probanden

Sehr geehrte Probandin, sehr geehrter Proband,

vielen Dank für Ihr Interesse an einer Studie, bei der die Aktivität im Gehirn während der Bearbeitung einer Aufmerksamkeits-Aufgabe untersucht werden soll.

Wir möchten Sie zunächst über den Ablauf informieren, um Ihnen einen Überblick über die geplanten Messungen zu ermöglichen und Ihnen das Ziel der Untersuchung zu erklären. Die Untersuchungen werden mit Hilfe der Elektroenzephalographie (kurz EEG) durchgeführt, die Messungen der Nervenzell-Aktivität im Gehirn ohne Eingriff, schmerzfrei und ohne zusätzliche Gabe von Medikamenten ermöglicht.

Ziel der Untersuchung

Die Studie soll die Aktivität im Gehirn während der Durchführung einer visuell präsentierten Aufgabe bestimmen.

Was ist ein Elektroenzephalogramm (EEG)?

Aufgrund der Aktivität der Nervenzellen lässt sich an der Kopfoberfläche fortlaufend eine elektrische Spannung messen – das Elektroenzephalogramm (EEG). Für die EEG-Messung müssen an verschiedenen Stellen des Kopfes Elektroden platziert werden, die eine Verbindung zwischen Kopfoberfläche und Messgerät herstellen.

Die Elektroden bestehen aus Silber/Silberchlorid, Zinn oder Gold. Zur Verbesserung der Leitfähigkeit wird eine Paste verwendet, die im Wesentlichen aus Wasser, Kochsalz und Verdickungsmittel besteht. Um zwischen Haut und Elektrode einen hinreichend guten Kontakt herzustellen, werden die Elektroden an einer speziellen Haube, ähnlich einer Badekappe, fixiert.

Wie läuft die Untersuchung ab?

Vor der Untersuchung werden Sie vom Untersuchungsleiter ausführlich über die für den Tag geplanten Messungen und Ziele informiert. Sie haben das Recht, jederzeit ohne Angabe von Gründen und ohne persönlichen Nachteil, die Teilnahme an der Messung abzulehnen oder während der Messung abzubrechen.

Während der Messung sitzen Sie auf einem Stuhl. Um Störungen der Messung zu vermeiden, findet die Untersuchung in einem eigenen, abgeschirmten und störungsarmen Raum statt. Während der Messung wird eine Infrarotkamera Ihre Augenbewegungen aufzeichnen. Ein Mitarbeiter der Abteilung wird zusammen mit Ihnen in dem Raum bleiben, Sie können sich jederzeit an ihn wenden.

Mögliche Risiken der Methode?

Die EEG-Messung ist vollständig gefahrlos. Für das EEG werden nur solche Geräte verwendet, die den einschlägigen Sicherheitsbestimmungen genügen. Sie werden in gleicher Form auch für die klinische Routine eingesetzt.

Appendix G: Consent form for training session and EEG measurements.

Universität Bremen

Untersuchung von Aufmerksamkeitsprozessen - Studie 1

Dr. D. Galashan, Abt. für Neuropsychologie und Verhaltensneurobiologie

Einwilligungserklärung

Über die geplante elektrophysiologische Untersuchung im Rahmen einer wissenschaftlichen Studie hat mich Frau/Herr _____ in einem Aufklärungsgespräch ausführlich informiert.

Ich konnte alle mir wichtig erscheinenden Fragen, z.B. über die Neben- und Folgemaßnahmen stellen, die zur Vorbereitung oder während der Untersuchung erforderlich sind. Auch habe ich das entsprechende Informationsblatt gelesen.

Die mir erteilten Informationen habe ich inhaltlich verstanden. Mir ist bekannt, dass ich meine Einwilligung jederzeit ohne Angabe von Gründen widerrufen kann.

Ich weiß, dass die bei Untersuchungen mit mir gewonnenen Daten auf der Basis elektronischer Datenverarbeitung weiterverarbeitet und eventuell für wissenschaftliche Veröffentlichungen verwendet werden sollen. Ich bin mit der pseudonymisierten Verarbeitung und anonymisierten Veröffentlichung dieser Daten einverstanden. Ich habe davon Kenntnis genommen, dass die Key-Datei, also die Zuordnung meiner personenbezogenen Daten zu den Untersuchungsdaten, nach Abschluss des Projektes, spätestens 2 Jahre nach Beendigung der Datenauswertung, vollständig gelöscht wird. Auch diese Einwilligung kann ich jederzeit ohne Angabe von Gründen widerrufen. Informationen zu meiner Person werden im Rahmen datenschutzrechtlicher Bedingungen verwaltet.

Ich gebe hiermit meine Einwilligung, dass bei mir im Rahmen des Forschungsvorhabens "*Untersuchung von Aufmerksamkeitsprozessen*" eine psychophysikalische bzw. elektrophysiologische Untersuchung durchgeführt wird.

Trainings-Sitzung:

_____	_____	_____
Ort, Datum	Unterschrift Teilnehmer	Unterschrift Untersucher

EEG-Sitzung:

_____	_____	_____
Ort, Datum	Unterschrift Teilnehmer	Unterschrift Untersucher

Appendix H: Experiment I (spatial cueing): Plots of source sensitivity images showing source sensitivities (in percent) of the single regional sources.

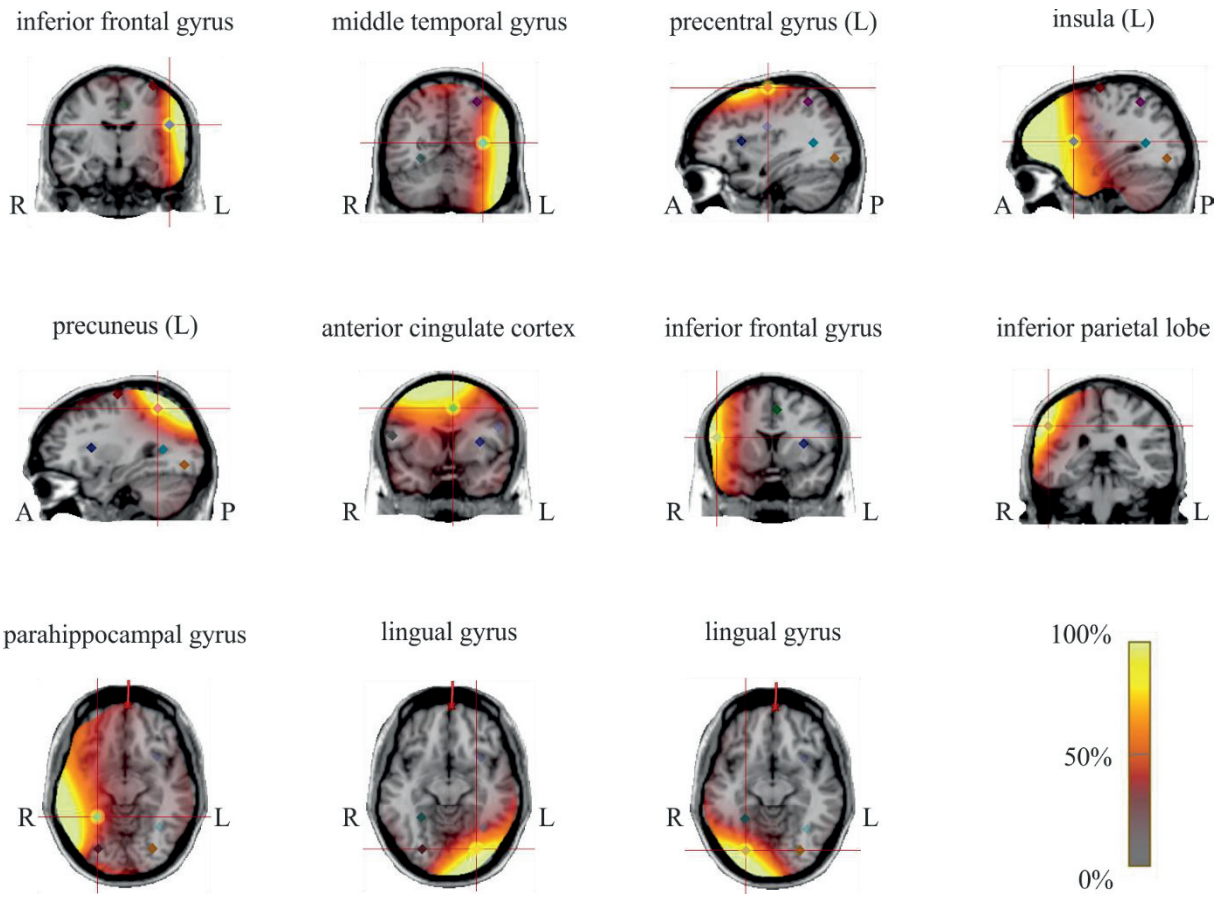

Appendix I1: ERPs of the congruent (light green) and incongruent (dark green) conditions with valid cueing. Top = experiment I (spatial cueing); bottom = experiment II (feature-based cueing). N = 18 (experiment I); N = 21 (experiment II).

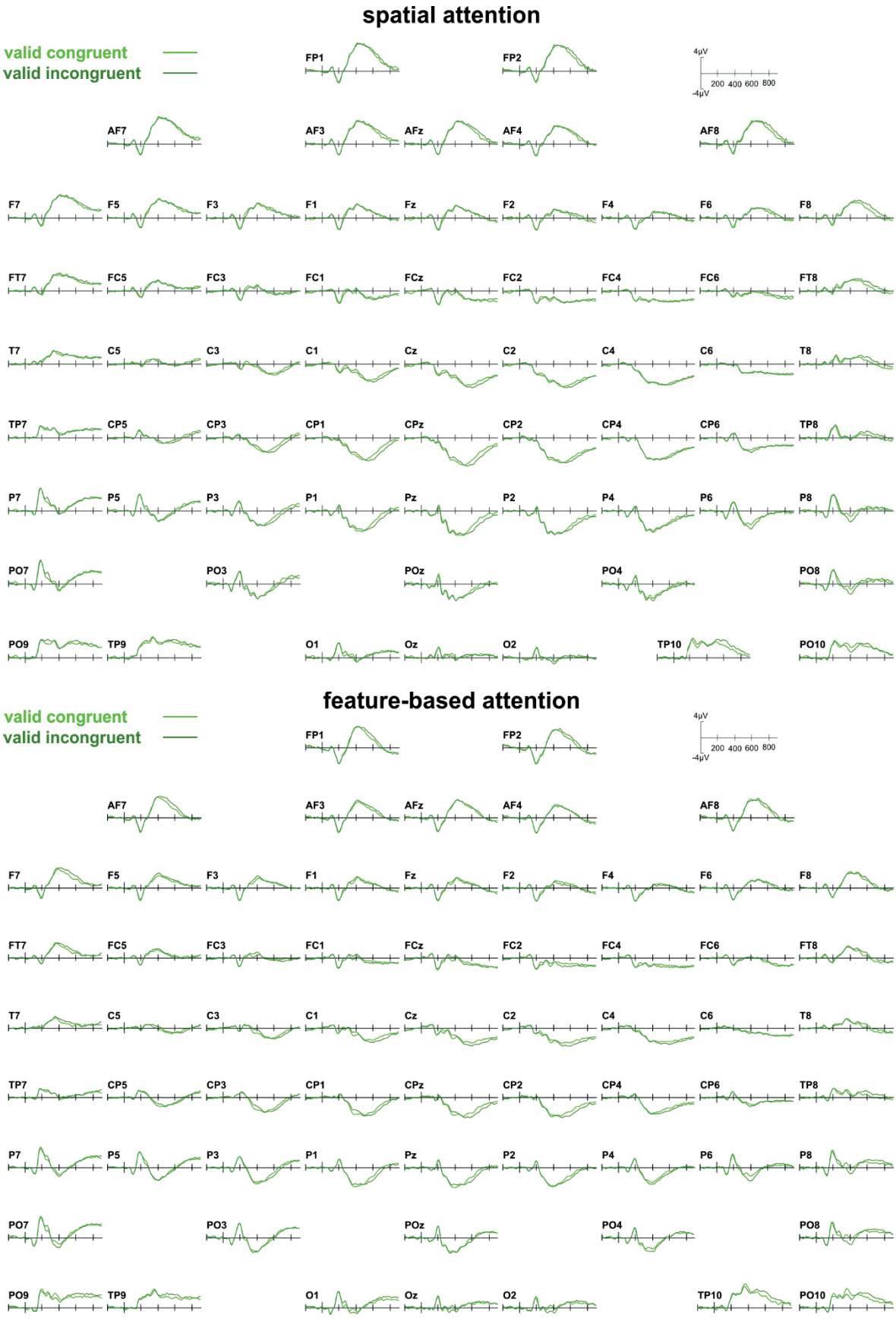

Appendix I2: ERPs of the congruent (light green) and incongruent (dark green) conditions with neutral cueing. Top = experiment I (spatial cueing); bottom = experiment II (feature-based cueing). N = 18 (experiment I); N = 21 (experiment II).

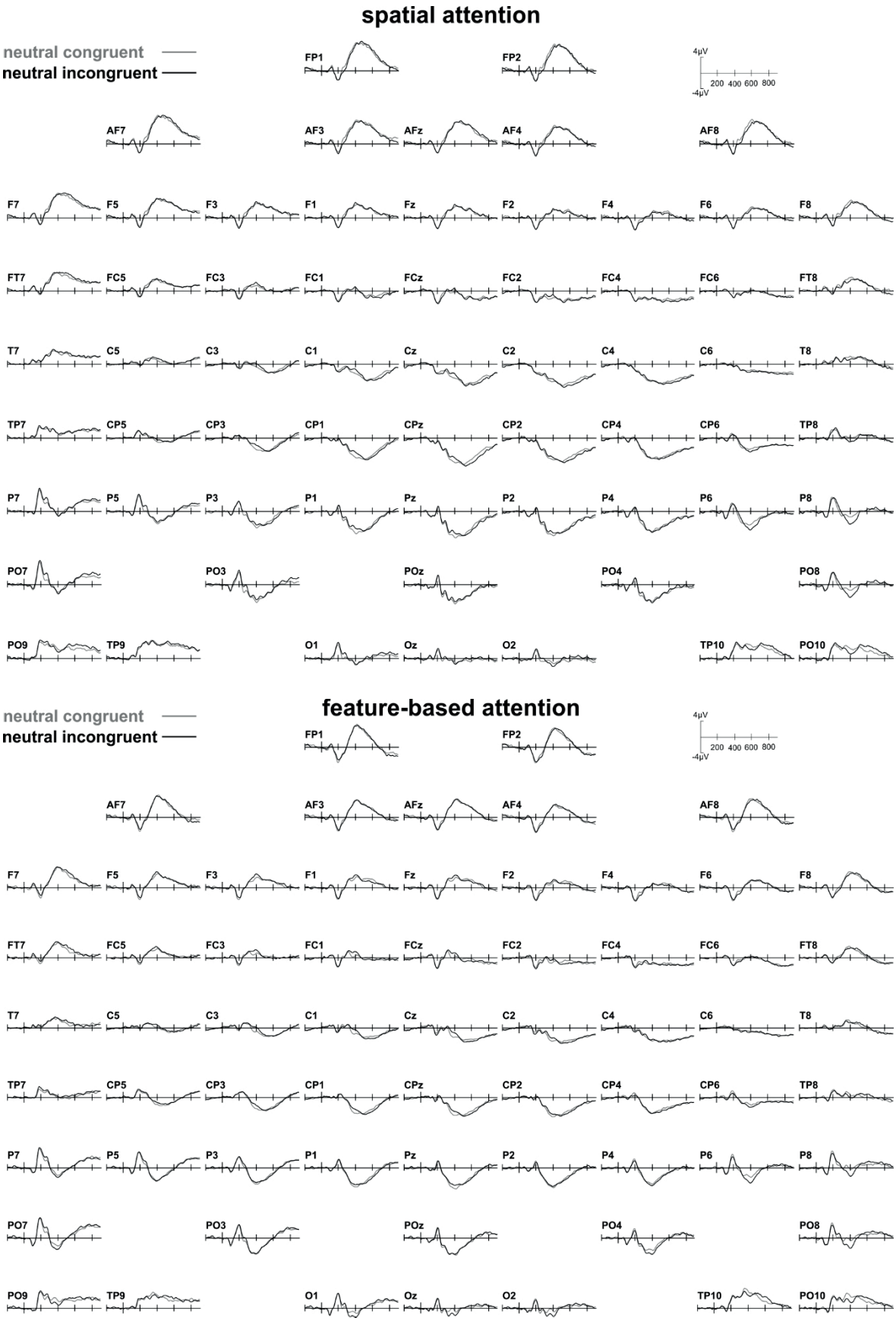

Appendix I3: ERPs of the congruent (light green) and incongruent (dark green) conditions with invalid cueing. Top = experiment I (spatial cueing); bottom = experiment II (feature-based cueing). N = 18 (experiment I); N = 21 (experiment II).

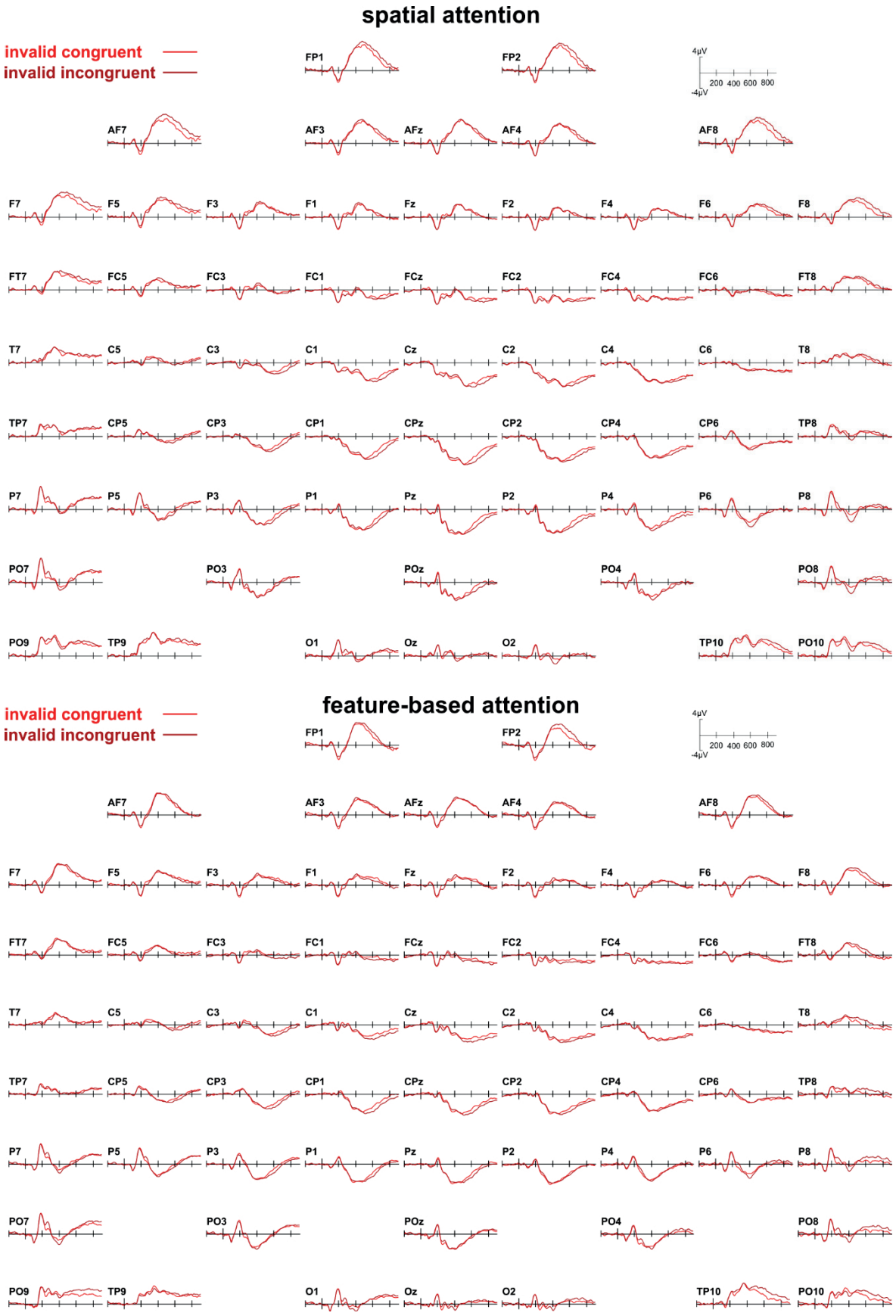

Appendix J: Experiment I (spatial cueing): Locations and source waveforms of all regional sources (green = congruent; red = incongruent; valid cueing = solid lines; invalid cueing = dotted lines). Difference waves are plotted below the source waveforms in the respective colors of the regional sources. Epochs deviating from zero are presented in green (congruent > incongruent) and red (incongruent > congruent. Grey area = bootstrap BCa 95%-confidence interval. N = 18.

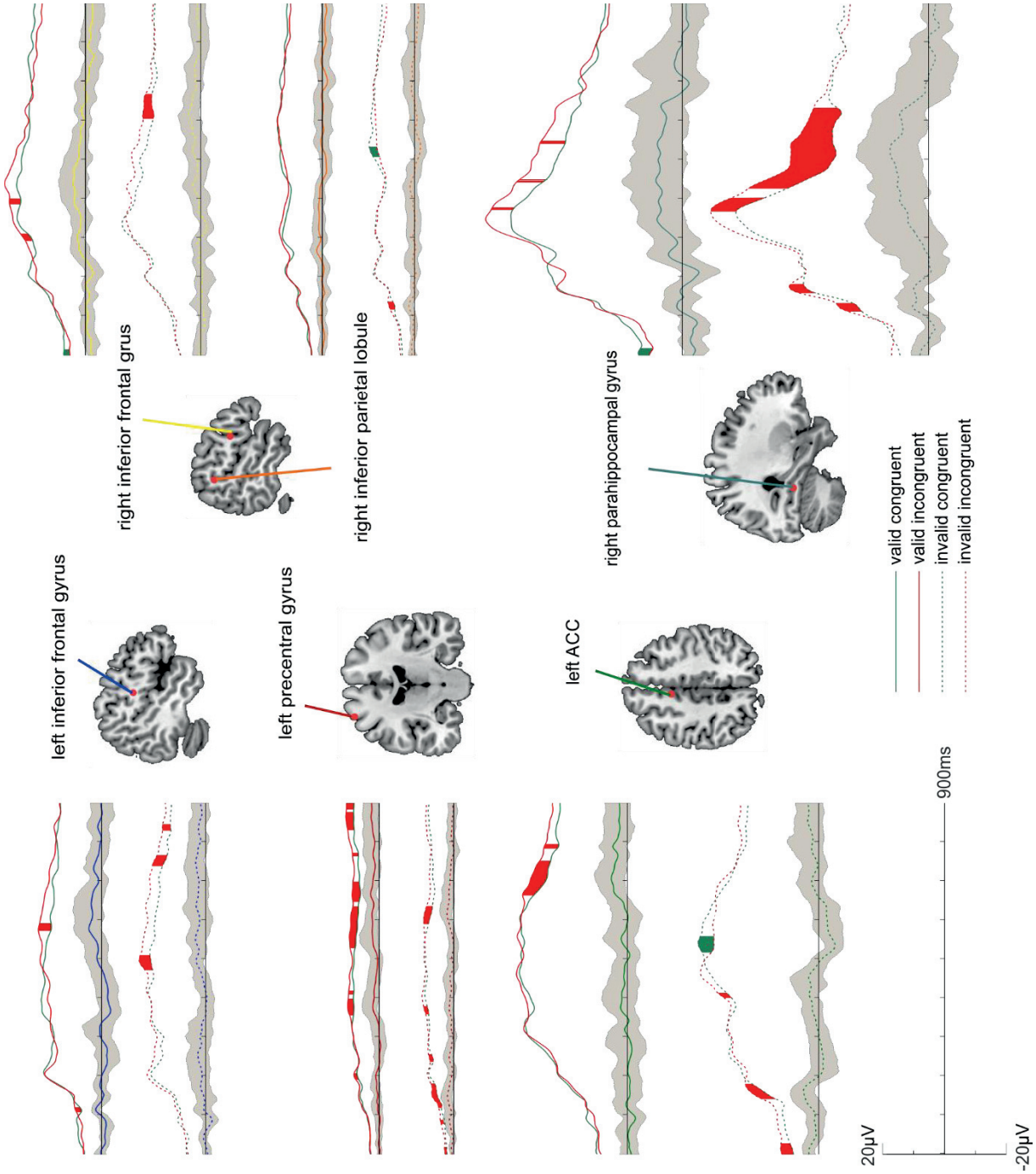

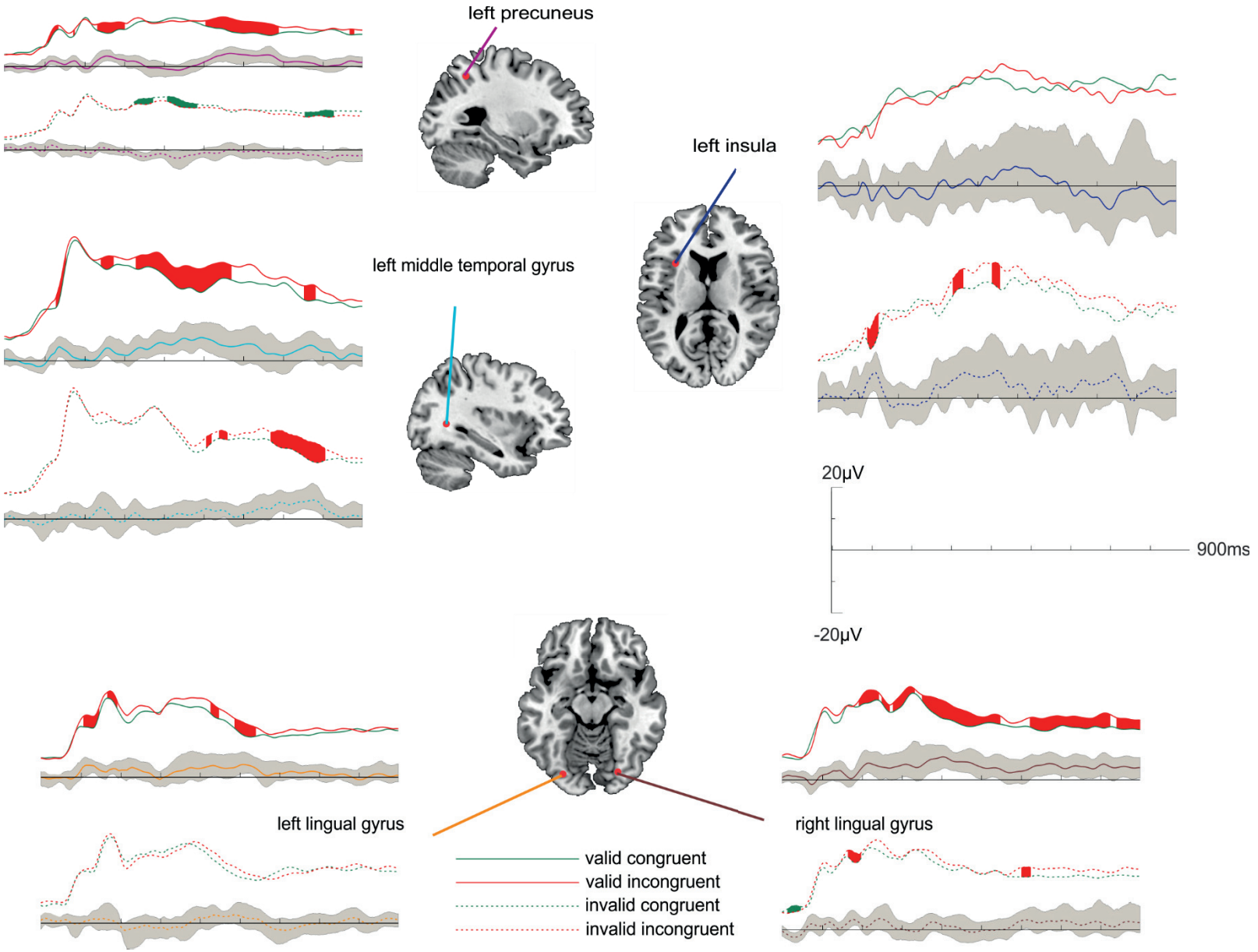
left precuneus
left middle temporal gyrus
left insula
20μV
900ms
-20μV
left lingual gyrus
right lingual gyrus
valid congruent
valid incongruent
invalid congruent
invalid incongruent

Appendix K: Experiment I (spatial cueing): Locations and source waveforms of all regional sources during neutrally cued trials (green = congruent; red = incongruent). Difference waves are plotted below the source waveforms in the respective colors of the regional sources. Epochs deviating from zero are presented in green (congruent > incongruent) and red (incongruent > congruent. Grey area = bootstrap BCa 95%-confidence interval. N= 18

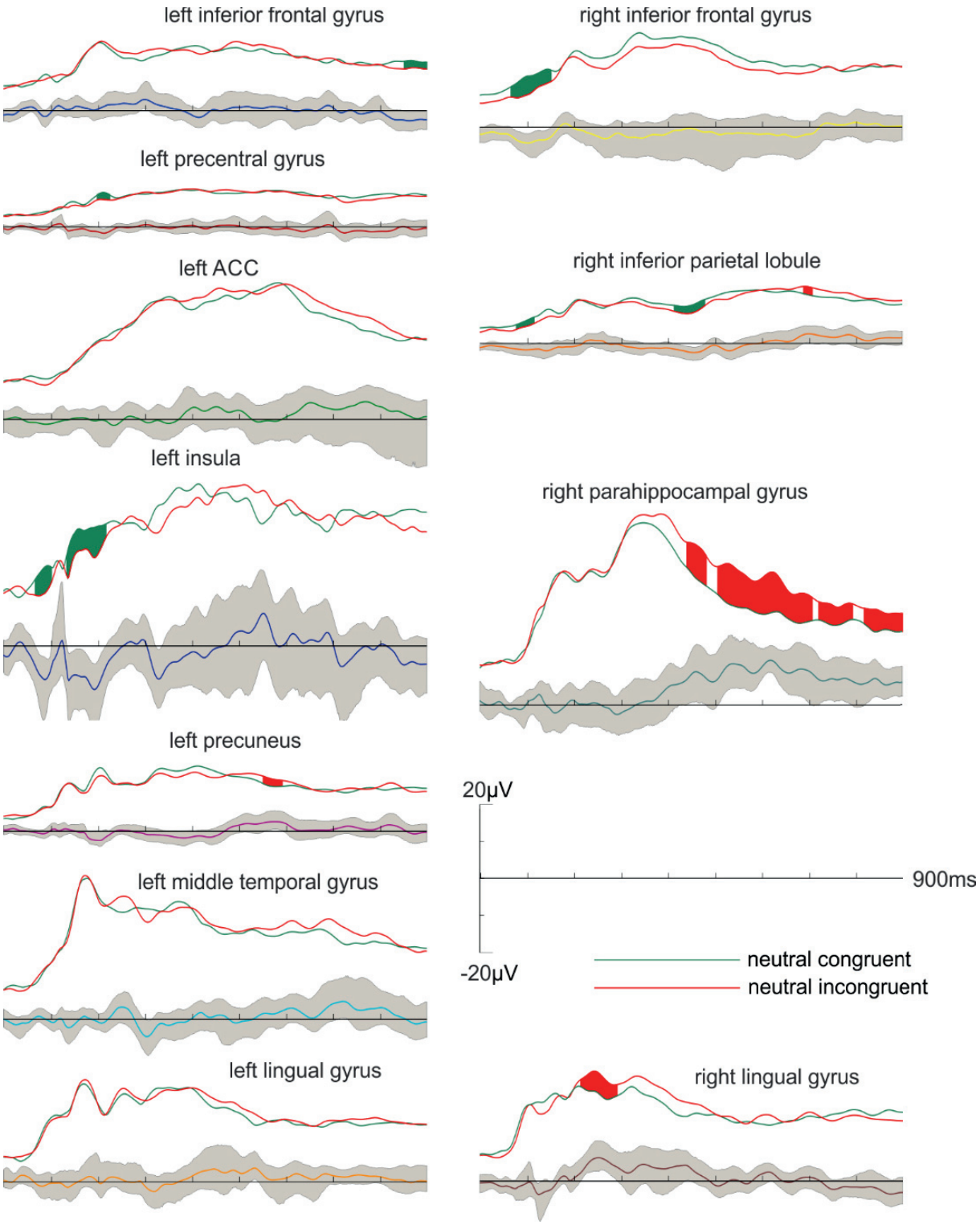

Appendix L: Experiment I (spatial cueing): Significant time epochs (ms) in which the BCa bootstrap 95%-confidence interval for the difference between incongruent and congruent trials did not include zero separately for each validity level (left = valid cueing; middle = neutral cueing; right = invalid cueing). N = 18.

	valid cues	neutral cues	invalid cues
left Inferior Frontal Gyrus	(106-119)	(288-307)	471-507
	570-590	850-900	735-765
			(827-844)
Middle Temporal Gyrus	126-154	(300-313)	(505-517)
	238-272	(712-722)	538-558
	326-575		669-804
	748-781		
Precentral Gyrus	(188-205)	193-224	(0-16)
	355-402		(77-86)
	(405-420)		116-179
	527-633		(235-254)
	645-698		357-385
	(761-772)		588-634
	828-876		
	879-900		
Insula		65-100	122-149
		132-215	337-363
		(321-335)	435-455
Precuneus	105-135	(179-194)	324-372
	(170-176)	(553-593)	404-484
	229-301		752-827
	503-690		
	(864-882)		
Anterior Cingulate Gyrus	660-749	(22-30)	0-25
	(781-792)	114-136	140-178
		505-531	(398-411)
			515-558
right Inferior Frontal Gyrus	(0-13)	64-150	604-670
	(291-309)		
	(385-397)		
Inferior Parietal Lobule	(260-268)	78-110	(22-30)
		(137-142)	114-136
	11-44	414-475	505-531
	(108-125)	685-713	
	163-196	(721-740)	
	(235-245)	(763-782)	
right Parahippocampal Gyrus	(0-17)	(426-433)	109-131
	(369-377)	439-479	157-181
	(436-442)	505-705	364-404
	(446-449)	715-791	424-631
	(538-546)	816-900	
left Lingual Gyrus	103-146	(524-540)	109-131
	165-190		157-181
	423-447		364-404
	486-540		424-631
right Lingual Gyrus	189-242	(117-130)	11-44
	248-269	(145-154)	(108-125)
	277-331	213-290	163-196
	350-546	(435-446)	(235-245)
	621-825		599-623
	839-900		(668-674)

Appendix M: Experiment II (feature-based cueing): Plots of source sensitivity images showing source sensitivities (in percent) of the single regional sources.

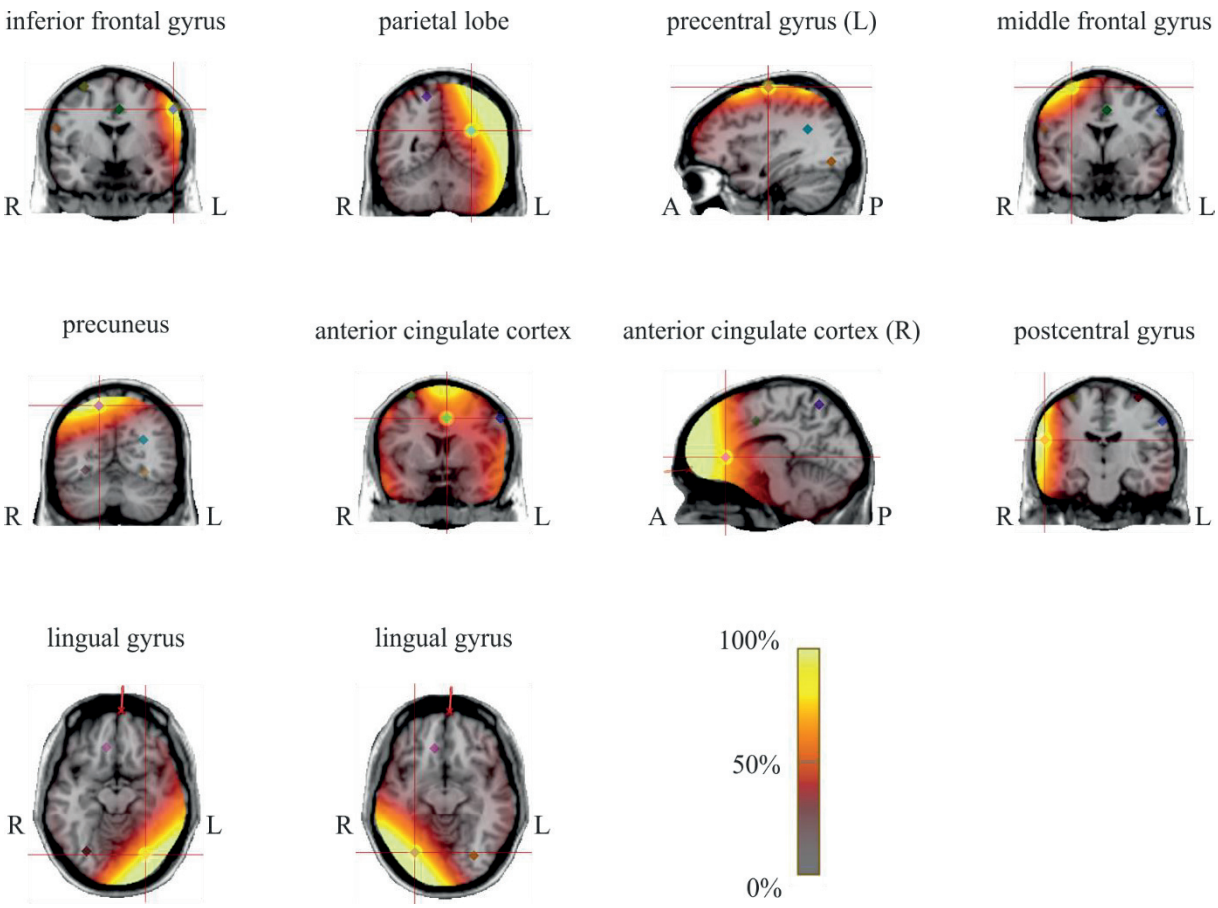

Appendix N: Experiment II (feature-based cueing): Locations and source waveforms of all regional sources (green = congruent; red = incongruent; valid cueing = solid lines; invalid cueing = dotted lines). Difference waves are plotted below the source waveforms in the respective colors of the regional sources. Epochs deviating from zero are presented in green (congruent > incongruent) and red (incongruent > congruent. Grey area = bootstrap BCa 95%-confidence interval. N = 21.

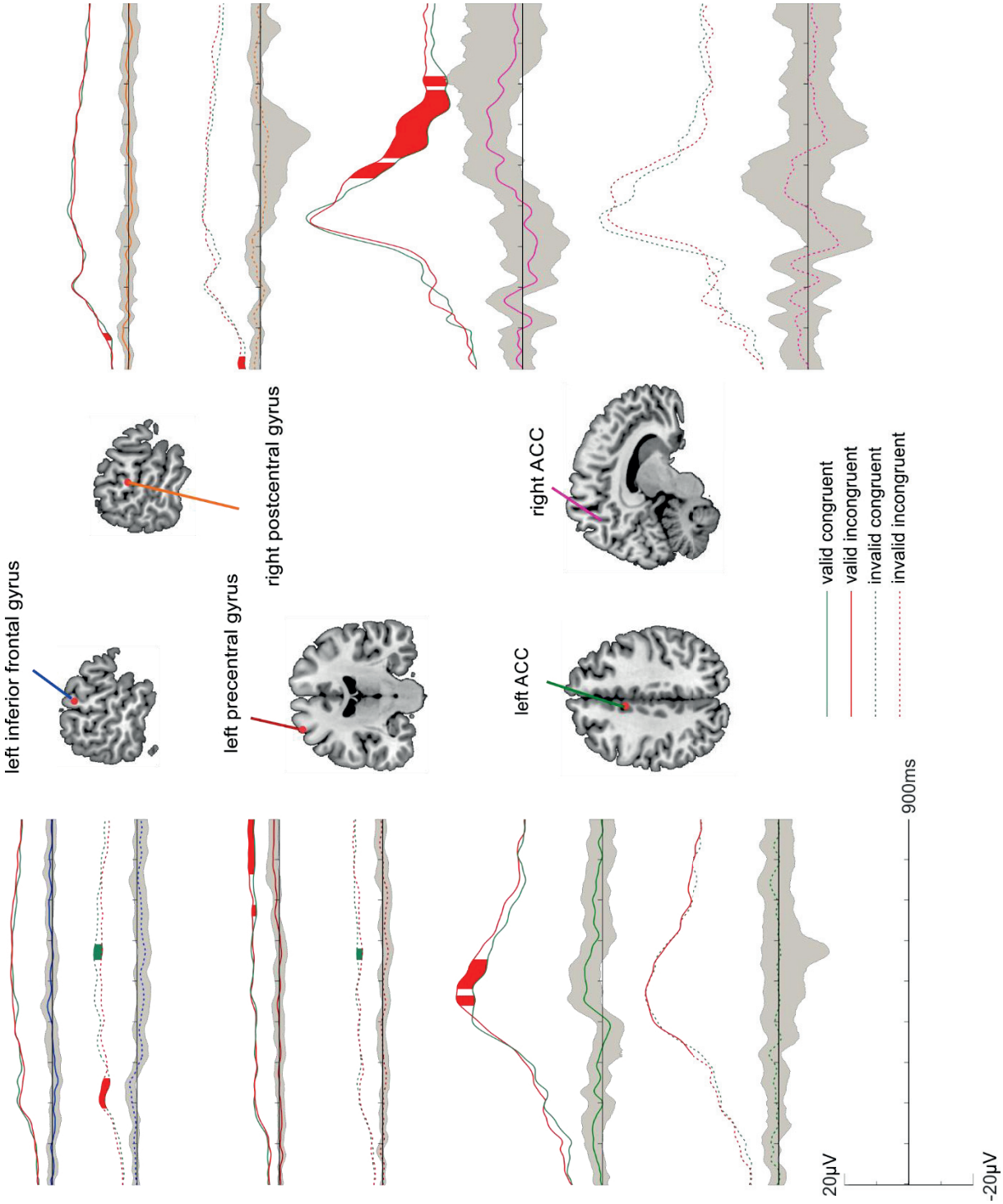

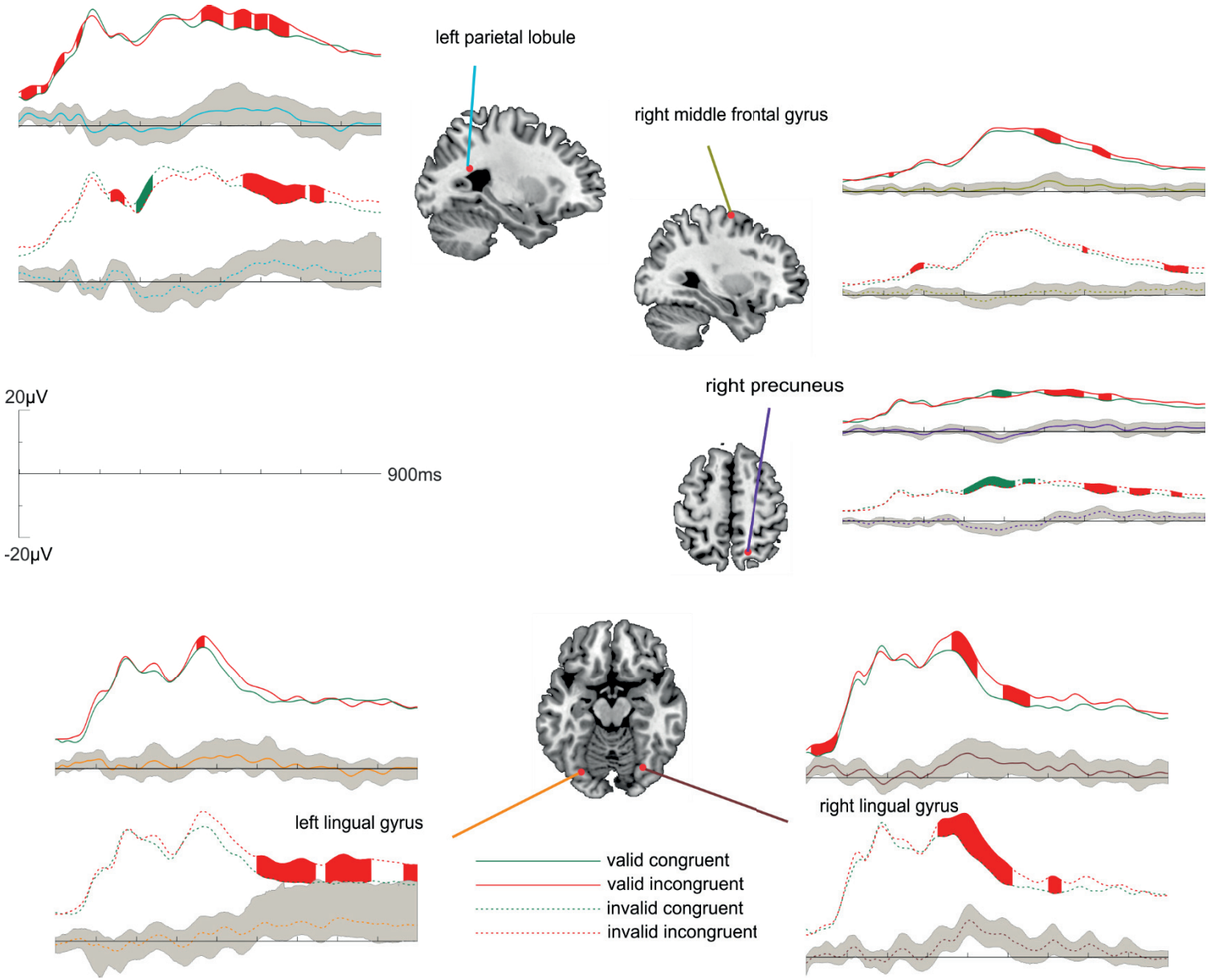
left parietal lobule
right middle frontal gyrus
right precuneus
20μV
900ms
-20μV
left lingual gyrus
right lingual gyrus
valid congruent
valid incongruent
invalid congruent
invalid incongruent

Appendix O: Experiment II (feature-based cueing): Locations and source waveforms of all regional sources during neutrally cued trials (green = congruent; red = incongruent). Difference waves are plotted below the source waveforms in the respective colors of the regional sources. Epochs deviating from zero are presented in green (congruent > incongruent) and red (incongruent > congruent. Grey area = bootstrap BCa 95%-confidence interval. N = 21.

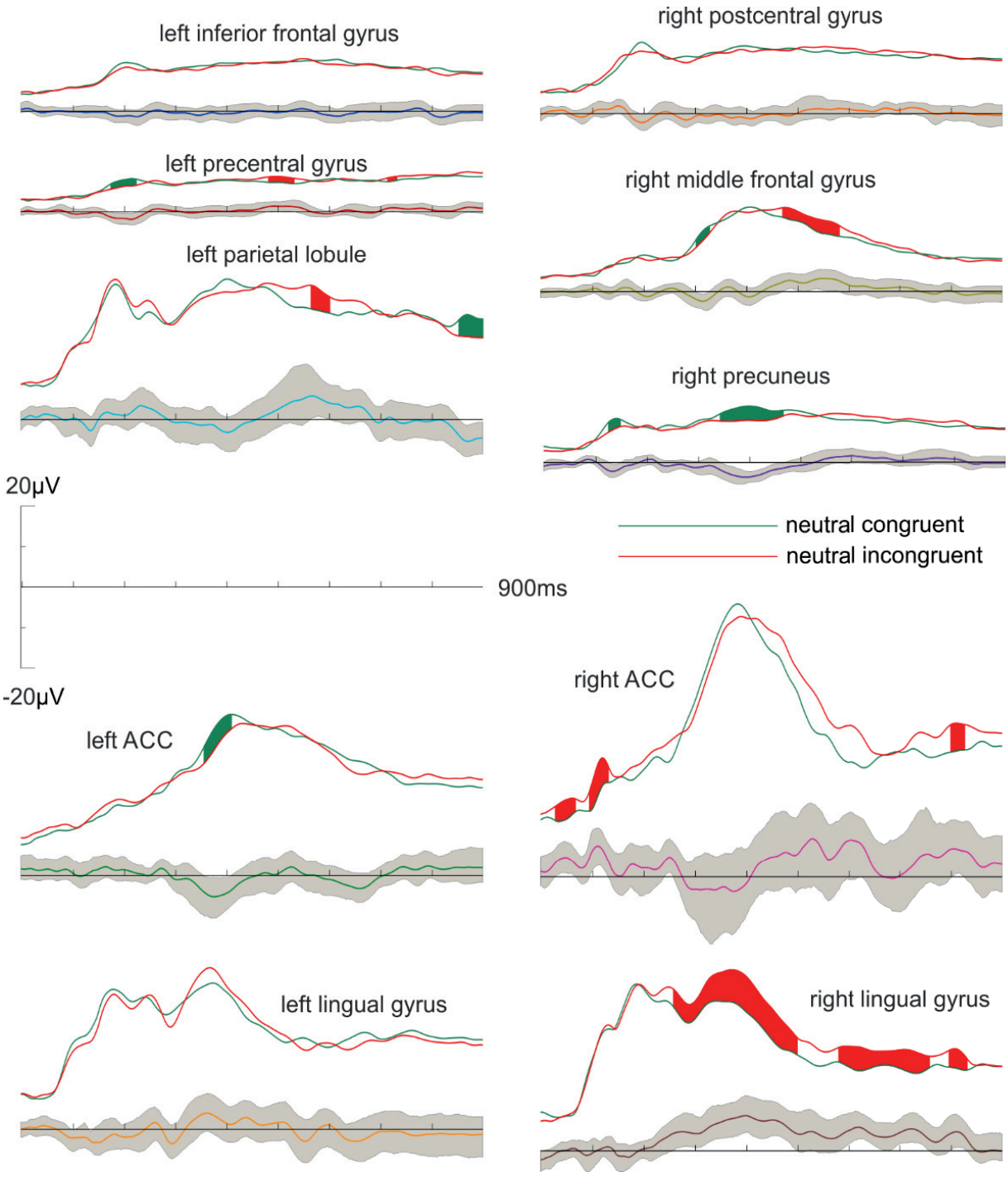

Appendix P: Experiment II (feature-based cueing): Significant time epochs (ms) in which the BCa bootstrap 95%-confidence interval for the difference between incongruent and congruent trials did not include zero separately for each validity level (left = valid cueing; middle = neutral cueing; right = invalid cueing). N = 21.

Regional Source	valid cueing [ms]	neutral cueing [ms]	invalid cueing [ms]
left Inferior Frontal Gyrus		0-30 (123-140) (267-276)	183-261 (454-473) 553-589
right Postcentral Gyrus	69-89	(142-155) (191-206)	0-30 (123-140) (267-276)
left Anterior Cingulate Gyrus	(85-103) 439-466 479-553	355-408	(52-67) 96-164
left Precentral Gyrus	(57-75) 661-689 763-900	172-225 476-533 712-734	553-580
left Parietal Lobe	4-50 (53-70) 84-111 (142-155) 446-516 534-576 582-617 622-670	563-600 853-900 300-326 470-581	(0-17) (117-135) (157-170) 228-260 291-329 555-711 718-757
right Middle Frontal Gyrus	(113-126) 475-540 618-664	300-326 470-581	168-200 (593-605) 797-857
right Precuneus	(195-211) 371-417 500-603 632-667 (831-840)	126-148 343-467	300-427 433-474 600-680 711-764 815-845
right Anterior Cingulate Gyrus	(162-176) 469-507 517-684 690-719	26-67 93-130 (240-257) 800-825	
left Lingual Gyrus	(74-81) (89-106) 348-369 (442-460)	(99-103) (130-139)	500-644 670-784 862-900
right Lingual Gyrus	11-76 360-423 487-554 (599-609) (653-661)	256-500 (519-534) 580-757 796-830	116-125 325-510 601-635 796-830

Appendix Q: Experiment I (spatial cueing): ERPs of valid (blue), neutral (black), and invalid (red) conditions pooled over congruency levels. Difference waves are plotted in dotted lines (blue = valid > neutral; red = invalid > neutral). N = 18.

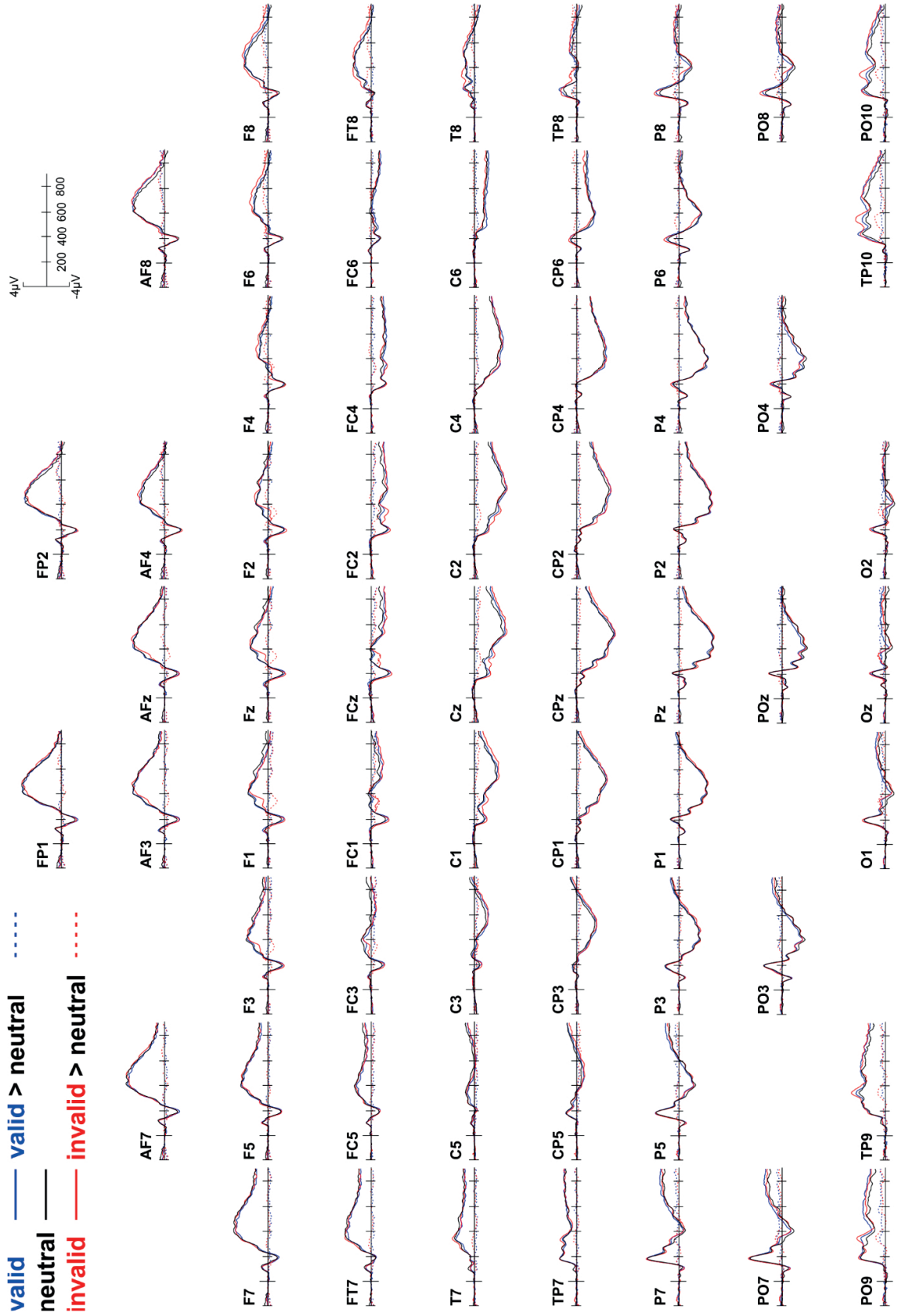

Appendix R: Experiment II (feature-based cueing): ERPs of valid (blue), neutral (black), and invalid (red) conditions pooled over congruency levels. Difference waves are plotted in dotted lines (blue = valid > neutral; red = invalid > neutral). N = 21.